INVITED REVIEW

Origin of the lunar highlands Mg-suite: An integrated petrology, geochemistry, chronology, and remote sensing perspective

Charles K. Shearer[1,*], Stephen M. Elardo[1], Noah E. Petro[2], Lars E. Borg[3], and Francis M. McCubbin[1]

[1]Institute of Meteoritics, Department of Earth & Planetary Sciences, University of New Mexico, Albuquerque, NM 87131, USA

[2]NASA, Goddard Space Flight Center, Greenbelt, MD 20771, USA

[3]Chemical Sciences Division, Lawrence Livermore National Laboratory, Livermore, CA 94550, USA

*Author to whom correspondence should be addressed: cshearer@unm.edu

Submitted to
Second Lunar Highlands Conference Special Issue
American Mineralogist
November 24, 2013
Resubmitted
May 23, 2014
Version 3 submitted
June 17, 2014

ABSTRACT

The Mg-suite represents an enigmatic episode of lunar highlands magmatism that presumably represents the first stage of crustal building following primordial differentiation. This review examines the mineralogy, geochemistry, petrology, chronology, and the planetary-scale distribution of this suite of highlands plutonic rocks, presents models for their origin, examines petrogenetic relationships to other highlands rocks, and explores the link between this style of magmatism and early stages of lunar differentiation. Of the models considered for the origin of the parent magmas for the Mg-suite, the data best fit a process in which hot (solidus temperature at ≥2 GPa = 1600 to 1800°C) and less dense (ρ~3100 kg/m^3) early lunar magma ocean cumulates rise to the base of the crust during cumulate pile overturn. Some decompressional melting would occur, but placing a hot cumulate horizon adjacent to the plagioclase-rich primordial crust and KREEP-rich lithologies (at temperatures of <1300°C) would result in the hybridization of these divergent primordial lithologies, producing Mg-suite parent magmas. As urKREEP is not the "petrologic driver" of this style of magmatism, outside of the Procellarum KREEP Terrane (PKT), Mg-suite magmas are not required to have a KREEP signature. Evaluation of the chronology of this episode of highlands evolution indicates that Mg-suite magmatism was initiated soon after primordial differentiation (<10 m.y.). Alternatively, the thermal event associated with the mantle overturn may have disrupted the chronometers utilized to date the primordial crust. Petrogenetic relationships between the Mg-suite and other highlands suites (e.g. alkali-suite and magnesian anorthositic granulites) are consistent with both fractional crystallization processes and melting of distinctly different hybrid sources.

INTRODUCTION

The lunar highlands crust is dominated by numerous "pristine" magmatic lithologies. These "pristine" igneous rocks include the ferroan anorthosites (FANs) and Mg-rich rocks (Warren, 1993; Papike et al., 1998). Dowty et al. (1974) recognized that FANs typically have greater than 90 volume percent plagioclase, very calcic plagioclase (>An_{96}), and pyroxene and olivine compositions that are relatively iron-rich (Mg# <70, where Mg# = molar [Mg/Mg+Fe]*100). Recent studies (Norman et al., 2003; Borg et al., 2011; Shearer et al. 2013) identified FAN rocks with similar mineral compositions but with higher abundances of mafic minerals (10-20 volume percent). The compositional range for the Mg-rich rocks, however, is not well-defined and they are a lithologically very diverse group (e.g., Norman and Ryder 1980; James, 1980; James and Flohr; 1983; Warren, 1986; Papike et al., 1998; Shearer and Papike, 2005; Shearer et al., 2006). Papike et al. (1998) subdivided the Mg-rich highlands rocks into the magnesian plutonic rocks (also known as (aka) Mg-suite, highlands magnesian suite), alkali rocks (aka the alkali-suite), and KREEP basalts (see their Table 10). Unlike Heiken et al., 1991), Papike et al. (1998) grouped these compositionally diverse rocks together because recent interpretations had petrogenetically linked some of these rocks to each other and to the Mg-suite (Snyder et al. 1995). The Mg-suite rocks are distinguished from all other Mg-rich rocks based on their lower alkali element content (e.g. K_2O generally less than 0.1 wt%, plagioclase >An_{90}) and more magnesian mafic silicates (Mg# generally > 78; Fig. 1). The Mg-suite rocks in the Apollo collection have the paradoxical chemical characteristics of very Mg-rich mafic silicates, which indicate a primitive parental magma (e.g., Hess, 1994), and highly elevated abundances of incompatible trace elements (REE, but not alkali elements), indicating an evolved parental magma (e.g., Papike et al., 1994; 1996). The Mg-suite rocks are plutonic to hypabyssal in origin with a range of rock types including ultramafics (e.g., dunites, pyroxenites, harzburgites, and peridotites), troctolites, spinel troctolites, anorthositic troctolites, norites, and gabbronorites (Warner et al., 1976a; James and Flohr, 1983; McCallum and O'Brien, 1996; Papike et al., 1998; Warren, 1993; Shearer and Papike, 2005, Shearer et al., 2006). In the Apollo collection, samples range from very large single specimens (e.g. 465 grams troctolite 76335) to tiny clasts within breccias (e.g. < 0.1 gram spinel troctolite clast in 72435). Mg-spinel-bearing lithologies and Mg-anorthosites have been identified in lunar meteorites and through remote-sensing observations (e.g. Kurat and Brandstatter, 1983; Lindstrom and Lindstrom, 1986; Treiman et al, 2010; Gross and Treiman, 2011; Pieters et al., 2011), but their relationship to the Mg-suite has not fully been appreciated. The alkali rocks (alkali-suite) making up the lunar highlands are distinguished from the Mg-suite (Papike et al., 1998) by their higher alkali-element content, more sodic plagioclase, and more Fe-rich mafic silicates (Fig. 1).

It is generally assumed that the Mg-suite was emplaced into the primordial FAN crust and that they formed layered intrusions (e.g., Warner et al., 1976a; James, 1980; Hess, 1994; Shearer and Papike, 2005). However, incontrovertible evidence, such as large-scale stratigraphic layering or clear genetic relationships among samples of different petrologic types, for this scenario does not exist. On the basis of the Apollo sample suite, the distribution of FANs and Mg-suite rocks implies a lateral and vertical crustal association rather than an intrusive relationship (Papike et al., 1998; Shearer and Papike, 2005). Furthermore, while the remnant magmatic textures and mineral chemistries in the Mg-suite rocks indicate an origin involving accumulation of crystals during the crystallization of basaltic magmas, there is no evidence for layering in these samples.

In this review, we examine the petrology, geochemistry, chronology, and distribution of the Mg-suite, using these combined data sets to evaluate models for Mg-suite petrogenesis, its relationship to other suites of crustal lithologies, and its links to early stages of lunar differentiation.

PETROLOGY, MINERALOGY, AND GEOCHEMISTRY OF THE MG-SUITE

Definition of the Mg-suite

The Mg-suite of plutonic highlands rocks has been distinguished from other lunar magmatic rocks using a variety of textural, mineralogical, and geochemical criteria. Firstly, they are plutonic to hypabyssal with textures and bulk compositions consistent with the accumulation of mineral phases (e.g., Haskin et al., 1974). The mineral assemblage generally contains calcic plagioclase (An_{98-84}) coexisting with Mg-rich mafic silicates (Mg# 95-60; Fig. 1). Secondly, the Mg-suite in the Apollo sample collection is typified by a KREEP component that is reflected in elevated REE abundances and LREE/HREE, and low Ti/Sm and Sc/Sm relative to other lunar lithologies. Olivine in Mg-suite rocks has low abundances of Ni, Co, and Cr for its relatively high Mg# compared to other lunar lithologies (Shearer and Papike, 2005; Longhi et al., 2010; Elardo et al., 2011), and plagioclase in the Mg-suite rocks has higher abundances of Ba, Y, and Sr (Papike et al., 1996; 1997; Shervais and McGee, 1998; Zeigler et al., 2008). Fluorapatite is typically Cl-rich and OH-poor (McCubbin et al., 2011). Whether these trace element characteristics are typical of all Mg-suite rocks, or only those in the PKT region of the Moon, is a point of debate that is closely related to petrogenetic models of origin of the Mg-suite. For example, Mg spinel-rich lithologies and magnesian anorthosites that have been identified in lunar meteorites (e.g. Takeda et al., 2006; Treiman et al., 2010; Gross and Treiman, 2011) plot within the Mg-suite field on a plot of Mg# in mafic silicates vs. An in plagioclase (Fig. 1). These rocks generally have major element mineral chemistries similar to the Mg-suite, but without many of their trace element characteristics. Lastly, Mg-suite rocks typically date to ~4.5 – 4.1 Ga, although whether this is representative of the true extent of Mg-suite magmatism is a point of dispute.

Mg-suite samples in the Apollo collection

Samples that fall within the general compositional ranges of the Mg-suite have been found at every Apollo landing site with the exception of the Apollo 11 site in Mare Tranquillitatus (Papike et al., 1998; Shearer and Papike, 2005). Samples of the Mg-suite are common at the Apollo 14 (Fra Mauro), Apollo 15 (Apennine Mountains), and especially the Apollo 17 (Taurus-Littrow Valley) landing sites, but are sparser at the Apollo 12 (Oceanus Procellarum) and Apollo 16 (Cayley Plains) landing sites (Papike et al., 1998). The lithologies making up the Mg-suite are cumulate igneous rocks and consist of ultramafics, troctolites, Mg-spinel troctolites, norites, and gabbronorites (Warner et al., 1976a; James, 1980; Norman and Ryder, 1980; Warren, 1993; Papike et al., 1998; Shearer and Papike, 2005). There are some samples that are classified based on modal abundances as magnesian anorthosites (e.g. Lindstrom et al., 1984), but in most cases the samples are small and modal abundance determinations are of questionable accuracy. Additionally, many of the ultramafic samples are very small (<0.1 g), making the relative importance of ultramafic samples in the Mg-suite debatable. Mg-suite samples display a near-continuous range in mineralogy from dunites to gabbronorites that generally approximates a fractional crystallization sequence, and this is also reflected in mineral chemistry (Snyder et al., 1995; Shervais and McGee, 1998). Similar mineralogical and geochemical trends are observed in the plutonic cumulate lithologies of terrestrial layered mafic intrusions such as the Stillwater Complex, Montana (e.g. McCallum et al., 1980; Raedeke and McCallum, 1984). Furthermore, the Mg-suite cumulate rocks have mineralogical and geochemical differences when compared to FANs that have led to the interpretation that they are derived from different parental liquids (Warner et al., 1976a; Warren, 1986; Shearer and Papike, 2005). Compared to the Mg-suite, the plutonic rocks represented by the alkali-suite have mafic phases which have lower Mg#s and plagioclase compositions that are lower in their Ca/(Ca+Na) (Fig.1). The compositional relationship presented in Figure 1 and incompatible element enrichments have been used as evidence to suggest that fractional crystallization of the parent magmas to the Mg-suite would produce the alkali-suite lithologies. A list of Mg-suite samples is shown in Tables 1-5, and their petrography, mineralogy, and geochemistry are reviewed in the sections below. For brevity, we focus on a few examples of each lithologic type, but a main reference for each Mg-suite sample can be found in Tables 1-5 and the reader is also directed to the online Lunar Sample Compendium for additional information and references.

Petrography of the Mg-suite

Any discussion of rocks derived from the ancient lunar crust needs to consider the concept of pristinity. Without such considerations, even careful workers may be led to erroneous interpretations regarding the origin and evolution of the lunar crust, as the effects of ~4.4 Gyr of impact alteration of ancient crustal samples are not always obvious. Warren and Wasson (1977) were the first authors to establish a set of criteria for establishing the level of pristinity retained in ancient lunar crustal samples. Warren (1993) compiled the results of numerous pristinity quantification efforts with a thorough compilation of non-mare lunar rocks in which he evaluated their pristinity based on siderophile element abundances, Fe-Ni-metal composition, textural characteristics, phase homogeneity, incompatible element abundances, plausibility of a rock being a mixture, and ages. On the basis of these criteria, Warren (1993) assigned each sample a value from 9 (high confidence) to 3 (low confidence) reflecting the confidence that the sample represents a pristine lithology from the ancient lunar crust. Much of the information used here is from Warren (1993) and the interested reader is referred to that compilation for detailed information on pristinity assessment.

Ultramafics

Ultramafic samples of the Mg-suite are rare in the Apollo collection. The only ultramafic sample with a mass over 0.1 grams is dunite 72415-72418 (58.74 g), collected as several fragments chipped off of a ~10 cm clast within Boulder 3 at Station 2 during the Apollo 17 mission (spinel troctolite 72435 was chipped from the same boulder). The lack of ultramafic samples over 0.1 grams besides 72415 and their coarse-grained nature cast doubt on the significance of other "ultramafic" samples in Table 1. For example, "pyroxenite" 14305c389 is essentially a single large grain of OPX (Shervais et al., 1984).

Dunite 72415-8 (Fig. 2a) has a modal mineralogy dominated by 93 vol.% olivine with minor plagioclase, OPX, CPX, Cr-spinel typically occurring in symplectites (see below), Fe-Ni metal, apatite that sometimes occurs as veining along mineral boundaries (see below), troilite, and armalcolite (Dymek et al., 1975; Laul and Schmitt, 1975; Ryder, 1992). Olivine (Fo_{89-86}) and plagioclase (An_{97-94}) have very narrow compositional ranges. 72415-8 has been cataclasized and in thin section appears as large olivine crystals set in a matrix dominated by crushed olivine (Fig. 2a). The fragmented nature of the olivine, combined with the observation of strain bands, subgrains, and some maskelynization of plagioclase indicate a complex shock history (Snee and Ahrens, 1975; Lally et al., 1976). Nevertheless, Warren (1993) assessed 72415-8 at a pristinity confidence level of 9, indicating this sample represents a nearly chemically unaltered Mg-suite lithology.

Warren et al. (1990) described harzburgite 12033,503, which is roughly 1.4mm across in thin section. It is dominated by olivine ($Fo_{89.5}$) and low-Ca pyroxene ($En_{91}Wo_{0.4}$) with minor Cr-spinel, Fe-Ni-metal, and no plagioclase. They determined that 12003,503 represents an igneous lithology and assessed it at a pristinity confidence level of 8. Lindstrom et al. (1984) described a dunite clast (1141,1236) in Apollo 14 breccia 14321. Although the sample proved very friable upon extraction, the clast contains coarse olivine grains up to 3 mm in diameter with very little plagioclase native to the clast. Lindstrom et al. (1984) also described magnesian anorthosites and troctolites from 14321 that may be related to the dunite. Sample 14321c1141 was assessed at a pristinity confidence level of 6 (Warren, 1993).

Troctolites

Troctolites are the most abundant Mg-suite sample type in the Apollo collection. They are perhaps the most studied as well, owing in part to the three large pristine troctolites, 76335, 76535, and 76536, collected during Apollo 17. The best preserved and most thoroughly studied troctolite, and perhaps sample of the entire Mg-suite, is sample 76535 (155.5g). It is a coarse-grained, unbrecciated olivine-plagioclase cumulate rock (Fig. 2b) that shows virtually no signs of impact modification, but extensive subsolidus annealing is apparent (Gooley et al., 1974; Haskin et al., 1974; Dymek et al., 1975). Plagioclase (An_{97}) and olivine (Fo_{88}), which are present in roughly cotectic proportions of 60% and 35%, respectively, show virtually no chemical zoning, and often meet at 120° triple junctions. Grain size in 76535 is typically ~2-3mm (Fig. 2b). OPX is a minor phase in 76535, making up ~5% of the rock. CPX and chromite are present as well, but both phases are primarily confined to symplectite assemblages consisting of chromite, CPX, and OPX (see below) that are typically in contact with both olivine and plagioclase (Gooley et al., 1974; Albee et al., 1975; Bell et al., 1975; Dymek et al., 1975; McCallum and Schwartz, 2001; Elardo et al., 2012). McCallum and Schwartz (2001) used the five phase symplectite assemblage to infer a depth of origin of 40-50 km, and two-pyroxene equilibration temperatures (i.e. Andersen et al., 1993) fall with the range of 800-900°C (McCallum and Schwartz, 2001; Elardo et al., 2012). The high apparent degree of equilibration at the temperatures and depths inferred indicates 76535 has experienced the equivalent of granulite-facies metamorphism, likely due to slow cooling in the plutonic environment. Other phases in 76535 include troilite, FeNi-metal, apatite, RE-merrillite, baddeleyite, zircon, and pyrochlore, most of which are confined to mesostasis areas and rare olivine-hosted holocrystalline melt inclusions (Dymek et al., 1975; Elardo et al., 2012). Elardo et al. (2012) documented veins consisting of CPX and troilite that were confined almost exclusively to intercumulus OPX grains (see below). 76535 has been assessed at a pristinity confidence level of 9 by Warren (1993). Its near-perfectly preserved texture, mineralogy, and composition have led to 76535 being extensively studied (e.g., Gooley et al., 1974; Haskin et al., 1974; Albee et al., 1975; Bogard et al., 1975; Dymek et al., 1975; Hinthorne et al., 1975; Huneke and Wasserburg, 1975; Lugmair et al., 1976; Papanastassiou and Wasserburg, 1976; Caffee et al., 1981; Premo and Tatsumoto, 1992a; McCallum and Schwartz, 2001; Shearer and Papike, 2005; McCallum et al., 2006; Garrick-Bethell et al., 2009; Day et al., 2010; Elardo et al., 2012).

The other large troctolites from Apollo 17, 76335 and 76536, are very similar in mineralogy (and bulk composition) to 76535, however they have experienced somewhat greater, but still relatively mild, degrees of impact modification, and appear to be somewhat more feldspathic (Papike et al., 1998). 76335 and 76536 are essentially monomict breccias. Given their compositional similarities and the coarse-grained nature of the Apollo 17 troctolites (Warren and Wasson, 1978; Ryder and Norman, 1979), 76335 and 76536 may simply be crushed versions of 76535.

Troctolites are also found at the Apollo 14 site, and thus far a single troctolite has been found at each of the Apollo 15 and 16 sites (Table 2). Samples from Apollo 14 are primarily found as clasts in the impact melt breccias that are common at the Fra Mauro site (Lindstrom et al., 1984; Shervais et al., 1984; Goodrich et al., 1986; Papike et al., 1998). The largest Apollo 14 troctolite is a clast (9 g) in breccia 14321 (Lindstrom et al., 1984) that has magnesian olivine (Fo_{87}) and calcic plagioclase (An_{95}) that are unzoned and over 2mm in grain size (although crushed). Modal abundances of Apollo 14 troctolites are sometimes very feldspathic, and have been described as magnesian anorthosites (e.g., Lindstrom et al., 1984); however the significance of this distinction is dubious because of the small size of the clasts. Compositions of olivine sometimes extend to more Fe-rich compositions (Fo_{77}).

Spinel Troctolites

The presence of several vol.% Mg-rich pleonaste, or “pink,” spinel differentiates the spinel troctolites from the troctolites, the latter of which never contain Mg-rich spinel. A list of Mg-suite spinel troctolite samples in the Apollo collection can be found in Table 3. The spinel troctolites all occur as clasts within polymict breccias and have been heavily shocked (Warren, 1993), which led to them sometimes being referred to as spinel cataclasites. Two spinel troctolite clasts (72425,8 and ,30; Fig. 2g, h) contain olivine (Fo_{74-72}) and plagioclase (An_{94}) along with Mg-rich spinel grains, and one sample (72435,8) contains a single grain of cordierite (Fig. 2; Dymek et al., 1976). 72435 was chipped from Boulder #3 at Station 2, the same boulder from which dunite 72415-8 was collected. A spinel troctolite in breccia 15295 also contains cordierite along with olivine (Fo_{91}), plagioclase (An_{94}), and pink Mg-rich spinel (Marvin et al., 1989). Prinz et al. (1973) and Ma et al. (1981) described a spinel troctolite clast in 67435 that retains cumulus texture. That clast contains olivine (Fo_{92}) and ~5 vol.% spinel poikilitically enclosed by plagioclase (An_{97}), along with Ni-rich metal (Papike et al., 1998). Due to their small sizes, it is unlikely that any of the spinel troctolites in the Apollo collection accurately reflect the true modal abundances and bulk composition of their parental lithologies.

Norites

The majority of norites in the Apollo sample collection were collected during the Apollo 15 and 17 missions. A list of all Mg-suite norite samples found in the Apollo collection can be found in Table 4. Two meter-sized noritic boulders were sampled during Apollo 17 at stations 7 and 8. The relatively large samples sizes and the abundance of OPX in these samples (allowing for more easily obtained mineral isochrons than OPX-poor samples) have led to the norites, alongside the large troctolite samples, being the most heavily studied members of the Mg-suite.

The two largest norite samples collected by Apollo 17 are 77075/77215 and 78235-78238. Examples of both norites are shown in Fig. 2c, d. 77075/77215 is one of the most ferroan samples of the Mg-suite. OPX in this sample is less magnesian ($En_{68-63}Wo_{5-3}$) compared to most other occurrences of OPX in Mg-suite samples, and it has CPX exsolution features (Fig. 2d) that indicate the OPX is inverted pigeonite (Chao et al., 1976; Papike et al., 1998). Most other occurrences of CPX in norites are in areas interstitial to the cumulus plagioclase and OPX, indicating it likely crystallized from trapped melt. This norite has minor abundances of FeNi metal, ilmenite, chromite, troilite, silica, RE-merrillite, and Zr-Ti-Ca-Fe oxide. Inclusions of either K-feldspar or granitic glass occur in the plagioclase. Sample 77075/77215 has been cataclasized and incorporated into an impact melt breccia (the station 7 boulder), however it has been assessed at a pristinity confidence level of 8 by Warren (1993).

The combined samples 78235, 78236, and 78238, represent the second largest norite sample (349.7g) returned during the Apollo missions. These samples were chipped from the top of the station 8 boulder, whereas norite 78255/6 (48.3g) was chipped from the bottom of the boulder; however 78235/6/8 and 78255/6 are very similar, if not identical. Sample 78235 has undergone some degree of shock as indicated by glass veins, some maskelynization of plagioclase, and some grain shattering, but it still retains a cumulate igneous texture (Fig. 2c). Plagioclase (An_{95-93}) and OPX ($En_{78}Wo_3$) are the only cumulus phases, however 78235 also contains trace amounts of CPX, chromite, ilmenite, high Ti-rutile, K-spar, RE-merrillite, apatite, Fe-metal, baddeleyite, zircon, and troilite (Dymek et al., 1975; Jackson et al., 1975; McCallum and Mathez, 1975; Steele, 1975; Nyquist et al., 1981; James and Flohr, 1983; Edmunson et al., 2009). The CPX present in 78235 is intercumulus and likely crystallized from trapped melt rather than from the inversion of pigeonite. Warren (1993) assessed this norite at a pristinity confidence level of 8.

The largest norite samples collected prior to Apollo 17 are norite clasts in breccias collected during Apollo 15. Clast B (~10g) from breccia 15445 is a highly cataclasized norite clast (Fig. 2e) with intermingled impact melt (Ryder and Bower, 1977; Shih et al., 1993; Shearer et al., 2012a). This clast has received attention due to its large size and variability in crystallization ages (Shih et al., 1993). Despite a high degree of shock, infiltration of impact melt, and possible mixing of lithologies, clast B of 15445 was assessed, at a pristinity confidence level of 8 by Warren (1993). The cataclasized anorthositic norite (CAN) clast in 15455 (~200g) has been described as being very similar in mineralogy and composition to clast B of 15445 (Ryder and Bower, 1977).

Gabbronorites

Gabbronorites are differentiated from the norites by the presence of CPX as a primary cumulus phase (James and Flohr, 1983; Papike et al., 1998). The gabbronorites also have a lower modal abundance of plagioclase than the norites. All samples of gabbronorites in the Apollo collection are clasts in breccias, all but two of which are under 1 g (Table 5).

The only large gabbronorite sample, clast 82 in 76255, is 300g and is very similar in mineralogy and composition to 76255 clast 72 (Fig. 2f). These clasts likely sample the same lithology. This gabbronorite sample contains 39% plagioclase, 4% OPX, and 57% CPX (Warner et al., 1976b). The plagioclase in 76255 (An_{86}) and other gabbronorites is the most sodic amongst Mg-suite lithologies (Table 5). Pyroxenes in 76255 have well-developed exsolution lamellae (Fig. 2f). Augite has an average composition of $En_{44}Wo_{43}$, whereas the orthopyroxene has an average composition of $En_{65}Wo_{3}$ (Warner et al., 1976b). Anderson and Lindsley (1982) and McCallum and O'Brien (1996) both calculated two-pyroxene equilibration temperatures of about 800° C for 76255, with the latter group inferring a shallow (0.5 km) emplacement depth. The backscattered electron (BSE) image in Fig. 2f reveals sulfide-rich veining in 76255. This texture in lunar crustal rocks is the result of secondary alteration resulting from a S-rich vapor (Norman et al., 1995; Shearer et al., 2011; Elardo et al., 2012), but these features in Apollo 17 samples have not been studied in detail. 76255 clast 72 has been assessed at a pristinity confidence level of 7 by Warren (1993).

A number of gabbronorites were also collected at the Apollo 16 site. Sample 67667 contains an unusual amount of olivine (50 vol.%) for relatively evolved Mg-suite samples (James and Flohr, 1983). 67667, which has been called a feldspathic lherzolite due to its high abundance of mafic minerals, is also one of the few Mg-suite samples that contains zoned cumulus minerals (Papike et al., 1998). Its olivine, for example, is zoned from Fo_{73} to Fo_{68}, and pyroxene and plagioclase also show magmatic zoning, indicating a shallow emplacement (James and Flohr, 1983).

Mineralogy of the Mg-suite

Olivine

Olivine in Mg-suite lithologies spans a narrow range in major element composition with the only exception being olivine in the gabbronorites (Fig. 3) (Papike et al., 1998; Shearer and Papike, 2005). The spinel troctolites have olivines with the highest Mg#s among Mg-suite lithologies, and span a range from Fo_{93-73}. Olivines in the ultramafics and troctolites overlap at the high end of the range in their olivine Mg#, but olivine in the troctolites reaches lower Mg#s than in the ultramafics. Olivine in the ultramafics spans a range from Fo_{90-85} whereas olivine in the troctolites ranges in composition from Fo_{90-80}. Olivine in the norites does not overlap in major element composition with the ultramafics and troctolites, ranging from $Fo_{78-70.}$ The gabbronorites exhibit the widest range in olivine compositions ranging from Fo_{71-32}. Very Mg-rich individual olivine grains in poikilitic melt breccias were studied by Ryder et al. (1997), and they argued that these grains were derived from Mg-suite lithologies. These individual grains reached Fo_{94}. The very magnesian olivine compositions found within Mg-suite lithologies demonstrate that the parental magmas for the Mg-suite were much more primitive in terms of major element composition than even the most primitive mare basalts and picritic glasses.

Electron and ion microprobe results (e.g., Ryder, 1983; Shearer and Papike, 2005) have shown that olivines from almost all Mg-suite lithologies have lower Cr, Ni, and Co contents than other lunar lithologies (Figs. 4, 5). Nickel contents of olivine are less than 200 ppm, and in most cases less than 100 ppm (Fig. 5). In comparison, olivines from mare basalts typically have Ni contents of 200-700 ppm (e.g., Papike et al., 1999; Karner et al., 2003; Shearer and Papike, 2005; Longhi et al., 2010; Elardo et al., 2014). The Ni contents of olivine from ferroan anorthosites are similar to those of the Mg-suite, however the Co contents of ferroan anorthosite olivine are higher than the Mg-suite and make them distinct. Mare basalt olivine also has distinctly higher Co contents than those of Mg-suite. Additionally, the Cr contents of Mg-suite olivine are lower for their Mg# than what would be expected given the trend observed in mare basalts (Fig. 4). Most Mg-suite olivines contain less than 500 ppm Cr, despite high Mg# (Shearer and Papike, 2005; Elardo et al., 2011; 2012). In contrast, olivines with the highest Mg# in mare basalts contain 2500-4000 ppm Cr. Yttrium contents of Mg-suite olivines are variable. The more primitive ultramafics and troctolites have olivine with low Y contents that are typically less than 2 ppm. These values are slightly greater or overlap with the Y contents of mare basalts (Shearer and Papike, 2005). Norites and gabbronorites, however, have olivine with elevated Y contents. These olivines range from 4-61 ppm in the norites and 8-13 ppm in the gabbronorites (Shearer and Papike, 2005). Mg-suite olivines consistently have greater Y contents than olivine in FANs, which typically contain less than 0.1 ppm Y.

Pyroxene

Mg-suite samples typically contain both OPX and CPX. However, with the exception of the gabbronorites, CPX occurs as either an intercumulus phase, or rarely as exsolution lamellae within OPX. Orthopyroxene in the Mg-suite shows a limited range in major element composition and very little major element zoning (Fig. 3; Papike et al., 1998). The Mg# of OPX in the ultramafics ranges from 92-86 and in the troctolites from 91-85. The Mg# of OPX in the spinel troctolites ranges from 91-70. Norite OPX ranges in Mg# from 89-67 and gabbronorite OPX ranges in Mg# from 78-60.

Papike et al. (1994) measured the REE abundances of OPX in Apollo 14, 15, and 17 norites, and Shearer and Papike (2005) measured Y as a REE proxy in Mg-suite samples of all types by ion microprobe. The REE patterns of OPX were parallel between samples from different landing sites. The Y data from Shearer and Papike (2005) showed that OPX in the norites and gabbronorites is much more enriched in Y (and by extension REEs) than OPX in the ultramafics and troctolites. Yttrium abundances in norite and gabbronorite OPX ranges from 12-4794 ppm, whereas Y abundances in OPX from the ultramafics and troctolites range from 0.14-6.50 ppm (Shearer and Papike, 2005). In contrast, OPX in the FANs typically has Y abundances less than 0.1 ppm.

Plagioclase

The major element composition of plagioclase in most Mg-suite lithologies is very limited (Fig. 3). Plagioclase in the ultramafic lithologies is found in low modal abundances (< 5 vol.%) and has very calcic compositions (An_{94-90}). Although plagioclase in the troctolites and spinel troctolites is far more abundant, it is similarly limited in major element composition (An_{97-92}). The norites (An_{95-83}) and gabbronorites (An_{96-63}) contain wider ranges in plagioclase composition; however the most calcic plagioclase overlaps in composition with the ultramafics, troctolites, and spinel troctolites (Papike et al., 1998; Shearer and Papike, 2005). Plagioclase in the Mg-suite has elevated abundances of Ba, Sr, and Y compared to other lunar lithologies (Fig. 6) such as FANs and mare basalts (Papike et al., 1997), most likely as a result of the KREEP-rich nature of their parental magmas. The REE abundances of plagioclase in Mg-suite lithologies have been measured by electron and ion microprobe by Papike et al. (1996), Shervais and

McGee (1998; 1999), and Shearer and Papike (2005). The REE patterns for the plagioclase from these studies are LREE-enriched with (La_N/Yb_N) > 10 with positive Eu anomalies. Inversion of these data to estimate parent melt compositions yielded extremely high REE concentrations similar to KREEP (Papike et al., 1996).

Spinels

Spinels (i.e., Mg-Al-bearing chromites, Mg-rich spinels), rather than Ti-rich oxides (i.e., ilmenite, ülvospinel, armalcolite), are the dominant oxides found in Mg-suite lithologies. Spinels in ultramafics, troctolites, norites, and gabbronorites are Mg-Al-chromite, whereas the spinel in spinel troctolites is a low-Cr Mg-rich (pink) spinel (Fig. 7). The major element compositions of chromites in the dunites and troctolites show significant overlap, with Cr# (molar Cr/[Cr+Al] *100) ranging from 72 to 61, and Mg# from 62 to 28 (e.g., Dymek et al., 1975; Haggerty, 1975; Shervais et al., 1984; Elardo et al., 2012). The chromite found in the norites is the most Fe- and Cr-rich in the Mg-suite, with Cr# ranging from 99 to 70, and Mg# ranging from 40 to 9 (e.g., Nehru et al., 1978; James and Flohr, 1983; Lindstrom et al., 1989). Chromites in the gabbronorites have lower Cr# than chromites in the norites, ranging from 67 to 53 (James and Flohr, 1983), and have Mg# of 23 to 31 that overlap with the Mg# of norites, but are lower than the Mg#'s of chromites in the ultramafics and troctolites (Fig. 7).

Phosphates

Phosphate minerals in the Mg-suite make up a very minor modal volume fraction of Mg-suite rocks (<1%). There are two phosphate minerals present in Mg-suite rocks: apatite [$Ca_5(PO_4)_3(F,Cl,OH)$] and RE-merrillite [$(Mg,Fe)_2(Ca_{18-x}(Y,REE)_x](Na_{2-x})(P,Si)_{14}O_{56}$ (Dymek et al., 1975; Lindstrom et al., 1984; Neal and Taylor, 1991; Jolliff et al., 1993; McCallum and Schwartz, 2001; Jolliff et al., 2006; McCubbin et al., 2011; Elardo et al., 2012). The earlier literature has many references to the mineral whitlockite $(Mg,Fe)_2Ca_{18}(PO_4)_{12}(PO_3OH)_2$ in lunar samples, but all of these reports represent misidentifications of the mineral RE-merrillite (Hughes et al., 2006; Jolliff et al., 2006; Hughes et al., 2008). The apatite in the Mg-suite ranges in grain shape from anhedral to euhedral and grain size from sub-micron up to approximately 300μm in the shortest direction (McCubbin et al., 2011). Mg-suite apatite is predominantly fluorapatite with chlorine abundances ranging from 0.7 to 1.8 wt.% and H_2O abundances ranging from below detection (>25 ppm) to 1800 ppm (Dymek et al., 1975; Jolliff et al., 1993; McCubbin et al., 2011; Barnes et al., 2014). The chlorine contents of Mg-suite apatite are elevated when compared to mare basalt and KREEP basalt apatite, and this chlorine enrichment seems to be an intrinsic geochemical feature of the lunar highlands (McCubbin et al., 2010a; b; McCubbin et al., 2011; Tartese et al., 2013; Barnes et al., 2014). In addition to elevated Cl abundances, Mg-suite apatites have isotopically heavier Cl and isotopically lighter H compared to mare basalts (Barnes et al., 2014; Greenwood et al. 2011; Sharp et al., 2010, 2013; Boyce et al., 2013). Despite their KREEP-rich nature, Mg-suite rocks have apatite with REE abundances that are generally lower than REE abundances in apatites from mare basalts (Fig. 8; Jolliff et al., 1993; McCubbin et al., 2010b; McCubbin et al., 2011; Tartese et al., 2013; Barnes et al., 2014; Elardo et al., 2014). On the surface, this observation seems counter-intuitive, but in many mare basalts apatite is the primary REE-hosting phase, whereas RE-merrillite is the primary REE-hosting phase in the Mg-suite rocks (McCubbin et al., 2011). In fact, RE-merrillite is present and more abundant than apatite in all Mg-suite samples that host phosphate minerals (Dymek et al., 1975; Jolliff et al., 1993; McCallum and Schwartz, 2001; Jolliff et al., 2006; McCubbin et al., 2011; Elardo et al., 2012). Although RE-merrillite is more abundant than apatite, fewer RE-merrillite analyses exist in the literature, and little is known about the variation in RE-merrillite composition within the Mg-suite. Of the analyses that are available, Mg-suite RE-merrillite consistently has an elevated Mg#, ranging from 85 to 98 (Neal et al., 1990; Neal and Taylor, 1991; Jolliff et al., 1993; Jolliff et al., 2006; Elardo et al., 2012; McCallum and Mathez, 1975), whereas RE-merrillite in mare basalts extend to much more Fe-rich compositions with a total Mg# ranging from 3 to 86 (Griffin et al., 1972; Frondel, 1975; Smith and Steele, 1976; Neal and Taylor, 1991; Zeigler et al., 2005; Jolliff et al., 2006; Elardo et al., 2014). Additional efforts to characterize RE-merrillite in lunar samples and its relationship to apatite is a clear topic requiring further development.

Geochemistry of the Mg-suite

Mg-suite rocks in the Apollo collection have the divergent chemical characteristics. Similar to primitive parental magma they have very Mg-rich mafic silicates (Fig. 1). Yet, much like many evolved parental magma, the Mg-suite has highly elevated abundances of incompatible trace elements (Fig. 9), but not alkali elements (e.g., Hess, 1984; Papike et al., 1994; 1996). Many of their other chemical characteristics further illustrate this chemical dichotomy.

The geochemistry of the Mg-suite rocks generally reflects their cumulate mineralogy. The bulk rock compositions generally have Mg# which range between 50 and 90 (Fig. 10) and normative plagioclase composition of An (molar Ca/[Ca+Na] x100) between 75 and 100. Olivine-rich lithologies generally have higher Mg#, but their normative plagioclase composition exhibits overlap between olivine-rich and olivine-poor lithologies. The Mg-suite generally have less than 0.1 wt. % K_2O. Compared to the ferroan anorthosites, the Mg-suite has lower Ti/Sm and lower Sc/Sm (Fig. 10a and b). These values are similar to other KREEP-rich magmatic- (KREEP basalts, monzogabbros) and impact-produced (e.g. fragmental breccias) lithologies.

The whole rock REE abundances of the Mg-suite exhibit a wide range of variations that include both positive and negative Eu anomalies, variable REE concentrations from 0.4 to 400 x chondrite La abundances, and variable $(La/Lu)_{Chondrite}$ (1.1 to 3.5) (Fig. 9). Some of these variations are likely the product of unrepresentative sampling during the analyses (e.g., variable amounts of trapped intercumulus melt) and the cumulate nature of the samples (e.g., the amount of cumulate plagioclase will control the Eu anomaly), and do not directly reflect the composition of the parental melt. Compared to FANs, the Mg-suite rocks are characteristically higher in REE and generally do not have large positive Eu anomalies. The olivine-bearing Mg-suite rocks from Apollo 17 generally have lower REE abundances than the olivine-poor varieties. The Apollo 14 olivine-rich rocks have higher REE abundances compared to similar Apollo 17 rocks. The norites generally have higher REE abundances than the Apollo 17 troctolites and most of the gabbronorites. Among the norites, there is a slight inverse correlation between Mg# and incompatible element abundances. Papike et al. (1998) observed that several of the gabbronorites have significantly different Ti/Sm (approaching chondritic values of 3600) than the other Mg-suite lithologies (Fig. 10). They concluded that this is evidence for the gabbronorites being distinctly different from other members of the Mg-suite (James and Flohr, 1983; Papike et al., 1998). Some caution should be taken from this conclusion as most of the gabbronorite lithologies from the Apollo collection are very small clasts (< 300 mg) and therefore may not represent representative compositions of the gabbronorites

Mineral/melt partition coefficients for the REEs have been used to calculate parental melt compositions for the Mg-suite rocks based on plagioclase and OPX REE contents (Papike et al. 1994; 1996; Shearer and Papike, 2005). Parental melts for the norites, gabbronorites, and Apollo 14 troctolites had similar REE abundances to high-K KREEP. However, Shearer and Papike

(2005) noted that plagioclase in many other troctolites are consistent with REE abundances similar to low-Ti mare basalts.

The Th content of the Mg-suite is elevated compared to the FANs and many of the mare basalts (Fig. 10c), however they are significantly lower than the KREEP basalts or the quartz-monzodiorites (QMD). The difference between the Mg-suite rocks and KREEP basalts and QMD should not be so surprising in that the former represent the accumulation of low Th mineral phases. Using the partitioning behavior of Th between mafic silicates (pyroxene, olivine) and basaltic melt (Hagerty et al., 2006), the calculated Th content of the melts parental to the Mg-suite are similar to the KREEP basalts.

Elements that are more compatible than the REE and Th in basaltic systems also illustrate an interesting contrast between the Mg-suite and mare basalts (Hagerty et al., 2006). Although the Mg# for the mafic silicates and bulk rock of the Mg-suite is higher than the mare basalts, Cr, Ni, and Co concentrations are generally lower in the Mg-suite rocks (Fig. 10d, e, f). The differences in these elements between the more primitive mare basalts (pyroclastic glasses) and the Mg-suite lithologies have been interpreted to indicate that parental magmas of this two magmatic suites were derived from significantly different lunar mantle sources (Shearer and Papike, 2005; Longhi et al., 2010; Elardo et al., 2012) These three elements in the Mg-suite overlap with KREEP basalts and QMD lithologies.

Candidate Mg-suite samples from the lunar meteorite collection

There are a number of lithologies found within lunar meteorites as clasts within breccias which have some chemical characteristics similar to Mg-suite lithologies collected during the Apollo missions. However, to date, there are no whole-rock samples in the lunar meteorite collection that have been convincingly argued to be members of the Mg-suite (Korotev, 2005).

Some of the uncertainty in classifying lithologies in lunar meteorites as Mg-suite lithologies stems from uncertainty in the petrogenesis of the Mg-suite itself, e.g., is KREEP involvement a defining characteristic of all Mg-suite parental magmas? Additionally, the provenance and pristinity of clasts in lunar brecciated meteorites is often difficult to assess, as mixing of lithologies due to impacts and thermal annealing have been widespread processes in the lunar crust (although these processes equally affect breccia clasts in returned samples). Below, we discuss a few examples of lithologies from lunar meteorites that we consider candidates for inclusion in the highlands Mg-suite.

Dhofar 489 – Magnesian Anorthosite and Spinel Troctolite Clasts

The brecciated feldspathic lunar meteorite Dhofar 489 contains clasts of both magnesian anorthosite and spinel troctolite that have geochemical characteristics similar to the Mg-suite (Takeda et al., 2006). Both lithologies have plagioclase with a composition of An_{96}. The spinel troctolite (4.1 x 1.3 mm in size) has olivine with Mg# of ~82-85 and the magnesian anorthosite (3 x 1.3 mm in size) has olivine with Mg# of ~75-79. The mineral major element compositions in the spinel troctolite are consistent with it being part of the Mg-suite, if it can be considered a pristine crustal lithology, which is debatable (Takeda et al., 2006). The magnesian anorthosite clast plots in the gap between the Mg-suite and ferroan anorthosite fields in Fig. 1. Many lunar granulites and other polymict samples plot within this gap; however such lithologies have been argued to represent impact-derived compositions (e.g., Lindstrom and Lindstrom, 1986), and this may be the case for magnesian anorthosites as well (Treiman et al., 2010). Dhofar 489 also has an age contemporaneous with Mg-suite magmatism. Ar-Ar dating indicates the breccia formed at ~4.23 Ga (Takeda et al., 2006), suggesting the spinel troctolite and magnesian anorthosite clasts, if igneous in origin, formed during the time numerous Mg-suite magmas were intruding the lunar crust. Furthermore, Dhofar 489 has some of the lowest abundances of incompatible trace elements (i.e., Th, REEs) among lunar feldspathic breccias, indicating it may have been derived from an area away from the Procellarum KREEP Terrane and possibly from the far side highlands (Takeda et al., 2006), although it should be noted that lighologies with low abundances of incompatible trace elements are also found within the Procellarum KREEP Terrane. If the spinel troctolite and magnesian anorthosite clasts in Dhohar 489 can be linked to the same magmatic events that produced the Mg-suite, it would imply that KREEP is the passenger rather than the driver of Mg-suite magmatism, and is likely a global magmatic event, rather than being confined to the Procellarum KREEP Terrane.

ALHA 81005 – Anorthositic Spinel Troctolite Clast

A single 350 x 150 μm clast containing 49% plagioclase, 30% spinel, 15% olivine, and 6% pyroxene in lunar meteorite ALHA 81005,9 was described by Gross and Treiman (2011). The spinel in this clast is an Mg-Al-rich spinel that is very similar in composition (Mg# of 65, Cr# of 6) to other Mg-suite spinel troctolites collected during the Apollo missions (e.g., Fig. 7). Olivine and pyroxene in the clast have Mg# of 75 and 78, respectively, whereas plagioclase is very calcic in composition (An 96). These mafic mineral and plagioclase compositions indicate that this anorthositic spinel troctolite clast has mineral compositions consistent with the Mg-suite (Fig. 1; Warner et al., 1976a), although it would be the most Fe-rich spinel troctolite yet discovered. However, the use of the Mg# vs. An# plot is intended for pristine lithologies from the lunar crust and the anorthositic spinel troctolite clast in ALHA 81005 may not represent such a lithology. Gross and Treiman (2011) suggested that the clast might originate as a crystallization product of an impact melt sheet or as the result of the interaction of a picritic magma with the anorthositic crust. Additional age and incompatible trace element data would be useful in assessing the potential relationship of this clast to the Mg-suite.

MIL 090034/70/75 and MIL 090036 – Troctolite and Gabbro Clasts

The samples MIL 090034/70/75 are three paired anorthositic regolith breccias and MIL 090036 is a similar breccia (not paired with the former 3 samples), all of which contain various lithic clasts and mineral fragments that have been suggested to be derived from Mg-suite lithologies (Liu et al., 2011). The clasts documented by Liu et al. (2011) range in size from ~100 µm x ~75 µm up to ~600 µm x 400 µm. Some clasts were described as troctolites and gabbros (Liu et al., 2011); however the small size of the clasts and limited number of mineral grains suggest they may not be representative of their parental rock. Nevertheless, olivine and pyroxene grains in the clasts and in the matrix have very Mg-rich compositions indicative of Mg-suite lithologies. Olivines range in composition from Fo_{91-59}, with the Fe-rich end of the compositional range sometimes limited to rims on Mg-rich grains. Pyroxene compositions reach $En_{87}Wo_4$ at the Mg-rich end of the compositional range; however compositions as Fe-rich as $En_{29}Wo_6$ are also observed. The Mg-rich olivines and pyroxenes in clasts in MIL 090034/70/75 and MIL 090036 have compositions that overlap the most primitive Mg-suite lithologies such as the Apollo 17 troctolites and dunites. Plagioclase compositions, including those found in association with Mg-rich mafic silicates, range from $An_{97-91.}$ On a plot of the Mg# of mafic minerals vs. An in plagioclase, some lithologies in MIL 090034/70/75 and MIL 090036 would plot in the Mg-suite field (Fig. 1); however, the question of whether these clasts represent pristine igneous lithologies or rather are mixtures of different lithologies juxtaposed by impact processes/melting is paramount. The bulk rock chemistry of MIL 090034/70/75 and MIL 090036 indicate a significant KREEP component (Liu et al., 2011; Shirai et al., 2012), which lends some degree of credence to the argument that the Mg-rich lithologies in these meteorites are derived from Mg-suite lithologies. However, additional mineral trace element analyses are needed to determine if the potential Mg-suite clasts themselves include a KREEP component.

Post-crystallization alteration of Mg-suite rocks

Following emplacement and crystallization of Mg-suite magmas, the cumulate mineralogy was subjected to varying degrees of subsolidus reequilibration, reheating and recrystallization due to impact, and post-crystallization alteration due to mobility of elements in the lunar crust. Several of these alteration features are illustrated below.

Chromite symplectites

Dunite 72415-72418 and troctolite 76535 contain chromite symplectites (Fig. 11), or wormy intergrowths of chromite and two pyroxenes (Gooley et al., 1974; Albee et al., 1975; Bell et al., 1975; Dymek et al., 1975; McCallum and Schwartz, 2001; Elardo et al., 2012). Of the two samples, 76535 best preserves original textural relations between the symplectites and cumulus minerals; 72415-72418 has been cataclasized and this has partially obscured textural relationships. Albee et al. (1975) and Dymek et al. (1975) favored a model in which the symplectites are the product of the crystallization of trapped interstitial melt, a process shown to produce similar textures in terrestrial layered mafic intrusions (e.g., Holness et al., 2011). Gooley et al. (1974), Bell et al. (1975), and McCallum and Schwartz (2001) suggested that the symplectites formed as a product of the high-pressure breakdown reaction of olivine and plagioclase to OPX, CPX, and spinel (i.e., Kushiro and Yoder, 1966) where the source of Cr was either pre-existing cumulus chromite or the diffusion of Cr out of olivine. However, Elardo et al. (2012) conducted a detailed petrologic study of the symplectites, cumulus minerals, and melt inclusions and concluded that the previously proposed symplectite formation mechanisms were inconsistent with textural relationships and mineral chemistry. Melt inclusion pyroxenes and cumulus olivine contain levels of Cr that are inconsistent with chromite saturation in the parental magma, and the sparse occurrence of symplectites and the lack of evidence for a Cr^{2+} oxidation reaction are inconsistent with the remobilization of cumulus chromite and/or diffusion of Cr out of olivine. Elardo et al. (2012) proposed a model in which the symplectites in 76535 are the product of infiltration metasomatism by exogenous, chromite-saturated melt. Elardo et al. (2012) also suggested that infiltration from a melt may provide enough heat to reset or delay closure of radioisotope chronometers, resulting in a younger date for 76535 than its true crystallization age.

Sulfide-pyroxene intergrowths

Elardo et al. (2012) documented veins consisting of CPX and sub-micron grains of troilite in troctolite 76535 (Fig. 12). The veining is not pervasive throughout the rock; it is primarily confined to intercumulus OPX grains and is typically not found within olivine and plagioclase. The boundaries between the CPX-troilite veins and intercumulus OPX are irregular, indicating a reaction texture. Elardo et al. (2012) suggested two possible formation models for the CPX-troilite veins in 76535. First, they could be direct crystallization products of the metasomatic melt responsible for crystallizing chromite in symplectite assemblages. Alternatively, the veins could be the result of S-rich vapor streaming in the lunar crust. Shearer et al. (2012b) invoked S-rich vapor streaming to explain sulfide replacement textures in olivine in other highlands lithologies, and Elardo et al. (2012) suggested that a similar process may have acted on 76535, perhaps after its excavation from the lower crust during a period of slow cooling in an ejecta blanket (McCallum et al., 2006).

Troilite replacement of olivine

Numerous studies have identified the replacement of mafic silicates with troilite in both magnesian-suite and FAN suite lithologies (Roedder and Weiblen, 1974; Norman, 1981; Lindstrom and Salpas, 1983; Norman et al., 1995; Shearer et al., 2012a,b). In the Mg-suite clasts such as the olivine-rich gabbronorite in 67915, low-Ca pyroxene-troilite intergrowths occur along the perimeter of the olivine and along fractures in the olivine. The troilite in the intergrowths is wormy in texture, and the long dimension length of the troilite ranges from < 1μm to 10μm (Fig. 13). These textural relationships (i.e. morphology of pseudomorphs, intergrowths of pyroxene-troilite) indicate that the reaction that is represented is that of olivine being replaced by troilite + low-Ca pyroxene. In this reaction, the fayalite component in the olivine reacts with sulfur to produce troilite via the reaction:

$$\mathbf{2\ Fe_2SiO_4 + S_2 = 2\ FeSiO_3 + 2\ FeS + O_2.} \qquad \mathbf{(1)}$$

In addition to the occurrences of troilite as veins and intergrowths with pyroxene, "wormy" shaped troilite will rarely occur adjacent to composite Fe-metal-oxide grains. The sulfide veining and replacement features are restricted to individual clasts and do not cut across the matrix surrounding the clasts, and thus predate the breccia-forming event.

This process occurs in the relatively shallow lunar crust on a scale that involves vapor interaction with multiple plutonic lithologies of various ages and compositions. These reactions occur at distinct conditions of f_{S2}, f_{O2}, and temperature. The reacting vapor is S-rich, and low in H. The reduction of oxides in the clasts was not a product of H-streaming as has been suggested for similar textures in lunar rocks (e.g. Sharp et al. 2013; Taylor et al. 2004), but more likely related to "S-streaming". Important S species in this vapor were COS, S_2 and CS_2. These vapors had the capability to transport other elements such as Fe and minor chalcophile-siderophile elements. However, a proportion of the minor elements making up the troilite (Fe, Ni, Co) did come directly from the olivine being replaced. The heat source driving the transport of elements is closely tied to the emplacement of magmas into the shallow lunar crust. These magmas could be related to episodes of either Mg-suite magmatism or the earliest stages of mare magmatism. These intrusions were probably the source for the S. The process that drove the derivation of the S-rich volatiles from these intrusions was also instrumental in fractionating the isotopic composition of S from 0‰ in the magmas to -5‰ in the vapor phase. This fractionation was not controlled by the proportions of SO_2^{-2} to H_2S in the vapor phase, but more likely COS, S_2 and CS_2 species (Shearer et al., 2012b; McCubbin et al. This Volume).

Phosphate veins

Apatite veins cut across olivine grains in dunites collected from the Apollo 17 site. This veining has not been examined in any substantial detail. The veins extend along fractures in the olivine and are 100s of micrometers in length and up to 10 micrometers in width (Fig. 14). The apatite in the veins have 0.2 to 0.6 wt.% Cl. The textures suggest that the apatite was mobilized following extensive episodes of brecciation experienced by the dunite. It is uncertain if the apatite represents mobilized apatite from the mesostasis in the original dunite cumulate or transport of an apatite component from outside the cumulate horizon.

Depth of Emplacement for Mg-suite rocks

The estimation of depth of emplacement for the Mg-suite rocks is somewhat difficult and subjected to substantial error because of the low pressure gradient (~0.05 kbar/km) in the lunar crust and the scarcity of minerals whose compositions, textures, and stabilities are sensitive to low-pressure regimes of the lunar crust. Given these difficulties, the thermobarometry calculations that have been made suggest that the Mg-suite plutons have been emplaced in numerous crustal environments. Many of these temperatures and pressures reflect subsolidus conditions tied to recrystallization or pyroxene exsolution textures. For troctolite 76535, McCallum and Schwartz (2001) calculated a recrystallization temperature and pressure for OPX + CPX + Cr-spinel symplectites (Fig. 11) at the boundaries between primary magmatic olivine and plagioclase of about 800-900°C and 220-250 MPa. This is equivalent to a depth of 42-50 km. Cataclastic spinel ± cordierite troctolite clasts were identified in Apollo 15 and 17 breccias (e.g., Fig. 2h) by Dymek et al. (1976), Herzberg (1978), and Marvin et al. (1989). Herzberg (1978) defined the cordierite to spinel boundary as representing the univariant equilibrium forsterite+cordierite ↔ enstatite+spinel. Baker and Herzberg (1980) concluded that the spinel-bearing troctolites reflect emplacement (and reequilibration) depths of between 12 to 32 km. McCallum and Schwartz (2001) reevaluated the temperature and depth of formation for the spinel-bearing troctolite assemblages and calculated equilibrium temperatures of 600-900°C at minimum pressures of 100-200MPa (20-40 km). Although these calculations imply an emplacement depth for the Mg-suite in the lower lunar crust, there are other observations that suggest the Mg-suite magmas were also emplaced in shallower crustal regimes (McCallum and O'Brien, 1996; McCallum, et al., 2006; Shearer et al., 2012a,b).

On the foundation of numerous terrestrial observations, McCallum and co-workers (McCallum and O'Brien, 1996; McCallum, et al., 2006) developed an approach to quantitatively determine the depth of origin for lunar crustal rocks by measuring the width, spacing, crystallographic orientation, structural state, and composition of exsolution lamellae in pyroxenes (Fig. 15). These exsolution characteristics can be exploited to calculate cooling rates that can then be used to calculate a depth of burial assuming specific models for thermal conductivities and lunar crustal cooling. Using pyroxenes from Apollo 16 and 17 breccias, McCallum and O'Brien (1996) were able to calculate depth of emplacement for a series of lunar plutonic rocks. For gabbronorite clasts in breccia 76255, they calculated pyroxene exsolution in host-augite and host-pigeonite exsolved between 1130 and 800°C at a depth of approximately 0.5 km. They calculated similar conditions for the emplacement of an alkali suite sodic ferrogabbro clast from the Apollo 16 site (67915). Using a similar approach, Shearer et al. (2012b) calculated a crystallization depth of an olivine-rich gabbronorite clast in 67915 (referred to as a ferroperidotite by Roedder and Weiblen, 1974) of less than 1 km (Fig. 15). On the basis of observed Fe-Mg gradients in olivine and CaO content of olivine, Ryder (1992) concluded that the Apollo 17 dunite (72415) was emplaced at shallow, hypabyssal environments in the lunar crust perhaps at depths less than 1 km. This is curious as chromite symplectites similar to those observed in troctolite 76535 have also been identified in this dunite. Perhaps a reasonable interpretation of these apparent divergent conclusions, is that both the Mg-suite magma was emplaced and the symplectites formed within the deep lunar crust (Elardo et al., 2012). The Fe-Mg gradients were superimposed on the olivine at much shallower depths following excavation and rapid cooling.

GLOBAL DISTRIBUTION OF THE MG-SUITE

Given that the Apollo and Luna sample sites are all located near the Moon's equator on the nearside (Fig. 16), and that lunar meteorites are derived from unknown locales, we are forced to rely on global remote sensing datasets in order to infer the distribution of the Mg-suite. Fortunately with the improvement over nearly two decades worth of global lunar remote sensing data, it is possible to assess the distribution of surface exposures of lithologies that could be interpreted as outcrops of Mg-suite rocks. Based on the understanding of Apollo samples (see above sections), remotely identifying possible Mg-suite materials is accomplished using near-infrared (NIR) spectral data. Because of the sensitivity of the NIR wavelength range to compositional variability within olivine- and pyroxene-bearing mineral assemblages (Burns, 1970; Adams, 1974, 1975; Pieters, 1993), it is possible to identify possible exposures of Mg-suite material on the lunar surface. Near-infrared spectroscopy is a powerful tool in delineating olivine and pyroxene compositions. A number of approaches enable the identification of specific mineral assemblages on the surface, one of the most powerful being the Modified Gaussian Model (MGM; Sunshine et al., 1990). The MGM is used to characterize continuum-removed spectra of the Moon that are then compared to well-characterized laboratory spectra of lunar and synthetic mafic minerals of known composition, including the full diversity of pyroxene and olivine compositions (e.g., Klima et al., 2007, 2011a,b; Isaacson and Pieters, 2010). This detailed characterization enables a remote assessment of the surface mineralogy and an estimation of its composition (Klima et al., 2011b; Issacson et al., 2011) and in turn the identification of surfaces that are consistent with Mg-suite materials. Additionally, with ~0.5° per pixel (~15km per pixel) thorium data from the Lunar Prospector mission (Lawrence et al., 2003), the association between possible Mg-suite surfaces (as inferred by NIR spectra) with potential KREEP-bearing materials can often be made (e.g., Klima et al., 2011a,b).

Recently, using data from the Moon Mineralogy Mapper (M^3) -- a high spatial and spectral resolution imaging spectrometer on India's Chandrayaan-1 (Green et al., 2011) was used to characterize the lunar-wide distribution of low-Ca pyroxenes (Klima et al., 2011b), olivine (Isaacson et al., 2011; Mustard et al., 2011), and Mg-spinel (Pieters et al., 2011, 2014; Dhingra et al., 2011; Lal et al., 2012). The high spectral resolution of the M^3 instrument (20–40 nm depending on the wavelength range, see Green et al., 2011) allows for detailed MGM analysis with uncertainties in band centers of +/- 10nm for the 1μm absorption feature and +/- 20-50 nm for the 2μm band. Given the systematic spectral variability in low-Ca pyroxenes changes on the scale of 40 nm at the 1μm absorption feature and 270 nm at the 2μm absorption feature, calibrated M^3 data is well suited to differentiate pyroxene compositions (Klima et al., 2011b). These measurement uncertainties still allow for broad Mg# classifications but not a direct determination of a specific Mg#. Despite operational difficulties experienced by Chandryaan-1, M^3 was able to obtain coverage of nearly 95% of the lunar surface at spatial resolutions between 140 and 280 meters, depending on the altitude of the spacecraft (Boardman et al., 2011). Contiguous areas lacking any M^3 coverage are limited to narrow longitude swaths centered at 21º, 90º, 151º, 193º, and 234º (see Boardman et al., 2011 Figure 5). Data from the Spectral Profiler on the Japanese Kaguya mission have been used to identify additional exposures of pyroxene and olivine-bearing compositions (Matsunaga et al., 2008; Yamamoto et al., 2010; 2011) and Fe- and Cr-spinel (Yamamoto et al., 2013).

These remote observations have revealed, at the ~100s meters scale, small exposures of mineral assemblages consistent with the Mg-suite (meaning low-Ca pyroxenes). Although these remote detections of the Mg-suite are typically based on identifications of low-Ca pyroxene (Klima et al., 2011b), there are excellent connections between what we measure from orbit and in the lab that lend confidence that the measurements are likely of the Mg-suite and not other lithologies such as ferroan anorthosite (Cahill et al., 2009). Klima et al. (2011b) described the distribution of low-Ca pyroxenes in two large regions, eastern South Pole-Aitken Basin (SPA) and south of Mare Frigoris (coincident with the Northern Imbrium Noritic region characterized by Isaacson and Pieters, 2009). Within eastern SPA, nine exposures of low-Ca pyroxenes were identified, of those are two that have spectra apparently related to Mg# >75 and are candidates for exposures of the Mg-suite (Klima et al., 2011b). These two exposures are located near the inner ring of the Apollo Basin (Fig. 16, green squares), the location of some of the thinnest crust on the Moon and possible location of lower-crust/upper mantle material (Ishihara et al., 2009; Petro et al., 2010; Klima et al., 2011b; Wieczorek et al., 2012). On the nearside, Klima et al. (2011b) identified four sites south of Mare Frigoris along the northern rim of the Imbium Basin with inferred Mg# between 80-90 (Fig. 15, blue squares) Near these low-Ca pyroxenes, Yamamoto et al. (2010), using data from Kaguya's Spectral Profiler, identified olivine-rich exposures indicating possible diversity in the Mg-suite materials in the region. The survey of Klima et al. (2011b) broadly agrees with the findings of Lucey and Cahill (2009), which used Clementine NIR data to show possible Mg-suite exposures across SPA and surrounding the Imbrium Basin as well as exposures surrounding Mare Australe, Crisum, and Procellarum.

On smaller scales, outcrops of potential Mg-suite materials have been identified in three distinct areas, two on the nearside and one on the far side. One, located in the central peak of Bullialdus Crater (Fig. 16, red square) has an inferred Mg# > 75, is located within the Procellarum KREEP Terrane (Jolliff et al., 2000), and is associated with a localized Thorium enhancement on the order of 16.5 ppm +/- 2.5 ppm (Klima et al., 2013). Dhingra et al. (2011) identified a distinct Mg-suite mineralogy, possibly a pink spinel anorthosite within the central peak of Theophilus Crater (Fig. 16). The Mg-spinel exposures are surrounded by anorthositic material, with trace exposures of olivine and pyroxene nearby within the central peaks. Similarly, a group of small exposures of mafic and Mg-spinel mineral assemblages were identified on the rim of the Moscoviense Basin (Fig. 16). The small, distinct exposures of low-Ca pyroxene, olivine, and Mg-spinel rich exposures (Pieters et al., 2011) are slightly more Fe-rich than the exposures described by Klima et al. (2011b). Both of these Mg-spinels occur in areas that expose deep-seated materials. In the case of Theophilus, the crater sits on the rim of the Nectaris Basin and the material along the inner ring of Moscoviense is near very thin crust (Ishihara et al., 2009;

Wieczorek et al., 2012), possibly the result of two large and overlapping impact craters (Ishihara et al., 2011).

Using Clementine UVVIS and NIR data, Cahill et al. (2009) evaluated the compositions of central peaks of 55 craters across the lunar surface. Following on the similar study using just the UVVIS data (Tompkins and Pieters, 1999), they observed a range of inferred compositions with Mg# > 78 for a number of central peaks, including pyroxenites, spinel-troctolites, and anorthositic troctolites. The host craters are observed across the entire Moon and are, as the work of Tompkins and Pieters (1999) and Klima et al. (2011b) showed, not restricted to a single region of the Moon. Interestingly, there is a suggestion that regions containing mafic minerals with the highest Mg#'s may be restricted to areas where the crust is ~40 km thick (Cahill et al., 2009), a relationship that was later noted and developed by Ohtake et al. (2012).

Although these surveys reveal that there are clusters of Mg-suite material in the eastern SPA and the northern rim of the Imbrium Basin, possible exposures of Mg-suite material are found, in small exposures, across the lunar surface. There clearly needs to be additional, detailed analysis of crater central peaks, basin rings, and other possible areas that sample or concentrate crustal lithologies to identify additional potential Mg-suite exposures. For example, preliminary work by Petro and Klima (2013) has shown that the Sculptured Hills near the Apollo 17 landing site may contain a range of Mg-suite lithologies. A more extensive survey of crater peaks and basin rings integrating new data sets will also help clarify the distribution of the Mg-suite vertically in the crustal column. Based on the distribution described above, it is apparent that exposures of Mg-suite material may be restricted to exposures of originally deep-seated material (>40 km) (e.g., Cahill et al., 2009). A more recent global survey of the character and distribution of Mg-spinel anorthosite by Pieters et al. (2014, these volumes) strongly support the deep-seated nature of anorthositic Mg-rich lithologies.

Global Variation of Thorium within the Mg-suite

Whereas the visible and NIR remote sensing approaches described above reveal possible Mg-suite assemblages, other remote sensing datasets reveal their association with possible KREEP-bearing lithologies. Using the Lunar Prospector gamma ray data, a potential, broad connection between the Mg-suite and KREEP can be drawn. As described above, some exposures of possible Mg-suite material, such as at the central peak of Bullialdus or the northern rim of the Imbrium Basin, are associated with enhancements of Th (and by association KREEP) (Lawrence et al., 2003; Klima et al., 2011). In these cases the abundance of Th is greater than ~8 ppm (Lawrence et al., 2003), with the Bullialdus central peak having as much as 16.5 ppm (Klima et al., 2011; 2013). However, given the broad distribution of possible Mg-suite materials, there are some areas, such as the exposures within the Moscoviense Basin (Pieters et al., 2011) and Theophilus (Dhingra et al., 2011) that have no apparent Th enhancements. It is important to note, especially at the very small scale of the exposures of Mg-suite material in Moscoviense, that the Lunar Prospector data may not have sufficient resolution as the unique compositions are on the 100's of meters scale while the resolution of the Th data is on the scale of ~10s kilometers. But as Klima et al. (2011) and Cahill et al. (2009) showed, there are possible Mg-suite materials within SPA. The floor of SPA has a moderate enhancement in Th relative to the surrounding PKT (Jolliff et al., 2000), not including the two small area enhancements that are not associated with Mg-suite materials (Lawrence et al., 2003). It appears, based solely on the available remote sensing data, that there is no direct relationship between KREEP and the Mg-suite (or Mg-suite mineral assemblages).

Relationship between lunar terranes and Mg-suite distribution and composition

Using remotely sensed measurements of Th and estimated of FeO, Jolliff et al. (2000) defined three compositional terranes: the Procellarum KREEP Terrane (PKT), the Feldspathic Highlands Terrane, and the South Pole-Aitken Terrane (SPAT). Remote sensing data suggests that there are exposures of candidate Mg-suite material within each terrane. In the global survey by Lucey and Cahill (2009), exposures of the Mg-suite are inferred in both the SPAT and the PKT, while the detailed surveys (Tompkins and Pieters, 1999; Cahill et al.,2009; Klima et al., 2011b; Yamamoto et al., 2010; Pieters et al., 2014) reveal small exposures in all three terranes. These remote sensing surveys demonstrate that there is compositional variability across the exposures that span the range of Mg-suite compositions, regardless of the terrane (Dhingra et al., 2011).

Tompkins and Pieters (1999) and Cahill et al. (2009) identified compositions ranging from gabbros to norites to troctolitic anorthosites in the central peaks of selected craters. In addition to lunar-wide diversity, Klima et al. (2011b) identifies a regional diversity, for example the norites south of Mare Frigoris, within the PKT, span a range of Mg# from 80-90. However, the exposures located in SPA span a similar range of Mg#, albeit without the Th enhancement associated with the SPAT. The two exposures of Mg-spinel described here occur within the Feldspathic Highlands Terrane, however the detailed criteria and global assessment of Pieters et al. (2014) clearly indicates that those too are found in the three major compositional terranes. Based on the distribution of candidate Mg-suite materials it appears that there may be no direct relationship between compositional terrane and the formation of the Mg-suite.

Layering within the lunar highlands and Mg-suite

As noted above, there are no direct samples or remote observations that indicate layering within the Mg-suite (Papike et al., 1999). Most of the supposition is tied to the family of rocks making up the Mg-suite (e.g. dunites, troctolites, norites, and gabbronorites) and their relationships to experimental studies. More recently, Lunar Reconnaissance Orbiter and M^3 observations have been interpreted to indicate compositional and mineralogical variation on the outcrop-scale within the lunar highlands. For example, Cheek and Pieters (2012) were able to distinguish between anorthosites with high plagioclase content (100%) and anorthosites with small abundances of pyroxene (6% pyroxene). They suggested the possibly that hundred-meter scale variation in the mineralogy of the anorthositic bedrock occurs in the Tsiolkovsky central peak. The Mg-rich lithologies seen at both Moscoviense and Theophilus (Fig. 15) occur as discrete small areas, all within a highly feldspathic matrix (Pieters et al., 2011, 2014; Dhingra et al., 2011; Lal, 2012). Further, at the best scale currently available (~140 m), no two mafic crustal lithologies discussed here have yet been detected in a contiguous manner to suggest layering.

Global distribution of the Mg-suite as implied by lunar meteorites

As lunar meteorites are a random sampling of the lunar surface, they offer an alternative perspective concerning the global distribution of Mg-suite (Korotev et al., 2003, 2009; Korotev, 2005). The feldspathic lunar meteorites indicate the lunar highlands away from the PKT have a greater Mg/Fe than the crust at the Apollo landing sites, but show little evidence for Mg-suite lithologies. Feldspathic lunar meteorites with FeO and Th abundances indicating they are sourced from areas of the feldspathic lunar highlands away from the PKT do not exhibit chemical trends consistent with mixing involving an Mg-suite like end-member, nor do they contain lithologic clasts that are demonstrably from Mg-suite precursors (Korotev et al., 2003; Korotev, 2005). As discussed above, there are some clasts in brecciated lunar meteorites that we consider candidates for inclusion in the Mg-suite, but very often clasts in brecciated meteorites are themselves brecciated or possibly the crystallization products of impact melts (e.g., Korotev, 2005; Korotev et al. 2009). Therefore, one interpretation of the current collection of feldspathic lunar meteorites is that it contradicts remote sensing data and suggests the Mg-suite is a product of magmatic processes restricted to the PKT, and was not a global magmatic event (Korotev, 2005). A similar interpretation could also be reached concerning the abundance of high-Ti mare basalts and their general absence in the lunar meteoritecollection.

Part of this interpretive ambiguity between the meteorites and orbital data is that Apollo Mg-suite samples exhibit the characteristics of KREEP-rich parental magmas. As stated above, and discussed further below, the question of whether the Mg-suite is meticulously defined by a KREEP component is an ongoing topic of debate that has implications for lunar crust building and magmatism on a global scale. This further leads to the non-trivial issue of the ability to recognize a KREEP-free Mg-suite lithology in a lunar meteorite when the known examples of the Mg-suite from the Apollo collection are characteristically KREEPy. Further study of brecciated lunar meteorites, particularly the clasts contained within them, will undoubted prove a fruitful area for future research.

CHRONOLOGY OF THE MG-SUITE

Complexities of establishing Mg-suite chronology.

A generalized chronology for events on the Moon is presented in Figure 17 (after Spudis, 1998). In a general sense, the Mg-suite is emplaced into the crust soon after the crystallization of the LMO and prior to many episodes of lunar magmatism. This generalized chronology for lunar events agrees with the “geochemical chronology” of lunar differentiation (very low-Ti mare basalt source $\Rightarrow$ FANs $\Rightarrow$ high-Ti basalt source $\Rightarrow$ KREEP source) and impact history. However, the specific chronology of the Mg-suite and its age relationship to other highlands lithologies are obscured to various degrees by the effects of the late heavy bombardment (e.g. Alibert et al., 1994; Borg et al., 1999; Borg et al., 2011), and the prolonged and potentially complex subsolidus cooling history they experienced at both the depth of emplacement and in ejecta blankets (e.g., McCallum et al., 2006). The most common "whole-rock" chronometers used to date crystallization of highlands rocks are Rb-Sr, Sm-Nd, and U-Pb. These chronometers not only provide crystallization ages of individual samples, but are the basis for model ages determined on suites of samples. With one exception (^{146}Sm-^{142}Nd; half-life 1.03 x 10^8 years) the short-lived chronometers that have improved the age estimates for meteorite differentiation cannot be applied to lunar rocks because even the oldest lunar rocks are too young to have formed when ^{26}Al (half-life 7.17 x 10^5 years), ^{53}Mn (half-life 3.7 x 10^6 years), or ^{182}Hf (half-life 8.90 x 10^6 years) were extant. There is only limited variation in ^{142}Nd in lunar samples indicating that this short-lived isotopic system was almost extinct at the time the Moon formed and differentiated. Additionally, U-Pb geochronology derived from individual zircon and baddeleyite grains from highlands lithologies (Apollo and lunar meteorite samples) have been explored using secondary ion mass spectrometry ion microprobe analyses.

Borg et al. (2013) identified several reasons for the ambiguity in the interpretation of various chronometers and established criteria for evaluating the reliability of ages of highlands rocks. Reasons for this ambiguity are numerous and include: (1) disturbance of the isotopic systematics of lunar samples by secondary processes associated with impacts, (2) the analytical difficulty associated with dating mono- or bi-mineralic samples that have low abundances of the parent isotope, (3) the large uncertainties in age determinations that obscure potential temporal differences among lunar rock suites, and (4) inter-laboratory differences in measurement techniques and age calculations that make age comparisons difficult. Experimental investigations of shocked and heated lunar samples demonstrate that Sm-Nd is the least mobile during shock metamorphism and therefore is the most reliable recorder of igneous events (Gaffney et al., 2011). In contrast, Ar-Ar, Rb-Sr, U-Pb, and Pb-Pb systems are more easily disturbed, accounting for the wide range of ages reported for highlands samples. Despite the perception that the Sm-Nd system is resistant to disturbance by shock processes, replicate Sm-Nd ages on single samples usually are also discordant. For example, the range of published Sm-Nd ages determined on FAN 60025 is 4.359 to 4.440 Ga (Carlson and Lugmair, 1981a,b; 1988; Borg et al., 2011).

Ages of the Mg-suite lithologies.

There are a number of ages determined for Mg-suite rocks. As a whole these data provide a somewhat shadowy picture about the emplacement history of the Mg-suite. Summaries of ages and interpretations have been compiled and summarized by Nyquist and Shih (1992), Nyquist et al. (2001), Snyder et al. (1995, 2000), Papike et al. (1998), Shearer and Papike (2005), Shearer et al. (2006), and Borg et al. (2013). A brief summary of these data are shown in Figure 18 and discussed in the context of lithology in the following text.

Only one of the ultramafic lithologies making up the Mg-suite has been dated, due to the small mass of most of the ultramafic samples. The largest ultramafic sample, the dunite represented by samples 72415-72418 has been dated using Rb-Sr, Pb-Pb, and U-Pb. Papanastassiou and Wasserburg (1975) defined an ancient Rb-Sr age of 4.55 ±0.10 Ga that they interpreted as a crystallization age. The U-Pb age is 4.52 ±0.06 Ga and within analytical uncertainty is concordant with the Rb-Sr age (Premo and Tatsumoto, 1992b). The Pb-Pb age is within the uncertainty of these other ages given the large uncertainty of 4.37±0.23 Ga (Premo and Tatsumoto, 1992b).

Radiometric ages for the troctolites are few in number, although a significant number of K-Ar, Rb-Sr, Sm-Nd, and U-Th-Pb ages have been published for 76535. Although the Rb-Sr data produced by Papanastassiou and Wasserburg (1976) have been interpreted as suggesting an ancient crystallization age of 4.61 ±0.07 Ga, most other systems point to a younger age (Premo and Tatsumoto, 1992a; Papike et al., 1998). Premo and Tatsumoto (1992a) determined a U-Pb age of 4.236 ±0.015 Ga. K-Ar ages range from 4.16 to 4.27 (Husain and Schaeffer, 1975; Huneke and Wasserburg, 1975; Bogard et al., 1975), whereas Hinthorne et al. (1975) determined a Pb-Pb age of 4.375 ± 0.002 Ga. Published Sm-Nd ages for troctolite 76535 range from 4.260 to 4.439 Ga (Lugmair et al., 1976; Premo and Tatsumoto, 1992a; Nyquist et al., 2012; Borg et al. 2013). Despite its pristinity, 76535 has a complex thermal history (Nord, 1976; Domeneghetti et al., 2001; McCallum et al., 2006; Elardo et al., 2012) and this has led to multiple interpretations of the radiometric age data. Papanastassiou and Wasserburg (1976) and Domeneghetti et al., (2001) interpreted these discordant ages as representing different, mineral-specific, isotopic closure ages in which the Rb-Sr isochron dates the crystallization age via the isolation of Rb-rich inclusions in olivine. Younger ages determined by many of the other isotopic systems have been interpreted to represent the subsolidus event that is represented by cation ordering in the orthopyroxene, and symplectite formation along plagioclase-olivine boundaries (e.g., McCallum and Schwartz, 2001; Elardo et al., 2012). On the other hand, Premo and Tatsumoto (1992a) and Borg et al., (2013) concluded that this troctolite formed between 4.23 and 4.37 Gya. If this is correct, the ancient age derived from the Rb-Sr may reflect the lack of isolation of the Rb-rich component that not only occurs as inclusions but also occurs along gain boundaries.

Snyder et al. (1995) reported whole-rock Nd and Sr isotopic ratios for a troctolitic anorthosite clast in sample 14303 and concluded that these isotopic data are compatible with an age of 4.2 Ga. Meyer et al. (1989) reported a U-Pb zircon age of 4.245±0.075 Ga for a troctolite clast in sample 14306, but the presence of zircon and the small sample mass make its affinity ambiguous (Papike et al., 1998). Edmunson et al. (2007) were able to date troctolite sample 76335 and obtain a Sm-Nd age of 4.278±0.06. Unfortunately, there are no radiometric age dates for the spinel troctolites due to their overall small mass.

The norite lithologies have considerably more radiometric age data than other Mg-suite lithologies because of the availability of samples with significant mass and their abundance of pyroxene. Shih et al. (1993) determined Sm-Nd ages for two Mg-suite norites in a clast from 15445: 4.46±0.07 Ga (,17) and 4.28±0.03 Ga (,247). Norite clast 15445,17 is the oldest dated norite, but the Sm-Nd isochron may be disturbed. As Shih et al. (1993) recognized 15445,17 and ,247 represent the same clast, and they interpreted that this contrast in ages represented two distinct norite lithologies in a single clast. However, after examining the mineralogy of the clast with both EPMA and SIMS, Shearer et al. (2011) concluded that this clast represented only one norite lithology. Shih et al. (1993) also determined Rb-Sr age for another norite clast in 15455 (15455,228: 4.55±0.13 Ga). Sm-Nd ages for norite 78235 (along with 78236 and 78238 were chipped off of the same small boulder) range from 4334 to 4448 (Carlson and Lugmair, 1981; Nyquist et al., 1981; Edmunson et al., 2007; Andreasen et al. 2013). Nyquist et al. (1981) reported a Rb-Sr age of 4.38±0.02 Ga. Premo and Tatsumoto (1991, 1992c) have studied the U-Th-Pb isotopic systematics of 78235 and determined an initial crystallization age of 4.426 ± 0.065 Ga with a disturbance at 3.93 ± 0.21. Ga. Hinthorne et al. (1977) dated 78235 by Pb-Pb ion microprobe analyses of baddeleyites and zircon. They produced an age of 4.25±0.09 Ga. For norite samples 77215 and 77075, Nakamura et al. (1976) and Nakamura and Tatsumoto (1977) derived a Sm-Nd crystallization ages of 4.37±0.07 and 4.13±0.82 and concordant Rb-Sr age of

4.42±0.04 and 4.18±0.08 Ga. One of the youngest norite ages was derived from the Civet Cat norite clast in 72255. On the basis of an internal Rb/Sr isochron approach, Compston et al. (1975) obtained an age of 4.08±0.05 for that sample. This is concordant with the Ar-Ar ages derived for this clast by Leich et al. (1975).

The gabbronorites make up a small portion of the highlands collection of Apollo samples both in number and mass. Therefore, there is a relative paucity of chronological data for this lithology. Carlson and Lugmair (1981a,b) reported a Sm-Nd isochron age of 4.18±0.07 Ga for small (7.9 grams) gabbronorite 67667. Warren and Wasson (1979) referred to this sample as a feldspathic lherzolite rake sample. A gabbronorite clast in impact-melt breccia 73255 has a Sm-Nd isochron age of 4.23±0.05 Ga (Carlson and Lugmair, 1981a,b). Meyer et al. (1989) reported U-Pb zircon ages (4.1-4.3 Ga) for gabbronorites collected from the Apollo 14 and 16 sites, but the affinity of these samples to the Mg-suite is unclear (Nyquist and Shih, 1992).

Highly relevant to the interpretation of the "crystallization ages" determined for individual Mg-suite rocks are the numerous model ages determined for the formation of potential sources for the Mg-suite: ur-KREEP and LMO cumulates. Several ur-KREEP Sm-Nd model ages were calculated by Carlson and Lugmair (1979), Nyquist and Shih (1992), and Edmunson et al. (2009) (4.36 ± 0.06, 4.42 ± 0.07 and 4.492 ± 0.061 Ga, respectively). On the basis of Lu-Hf isotopic analyses of KREEP-enriched breccias (Sprung et al., 2013) and a suite of igneous rocks with KREEP signatures (Gaffney and Borg, 2013), model ages for ur-KREEP formation of 4.402 ± 0.023 Ga and 4.353 ± 0.037 Ga, respectively, were determined. Model ages for the mare basalt source region have been estimated using the ^{146}Sm-^{142}Nd isotope system. Ages of 4.329 $^{+0.040}/_{-0.056}$ Ga (Nyquist et al., 1995), 4.352 $^{+0.023}/_{-0.021}$ Ga (Rankenburg et al., 2006), 4.313 $^{+0.025}/_{-0.030}$ Ga (Boyet and Carlson, 2007), and 4.340 $^{+0.020}/_{-0.024}$ Ga (Brandon et al., 2009) determined by this method yields a weighted average age for mare basalt source formation of 4.337 ± 0.028 Ga (Borg et al., 2014). Evidence from Hf-W chronology indicate that LMO solidification occurred after the extinction of ^{182}Hf and therefore later than 60 Myr after CAI formation.

On the basis of these Mg-suite age data, numerous (and conflicting) interpretations have been reached concerning the chronology of the Mg-suite and its relationship to other highlands lithologies (e.g. FANs, alkali suite) and lunar differentiation. These interpretations are based on the analysis and judgment of the reliability of the individual age dates within each study. This is typically done by essentially either (1) taking most precise ages at face value or (2) establishing criteria for evaluating ages (Borg et al., 2013, 2014).

There are numerous conclusions that can be reached based by a straight forward interpretation of all the precise ages. In this interpretive scenario, the range of Mg-suite rock ages (4.61±0.07 to 4.17±0.02 Ga) compiled by Nyquist and Shih (1992), Nyquist et al. (2001), Snyder et al. (1995, 2000), and Borg et al. (2014) represent an extensive period of Mg-suite magmatism (approximately 300-400 m.y.). Clearly, some of the older ages for the Mg-suite (e.g. 4.61±0.07 Ga) should be disregarded as they represent ages older than the Solar System. This extensive period of Mg-suite magmatism must be contemporaneous with FAN magmatism and implies that the lunar magma ocean solidified very early. Further, these data suggest that an episode of primitive Mg-suite magmatism (dunites and troctolites) predates less primitive Mg-suite magmatism (norites and gabbronorites). These early episodes of Mg-suite magmatism must predate the alkali-suite (Figure 1) episode of highlands crustal building. Snyder et al. (1995) suggested that the Mg-suite magmatism was initiated at different times in different regions of the Moon. Their interpretation was that Mg-suite magmatism on the nearside occurred first in the northeast and then swept slowly to the southwest over a period of 300-400 m.y. They speculated that this regional progression of magmatism could be due to the progressive crystallization of the residual liquids of the LMO. The common 4.35 Ga age likely records a secondary pulse of widespread and diverse FAN, Mg- and alkali-suite magmatism. These younger FANs must represent either a non-LMO igneous process or the resetting of FAN ages due to their thermal history. The relatively young models ages determined for ur-KREEP and the LMO cumulate pile must represent a mantle-wide thermal event that reset the isotopic systems, and this event may be mantle cumulate overturn.

More recently, Borg et al. (2013,2014) suggested criteria for assessing highlands chronological data. Using these criteria, they concluded that the oldest ages determined with confidence on FAN and Mg-suite highlands rocks are in fact ~4.35 Ga (Fig. 18). This age is concordant with ^{142}Nd model ages of mare source formation (Nyquist et al., 1995; Rakenburg et al., 2006; Boyet and Carlson, 2007; Brandon et al., 2009), a peak in zircon ages (Compston et al., 1984; Grange et al., 2009; 2011 Pidgeon et al. 20072010; Nemchin 2009a,b; 2011), and the Lu-Hf model KREEP formation age (Gaffney and Borg, 2013), all of which suggest a major event at ~4.35 Ga. In this case, if the ancient ages of individual samples are not correct, then the 4.35 Ga age most likely records either the primordial solidification of the Moon or a major, Moon-wide thermal event (cumulate overturn?). In the scenario that the 4.35 Ga age represents a differentiation event, FAN magmatism may precede Mg-suite magmatism, but only by a few Ma. In the second scenario, the Moon-wide thermal event completely resets the isotopic systems in the mantle and ancient primordial crust (FANs). The episode of Mg-suite magmatism at 4.35 Ga partially manifests this thermal event. These two potential interpretive scenarios need to be resolved with ages on additional Mg-suite and alkali-suite samples using multiple chronometers and additional modeling of the early thermal history of the Moon.

PETROGENESIS OF THE MG-SUITE

Models for the generation of the Mg-suite parent magmas.

Numerous petrogenetic models have been proposed to account for the contrasting primitive (e.g., high Mg#) and evolved (e.g., saturated with plagioclase, high concentrations of incompatible trace elements, low concentrations of Ni, Co, and Cr) characteristics of the Mg-suite and the relative ages of early highlands lithologies. Models for the petrogenesis of the Mg-suite fall into 6 end-members: (1) impact origin (Taylor et al., 1993; Hess, 1994) (Fig. 19a); (2) products of magma ocean crystallization (Wood, 1975; Longhi and Boudreau, 1979; McCallum, 1983) (Fig. 19b); (3) remelting and remobilization of late-stage magma ocean cumulates such as KREEP (Hess et al., 1978; Hess, 1989) (Fig. 19c); (4) Mg-rich magmas derived from lower portions of the cumulate pile that were enriched in Al and incompatible trace elements through assimilation of KREEP, anorthositic crust, or both (Warren and Wasson 1977; Longhi, 1981; James and Flohr, 1983; Warren, 1986; Ryder, 1991; Papike et al., 1994, 1996) (Fig. 19d); and (5) melting of hybrid mixed cumulate sources either in the deep or (6) shallow lunar mantle (e.g., Shearer et al., 2006; Shearer and Floss, 1999; Shearer and Papike, 1999; 2005; Elardo et al., 2011) (Fig. 19e and f).

Impact origin.

An impact origin for the Mg-suite has been proposed to explain the chemical paradox of primitive and evolved chemical signatures in the same rocks (Wanke and Dreibus, 1986; Taylor et al., 1993; Hess, 1994). The model proposed by Taylor et al. (1993) combined late accretion impactors (~bulk Moon composition) as a source for the primitive component with LMO crystallization products (anorthosite, KREEP) as a source for the evolved component (Fig. 19a). The impact of this material into the Moon during the end of LMO crystallization would have mixed this primitive material with remelted ferroan anorthosite and residual KREEP liquid. The resulting magmas pooled beneath the ferroan anorthositic crust and subsequently intruded the crust. Formation of the Mg-suite by impact also circumvented the problem of a heat source capable of producing large volumes of primitive, high-Mg magmas following LMO crystallization (Taylor et al., 1993). There are several difficulties with this version of the impact model for the origin of the Mg-suite. The trace element fingerprints for impactors, such as elevated siderophile element abundances, are not found in the Mg-suite. For example, the Cr/Ni ratios for the highlands Mg-suite show a typical lunar value (Cr/Ni >5) in contrast with primitive cosmic abundances (Cr/Ni = 0.25). There is also a mass-balance problem with this process. The ratio of the mass of the impactor to the mass of the impact melt is too small (O'Keefe and Ahrens, 1977) to make a substantial contribution to the high Mg# observed in the Mg-suite. Finally, circumventing potential problems with heat sources to produce magnesian magmas is not necessary as several studies have identified viable processes that could have triggered melting in the deep lunar mantle (Spera, 1992; Ryder, 1991; Warren and Kallemeyn, 1993; Shearer and Papike, 1993, 1999).

Hess (1994) explored the possibility that the Mg-suite was generated by impact melting of the plagioclase-rich lunar crust and olivine-rich cumulates of the magma ocean. This eliminates the mass-balance problem in the earlier model of Taylor et al. (1993). Hess (1994) postulated that large impact melt sheets that were superheated and sufficiently insulated could cool slowly and differentiate to produce the troctolite-norite-gabbro sequence observed in the Mg-suite. Variable incorporation of KREEP and crustal components during shock melting could explain the variation in the evolved component in the Mg-suite plutonic rocks. The siderophile element signature of the impactor would have been significantly diluted during these processes.

Vaughan et al. (2013) modeled the crystallization of large impact melt sheets (thickness ≥ 15 km, diameter ≥ 350 km) produced by the Orientale and South Pole Aitken basin events. Target material that would have been melted include crustal (anorthosite, anorthositic norite) and mantle (pyroxenite) target materials. In a variety of crystallization models, they predicted cumulate horizons which would be dominated by either anorthosite or norite with somewhat smaller volumes of "quartz diorite" (in the strictest sense a quartz gabbro), quartz pyroxenite, pyroxenites and/or dunites. Modifying proportions of the target lithologies, character of crystallization (fractional versus equilibrium), and homogeneity of the melt sheet would affect the composition of the melt sheet, cumulate mineralogy, and the proportion of lithologies. Vaughan et al. (2013) speculated that these "counterfeit" plutonic rocks could pass as highlands lithologies, but finally concluded that this process could not account for the Mg-suite.

There are several lines of rationale for why this model is probably invalid. There is a mass balance issue in that only very unique mixtures of crustal target rocks and upper mantle lithologies could contribute to the high Mg# observed in the mafic silicates of the Mg-suite. The inability of the impact process to produce magmas capable to crystallize high Mg# mafic silicates would disrupt the distinctly different ferroan anorthosite and Mg-suite chemical trends (Fig. 5). Furthermore, as documented above, the crystallization ages of the Mg-suite rocks are older than 4.1 Ga. These crystallization ages are older than the large impact basins preserved on the near-side of the Moon (e.g. Orientale ~3.75 Ga). This would require that the Mg-suite rocks were produced by the crystallization of even older impact melt sheets and that only the remnants of these older melt sheets were incorporated onto the lunar surface. Mg-suite rocks from these younger impact melt sheets are absent from the Apollo and lunar meteorite collections. In addition, thermobarometry of Mg-suite rocks indicate a range of crustal environments of emplacement from 40-50 km to only a few kilometers (e.g. McCallum and Schwartz, 2001; Shearer et al., 2012a,b). These ranges in emplacement depths are not consistent with the crystallization of a surface impact melt sheet. Finally, if a substantial upper mantle component was incorporated into surface impact melt sheets, it should be expected that upper mantle lithologies would have been excavated and incorporated into the lunar regolith. No such samples have been found in the lunar regolith.

Primordial differentiation origin (Co-magmatic relationship between Mg-suite and FANs).

Wood (1975), Longhi and Boudreau (1979) and Raedeke and McCallum (1980) proposed models in which the Mg-suite was produced during LMO crystallization and evolution (Fig. 19b). Wood (1975) suggested that the Mg-suite and ferroan anorthosites were simply contemporaneous products of crystal accumulation and trapped melts. In this scenario, the Mg-suite intrusions consist of cumulus olivine/pyroxene plus plagioclase, whereas the ferroan anorthosites consist of cumulus plagioclase with mafic crystals produced from intercumulus melts. In addition to the differential incorporation of cumulates and trapped melts, Longhi and Boudreau (1979) proposed that the cumulus minerals in both rock types were produced by different styles of crystallization. The plagioclases in the ferroan anorthosites were products of equilibrium crystallization. The cumulate mafic silicates of the Mg-suite precipitated at approximately the same time, but under conditions of fractional crystallization. Raedeke and McCallum (1980) demonstrated that minerals from the banded zone in the Stillwater Complex show two fractionation trends remarkably similar to the Mg# of mafic mineral vs. An in plagioclase fractionation exhibited by the lunar highlands plutonic rocks (Fig. 1). They attributed the bimodality of the Stillwater rocks to differences in the style of crystallization (fractional crystallization accompanied by crystal accumulation vs. equilibrium crystallization of trapped intercumulus liquid in a plagioclase-rich crystal mush). A near contemporaneous relationship between members of these suites is suggested by the overlapping ages for some of the Mg-suite rocks with the ferroan-anorthosite suite (Fig. 18).

These simple primordial models are not consistent with all the geochemical observations made for the Mg-suite, however. Although the relationships between the Mg-suite and the FAN suite shown in Figure 1 mimics the mineral chemistry fractionation trends observed in the banded zone of the Stillwater complex, Raedeke and McCallum (1980) demonstrated that the rocks of the FAN suite cannot be generated from the same magma that formed the rocks of the Mg-suite. Their detailed analysis of mineral compositions and hypothetical intercumulus melt confirmed the likelihood that the gap between the two suites in Figure 1 is real and that these two suites of rocks represent two distinctly different parent magmas. Trace element data confirm this conclusion reached from major element mineral compositions. For example, the Mg-suite parental magmas have high Eu/Al but low Sc/Sm and Ti/Sm relative to the melts parental to the ferroan anorthosites (Norman and Ryder, 1979; Raedeke and McCallum, 1980; Warren and Wasson, 1977; James and Flohr, 1983; Warren, 1983, 1986). If taken at face value, initial Sr and Sm isotopic compositions indicate differences between FAN and Mg-suite parental magmas. However, this difference may not necessarily be correct. For example Rb-Sr and Sm-Nd isotopic data from 60025 (FAN) and 76535 (Troctolite) suggest derivation from isotopically similar, undifferentiated sources. Although the chronology described above exhibits overlap between the crystallization ages of the Mg-suite and FAN-suite, the relative geochemical chronology suggested by Eu/Al, Sc/Sm, and Ti/Sm indicates that within the context of a lunar magma ocean, the Mg-suite source region (or at least the KREEP component of that source region) was produced after the crystallization of the FAN-suite and source regions for both high- and low-Ti basalts. One interpretation of the absolute chronology implies that these events were closely spaced in time and not resolvable by geochronologic measurements.

Post-Magma Ocean Models for the Mg-suite.

Because of these difficulties with impact and primordial melting models, numerous models have been proposed that advocate a post-magma ocean origin for the Mg-suite that involves the melting of LMO cumulates. These models call upon either the melting or remobilization of shallow, evolved magma ocean cumulates (e.g., urKREEP), or melting of early, magma ocean cumulates with incorporation of KREEP or a crustal component through assimilation or mixing.

Ur-KREEP remobilization or melting.

Hess et al. (1978), Hess (1989), Snyder et al. (1995), Papike (1996) and Papike et al. (1994, 1996, 1997) explored the possibility that the Mg-suite and temporally associated highlands basaltic magmas (e.g., KREEP basalts, high alumina basalts) originated by partial melting of LMO cumulates at a shallow depth (Fig. 19c). Although they did not draw a genetic connection between the Mg-suite and KREEP basalts, Hess et al. (1978) suggested that the basalts with a KREEPy signature were generated by partial melting of LMO cumulates that crystallized soon after extensive ilmenite crystallization, but prior to the formation of KREEP (between 95 and 99% crystallization of the magma ocean). These magmas may have assimilated KREEP. Alternatively, Hess (1989) suggested that the KREEP-rich magmas were a product of partial melting of a lower lunar crust that had been altered metasomatically by KREEP (also see McCallum, 1983). Pressure release melting and remobilization of these rock types may be related to catastrophic impacts on the lunar surface (Snyder et al. 1995; Papike 1996; Papike et al. 1994, 1996, 1997). Although derivation of the parental KREEP basaltic magma from very-late magma ocean cumulates may be consistent with some of the reconstructed trace-element melt compositions from individual minerals (Papike, 1996; Papike et al., 1994, 1996, 1997), the chemical signatures common in the more primitive Mg-suite (e.g., olivine-bearing, high Mg#, low Na/(Na+Ca)) cannot be accounted for by this model.

Interactions among LMO cumulate sources.

Models that require the Mg-suite to represent crystallization products of high Mg# magmas generated in the deep lunar mantle (Fig. 19d-f) were developed to resolve some of the problems with a shallow cumulate source (James 1980; Warren and Wasson, 1977; Longhi, 1981; Morse, 1982; Ryder, 1991; Smith, 1982; Hunter and Taylor, 1983; James and Flohr, 1983; Shirley, 1983; Shervais et al., 1984; Warren, 1986; Hess, 1994). These types of models stimulate many questions. Is the lunar mantle capable of producing primary magmas with Mg# >74? Do these magmas have Al contents that are appropriate for plagioclase saturation at Mg# >74? Can assimilation processes increase the Al and incompatible-element content in these primitive magmas without dramatically lowering the Mg#? Hess (1994) demonstrated that magmas with Mg# appropriate for Mg-suite parent magmas could be generated by melting of early LMO cumulates. A magma ocean with an Mg# value equivalent to the bulk Moon (80 to 84; Jones and Delano, 1989; O'Neill, 1991) upon crystallization at high pressures would produce early cumulates of olivine having Mg# greater than 91. Elardo et al. (2011) illustrated that a wide range of proposed LMO bulk compositions (e.g., Earth-like to highly refractory element-enriched LMO) would produce early LMO cumulate lithologies with appropriate Mg# (greater than 91). Subsequent melting of these cumulates would produce magmas with Mg# equivalent to that of the parental Mg-suite magmas. Because of the pressure dependence of the FeO-MgO exchange equilibrium between olivine and basaltic melt, crystallization of these high-pressure

(DOI will not work until issue is live.) DOI: http://dx.doi.org/10.2138/am-2015-4817 8/6

melts near the lunar surface would result in liquidus olivine that is slightly more magnesian than residual olivine in the mantle source. Higher Mg# values for the melt may also result from the reduction of small amounts of FeO to Fe in the source (Hess, 1994). Melting of the early magma ocean cumulates initially could have been triggered by either radioactive decay (Hess, 1994) and/or cumulate overturning (Hess and Parmentier, 1995). The deep lunar mantle materials would have been less dense and hotter than the overlying cumulates and tend to move upward and be subjected to pressure-release melting. The pressure release from 400 km to 100 km would have been on the order of 15 kbars. This resulted in relatively high degrees of melting (>30%; Ringwood 1976; Herbert 1980; Shearer and Papike, 1999). Partial melting of early magma ocean cumulates could have produced primitive melts with high Mg# but, as shown by Shearer and Papike (1999) and Elardo et al. (2011), these magmas would not have the same geochemical characteristics as the Mg-suite. For example, these primitive magmas would not possess the high incompatible-element enrichments, fractionated Eu/Al and Na/(Na+Ca), and plagioclase as a liquidus phase until the Mg# of the melt was <42. Three types of processes have been proposed to resolve this problem: (1) assimilation of evolved crystallization products of the magma ocean and melting of a hybrid cumulate sources in the (2) deep or (3) shallow lunar mantle.

Warren (1986) calculated that if these high-Mg magmas assimilated ferroan anorthosite and KREEP (Fig. 19d), they would have reached plagioclase saturation at values of Mg# appropriate for Mg-suite magmas. Such magmas also would have inherited a fractionated incompatible element signature (high REE, fractionated Eu/Al). Hess (1994) explored the thermal and chemical implications of anorthosite melting and plagioclase dissolution by magnesian (high Mg#) basaltic magmas. In his analysis of anorthosite melting and mixing as a mechanism to drive high Mg# magmas to plagioclase saturation, he concluded that the resulting crystallization of olivine and the mixing of relatively ferroan cotectic melts produced from the anorthosites would lower the Mg# of the hybrid melt below that expected for the Mg-suite parental magmas. In addition, diffusion rates for Al_2O_3 in basaltic melts are extremely slow (Finnila et al., 1994) and indicate that the time scales to dissolve even a small amount of plagioclase are of the same order as the characteristic times of solidification of a large magma body. Similar thermal constraints are less severe for the shallow melting-assimilation of a KREEP-like component into a primitive Mg-suite magma. Although assimilation of KREEP does not dramatically drive the magnesian basaltic magmas to plagioclase saturation, this mechanism may account for the evolved trace-element signatures in the Mg-suite. However, mixing of viscous melts of KREEP composition with more-fluid, magnesian magmas could be prohibitive (Finnila et al., 1994). In addition, melt compositions for the Mg-suite norites that were calculated from pyroxene and plagioclase trace element data have incompatible element concentrations that are equivalent to or slightly higher than urKREEP (Papike et al. 1996; 1997). Simple mass-balance calculations indicate that it is impossible for a primitive Mg-suite magma to assimilate such an abundant amount of KREEP (Shearer and Floss 1999).

As an alternative to assimilation at shallow mantle levels, is it possible that the KREEP component was added to the deep mantle source for the Mg-suite (Fig. 19e)? Hess (1994) proposed that the source for the Mg-suite may be a hybrid mantle consisting of early magma ocean cumulates (e.g., dunite) and a bulk Moon component that may be either primitive lunar mantle or an early quenched magma ocean rind. Polybaric fractional melting of a 50–50 mixture would produce melts with appropriate Mg# and reasonable Al_2O_3. However, mixing of these components would not produce some of the incompatible-element and isotopic signatures exhibited by the Mg-suite. As an alternative, Shearer et al. (1991, 1999) suggested a cumulate overturn mechanism to transport a KREEP component to the deep lunar mantle to explain the evolved KREEPy signature imprinted on selected picritic glasses associated with mare basaltic magmatism. A similar process may have produced the KREEP signature in the Mg-suite. There are potential shortcomings for this model. For example, most LMO cumulate overturn models for the Moon are driven by the density and temperature contrasts in the cumulate pile. These contrasts result in the sinking of evolved dense cumulates such as the late (90-96% LMO crystallization) high-Ti cumulate lithologies and upwelling of hot and less dense early (0-50% LMO crystallization) magnesian cumulates. In all of these cumulate overturn models, mechanisms are not identified for the transport of the less-dense and perhaps warm urKREEP and high-Al crustal lithologies (ρ<2900 kg/m^3) into the deep lower mantle. Perhaps, the sinking of the dense, high-Ti cumulates would act in pulling the urKREEP horizons into the deep lunar mantle, but this process would act to mix these two cumulate horizons into the hybrid, Mg-suite source rather than separate them as observed in the Ti/Sm characteristics of the Mg-suite. Shearer and Papike (1999, 2005) identified another potential issue for early, olivine-rich LMO cumulates being a major component in the Mg-suite source. They observed that the Ni content in olivine in most Mg-suite rocks were substantially lower than that observed in less magnesian olivine from the mare basalts. This observation was also made earlier by Ryder (1983). These observations imply that the mare basalt and Mg-suite magmas are distinctly different. Further, they indicate that the early, more magnesian cumulates are Ni-poor compared to much later LMO cumulate lithologies. This appears to be counterintuitive, as previous crystallization models for the LMO and observations of fractional crystallization of terrestrial basalts indicate enrichment of early olivine in Ni. This potential dilemma for models for the Mg-suite may be resolved by either the involvement of a metal phase either during early stages of LMO crystallization (e.g., core formation), melting of the source or during evolution of the basaltic magma (Shearer and Papike, 1999; Papike et al. 1997) or relatively low $Ni^{olivine/melt}$ partitioning during the very early stages of LMO crystallization (Jones, 1995; Longhi et al., 2010; Shearer and Papike, 2005; Elardo et al., 2011).

Rather than the hybridization of the early lithologies of the LMO cumulate pile occurring in the deep lunar mantle via overturn, another alternative would be for this hybridization to occur in the shallow mantle (Shearer et al., 2006, 2009; Elardo et al., 2011). In this model (Fig. 19f), the hot (solidus temperature at 2 GPa has been estimated to be from 1600 to 1800°C) and less dense (ρ~3100 kg/m^3) early cumulate horizon (Shearer et al., 2006; Elardo et al., 2011) would rise to the base of the crust during overturn. Some decompressional melting would occur, but more importantly this process brings a hot cumulate horizon adjacent to the plagioclase-rich and KREEP-rich lithologies that would melt at substantially lower temperatures (<1300°C). Some of the issues posed by Hess (1994) against an assimilation model that were presented above (e.g. heat loss during mixing, diffusion of Al_2O_3) are still relevant, but the constraints may be less severe. For example, the emplacement of a large mass of a hot LMO cumulate horizon at the base of the crust would introduce more heat into the upper mantle-lower crust than the emplacement of a smaller mass of lower temperature magnesian magmas.

This overturn model is consistent with the various LMO cumulate pile overturn models proposed by Hess and Parmentier (1995) Parmentier et al. (2002), Zhong et al. (2003), Stegman et al. (2003), Elkins-Tanton et al. (2002, 2003) and summarized by Shearer et al. (2006). The relative timescales of LMO crystallization and cumulate overturn influences the final cumulate stratigraphy and potentially the relationship between the FAN and Mg-suite chronology. Elkins-Tanton et al. (2003) illustrated that the overturn of the LMO cumulate pile involves the competition between the rate of thickening of the solidified layer and the time scale of Rayleigh-Taylor instability. In simple LMO models of very rapid, turbulent convective heat transfer to the surface, solidification may be more rapid than the estimated overturn time for the early olivine-orthopyroxene cumulates. However, once the plagioclase crust forms a conductive lid, the last stages of LMO solidification will be much slower. Therefore, overturn of the mafic cumulates may occur while the evolved portion of the LMO is still liquid (Hess and Parmentier, 1995; Elkins-Tanton et al., 2002, 2003; Shearer et al., 2006). This type of scenario could account for a thermal environment that would enable the production of Mg-suite magmas via interactions between LMO early cumulates, KREEP, and plagioclase flotation cumulates on the timescales suggested by many of the more recently-determined crystallization ages for FANs and Mg-suite rocks discussed in the chronology section (Borg et al., 2011, 2012; Carlson et al., 2013). Although the effect of the transport of the hot lower mantle to the base of the lunar crust has not been empirically modeled, Wieczorek and Phillips (2000) and Laneuville et al. (2013) used thermal conduction models to examine the response of the lunar crust and mantle to heat-producing elements in the KREEP horizon. They concluded that under their scenario, portions of the crust and mantle would be exposed to temperatures near their solidus at the end of LMO crystallization.

Petrogenetic relationships among Mg-suite lithologies.

Although field or orbital data to indicate that the Mg-suite rocks are related to one another by fractional crystallization of basaltic magmas within layered intrusive complexes do not exist, the mineral and chemical variations observed among the Mg-suite rocks have been interpreted as indicating such a petrogenetic scenario. As illustrated by Longhi and Boudreau (1979), Hess (1989), Shearer et al. (2006), and numerous others, the crystallization of the Mg-suite is well represented by the 1-atmosphere $(Fe,Mg)_2SiO_4$-$CaAl_2Si_2O_8$-SiO_2 pseudoternary system. Within this system, the liquid line of descent of a primitive Mg-suite liquid within the olivine stability field would first produce olivine cumulates (dunites), followed by olivine and plagioclase cumulates along the olivine-plagioclase cotectic (troctolites). This fractional crystallization would drive the melt composition to the olivine-plagioclase-low-Ca pyroxene peritectic and along the low-Ca pyroxene-plagioclase cotectic to produce norites. Specific parent melt compositions within the olivine stability field are required to produce this fractional crystallization sequence. If the parent liquid has a low abundance of the plagioclase component, troctolites will not be produced. The mineral compositions in the Mg-suite further illustrate this relationship among Mg-suite lithologies (Fig. 5). Using a KREEP basalt (from the Apollo 15 collection site) as a starting parental magma, Snyder et al. (1995) and Shervais and McGee (1998, 1999) demonstrated that fractional crystallization and the accumulation of mineral phases and trapped KREEP-like residual liquid (2–15%) could produce the range of mineral and rock compositions observed in the highlands Mg-suite. Snyder et al. (1995) proposed that approximately 0 to 43% fractional crystallization and accumulation would produce the observed major element mineral variation in the Mg-suite. The lower Mg# of KREEP basalts (~61–66) relative to the Mg# that would be expected for parental magmas for the Mg suite cumulates (mafic minerals with Mg#~ 95) and their non-contemporaneous nature is an issue for directly linking KREEP basalts to the Mg- suite parent magmas, but this potentially could be a result of sampling (Irving, 1977). Alternatively, as suggested by Shearer and Papike (1999), Borg et al. (2004), and Shearer et al. (2006) there most likely is a broad compositional array of lunar basalts with a KREEP signature that were produced in the lunar mantle over a 1-2 billion year period of time.

This is a preprint, the final version is subject to change, of the American Mineralogist (MSA)
Cite as Authors (Year) Title. American Mineralogist, in press.
(DOI will not work until issue is live.) DOI: http://dx.doi.org/10.2138/am-2015-4817

Petrogenetic relationships between the Mg-suite and alkali suite

Snyder et al. (1995) proposed that the Mg- and alkali-suites are a product of fractional crystallization of a parental KREEP basalt. The sequence of crystallization and accumulation that they proposed is Mg suite (0 to 43% crystallization) ⇒ alkali anorthosites, alkali norites (43 to 74% crystallization) ⇒ alkali gabbros, alkali norites (74 to 90% crystallization) ⇒ quartz monzodiorites (90 to 99.8% crystallization) ⇒ granites.

Alternatively, the Mg-suite and alkali-suite may represent contemporaneous, yet separate episodes of basaltic magmatism (Warren and Wasson, 1980; James, 1980; James et al., 1987). There is some compositional evidence to suggest genetically distinct highlands rock types. For example, James et al. (1987) subdivided many of these highlands rock types into various groups on the basis of their mineral chemistry and mineral associations. Whether these subdivisions are artificial or petrologically significant is debatable. Within this scenario, differences between these two suites may be attributed to the depth of initial melting prior to KREEP addition. For example, Mg suite magmatism would be a product of interaction between very early LMO cumulates-KREEP-FAN, whereas the alkali-suite magmatism would involve initial melting of later LMO cumulates and interactions with KREEP.

Petrogenetic relationships between the Mg-suite and magnesian anorthositic granulites

Magnesian anorthosites have been described in Apollo samples and in lunar meteorites (e.g. Lindstrom et al., 1984; Lindstrom and Lindstrom, 1986; Takeda et al., 2006, 2007, 2008; Treiman et al., 2010) and may represent a widespread rock type in the lunar highlands (Jolliff et al., 2000; Wieczorek et al., 2006). However, their relationship to other episodes of lunar highlands magmatism is undetermined. This suite of rocks has experienced significant degrees of metamorphism resulting in recrystallized textures and a broad range of compositions. These rocks have Ar-Ar ages ranging from 3.94 to 4.26 Ga (Lindstrom and Lindstrom, 1986). In a plot of Mg# versus plagioclase composition (Fig. 1), the magnesian anorthositic granulites are clearly distinct from the FAN suite, but plot in or near the Mg-Suite field. The magnesian anorthositic granulite clasts found in the Apollo samples have a positive Eu anomaly and a REE pattern that is parallel to the more magnesian lithologies of the Mg-suite. In contrast, the calculated REE patterns for clasts in lunar meteorites are substantially lower than most Mg-suite rocks (2-3xCI chondrite) (Treiman et al., 2010). Compared to the Mg-suite rocks, the magnesian anorthositic granulites have similar Sc/Sm and Ti/Sc ratios and overlapping Cr_2O_3 and Th abundances (Lindstrom and Lindstrom, 1986). They have higher Ni than the Mg-suite, but this may be attributed to a meteoritic component. Many of these trace element characteristics were not calculated for the meteorite clasts studied by Treiman et al. (2010).

Warner et al. (1977) identified numerous lunar granulites that plotted within and between FAN and Mg-suite fields in Figure 1 and concluded that they all are metamorphic polymict breccias from the early lunar crust. However, a detailed study by Lindstrom and Lindstrom (1986) concluded that the most magnesian granulites are at least as likely to represent Mg-suite precursors as fortuitous mixtures of unrelated highlands lithologies. Treiman et al. (2010) suggested that the magnesian anorthositic clasts in the lunar meteorites (and perhaps some of the clasts returned by the Apollo program) may represent Mg-suite plutons that did not contain a KREEP component. If this is correct, these conclusions may imply that KREEP was not an integral part in producing the initial parental magmas for Mg-suite. In this case, the latter model proposed above (Fig. 19e) may be appropriate. The implication for this model is that KREEP-rich Mg-suite magmas were emplaced in the lunar crust in the PKT, whereas Mg-suite magmas without a KREEP component may be a component in the crust on the lunar far-side. This model is also supported by numerous remote sensing observations from the far-side highlands.

FUTURE EXPLORATION OF THE MG-SUITE

Although the Mg-suite has been extensively studied since the return of samples by the Apollo Program, there are still numerous questions that could be resolved by further sample and remote sensing measurements and observation. These questions are particularly important in furthering our understanding of the role of the Mg-suite in early planetary formation, differentiation, and crustal formation and evolution.

What is the age of FAN and Mg-suites?

There are two interpretations of the ages of the FAN- and Mg-suites. One interpretation is that the Mg-suite magmatism clearly post-dates (<4.5 Ga) ancient FAN terranes (> 4.5 Ga) and that this style of magmatism occurred over a long duration of time (>400 million years). This interpretation requires a Moon that was formed very early in the Solar System, presumably by a giant impact with the proto Earth. Further, this requires a rapid formation of planetary objects in the Solar System, very early collisions among these objects, and a complete solidification of the LMO prior to follow-on episodes of lunar magmatism. The second interpretation is that the approximate 4.35 Ga age observed in many FANs and Mg-suite lithologies is meaningful and represents two major closely spaced episodes of lunar differentiation. This interpretation implies either the Moon is relatively young or that a major lunar thermal event (reheating of crust either as a result of urKREEP heating or emplacement of hot, deep mantle at the base of the crust) occurred at approximately 4.35 Ga.

What was the duration of Mg-suite magmatism?

It appears that Mg-suite magmatism is fairly limited in duration. Depending upon the time this stage of magmatism was initiated (4.5 or 4.35 Ga), it (and the possibly related Alkali-suite) appears to have waned by 4.1 Ga. This apparent end of Mg-suite magmatism may only be a reflection of sampling and a transition from this magmatism to KREEP basaltic volcanism (to at least 3.0 Ga). We conclude that neither is true. First, large basins were forming until 3.8-3.9 Ga, yet these events did not reveal younger Mg-suite lithologies. Second, mineralogical data seem to suggest that the Mg-suite is distinct from follow-on periods of KREEP basaltic magmatism. These distinctions include high Mg# and low Ni and Cr in mafic silicates, Cl enrichments in apatite, and low bulk-rock NiO and Cr_2O_3 concentrations. Our conclusion is that the incompatible element signature referred to as KREEP is incorporated into basaltic magmas produced by melting of many different mantle sources. Finally, the migration of Mg-suite magmatism in the lunar crust is at this time speculative due to the interpretation and limit of the crystallization ages.

How are the Mg-suite lithologies related?

Although there is in the very best case, little geological field evidence confirming the relationship among the different Mg-suite lithologies, similar mineralogical and geochemical fingerprints, experimental studies, analogies to terrestrial layered intrusions, and crystallization ages indicate a fundamental petrogenetic link that may be tied to fractional crystallization. However, it is clear that the limited and perhaps unrepresentative samples seem to suggest distinct Mg-suite magmas were emplaced into the lunar crust at a range of crustal pressure environments.

What is the distribution of the Mg-suite?

The distribution of the Mg-suite may only be regional and closely associated to the PKT or may be produced Moon-wide (with differing proportions of a KREEP component). Figure 15 seems to imply that Mg-suite magmatism may extend outside the PKT. If this is correct, the link between the Mg-suite and KREEP may be a regional association. However, the brecciated lunar meteorite collection shows little to no evidence for Mg-suite lithologies in the feldspathic highlands crust outside the PKT. Distinguishing between these differences in distribution is critical to understanding the origin of the Mg-suite magmas, and more broadly planetary differentiation and crustal building processes on an asymmetric planetary body.

What is the petrogenetic relationship between the Mg-suite and magnesian anorthositic granulites?

The magnesian anorthositic granulites appear to be an important crustal component making up the Feldspathic Highlands Terrane (Jolliff et al., 2000). Understanding their origin (recrystallized magmatic or impact lithologies) and potential petrogenetic relationship to the Mg-suite will enable an assessment of early post-LMO building of the highlands crust.

What are the necessary next steps for exploring the nature of the Mg-suite?

There are numerous sample measurements and mission observations that could answer some of the questions regarding the Mg-suite. Establishing a better chronology for highlands evolution could be done by conducting additional isotopic age measurements and evaluating and placing these data within a mineralogical-geochemical context for both large samples and clasts within Apollo samples and lunar meteorites. New highlands samples may be identified by conducting micro computerized tomography on lunar breccias. Robotic and human sample return missions from unexplored lunar terranes such as the South Pole Aitken Basin, the Feldspathic Highlands Terrane, and from selected central peaks or basin rings would provide an important

Moon-wide perspective for understanding the formation and evolution of the lunar highlands. Orbital missions that build upon the success of the Lunar Reconnaissance Orbiter, GRAIL, Kaguya, and Chandrayaan-1 missions could better establish the distribution and composition of the Mg-suite lithologies and the nature of the lunar highlands. For example, a mission that combines both Moon Mineralogy Mapper capabilities with geochemical instrumentation high spatial resolution could be used to explore the composition of the crust such as is exposed at central peaks. Integrating these data within the context of crustal structure and thickness would provide great insights into the lunar highlands.

ACKNOWLEDGEMENTS

The authors thank the conveners (Allan Treiman, Meenakshi Wadhwa, Charles Shearer) for their work in organizing the Second Conference on the Lunar Highlands Crust (July 13-15, 2012), which was as timely as it was informative, and Stu McCallum and Dave Mogk for providing expert field guidance during the excursions to the Stillwater Complex. Ryan Zeigler and Carle Pieters are thanked for their insightful reviews that substantially improved this review. Associate editor Peter Isaacson provided useful comments and timely reviews of this rather lengthy manuscript. Our group is also indebted to both Peter Isaacson and Rachel Klima for organizing this special issue. CKS acknowledges support from the NASA Cosmochemistry Program and NASA Lunar Advanced Science for Exploration Research Program during this study (Grant no. NNX13AH85G and NNX13AJ58G to CKS). SME acknowledges support from NASA Earth and Space Science Fellowship NNX12AO15H. NEP acknowledges the support of NASA Grant SCEX22013D from the LASER Program and the Lunar Reconnaissance Orbiter Project. LEB acknowledges support from the NASA Cosmochemistry Program (Grant no. NNH12AT841 to LEB). during this study. FMM acknowledges support from the NASA Lunar

Advanced Science for Exploration Research Program during this study (Grant no. NNX13AK32G to FM). This contribution has made use of the NASA Astrophysics Data System.

REFERENCES

Adams, J.B. (1974), Visible and near-infrared diffuse reflectance spectra of pyroxenes as applied to remote sensing of solid objects in the Solar System. Journal of Geophysical Research, 79, 4829-4836.

Adams, J.B. (1975), Interpretation of Visible and Near-Infrared Diffure Reflectance Spectra of Pyroxenes and Other Rock-Forming Minerals, in Infrared and Raman Spectroscopy of Lunar and Terrestrial Materials, edited by C. Karr, pp. 91-116, Acedemic Press, New York.

Albee, A.L., Dymek, R.F., and DePaolo, D.J. (1975) Spinel symplectites: high pressure solid-state reaction or late-stage magmatic crystallization? Proceedings 6th Lunar Science Conference, 1-3.

Alibert C., Norman M.D., and McCulloch M.T. (1994) An ancient age for a ferroan anorthosite clast from lunar breccia 67016. Geochimica et Cosmochimica Acta 58, 2921-2926.

Andersen, D.J., Lindsley, D.H., and Davidson, P.M. (1993) QUILF: a Pascal program to assess equilibria among Fe-Mg-Mn-Ti oxides, pyroxenes, olivine, and quartz. Computers & Geosciences 19, 1333-1350.

Anderson, D.J. and Lindsley, D.H., (1982) Application of a two-pyroxene thermometer. 13th Lunar and Planetary Science Conference (abs.), 15-16.

Andreasen R., Simmons, S.T., Righter, M., and Lapen T.J. (2013) Lutetium-Hafnium and Samarium-Neodymium Systematics of Apollo 17 Sample 78236: Age and the Importance of Thermal Neutron Fluence on the Lutetium-Hafnium System. Lunar and Planetary. Science Conference abstract #2887.

Baker, M.B. and Herzberg, C.T. (1980) Spinel cataclasites in 15445 and 72435: Petrology and criteria for equilibrium. Proceedings 11th Lunar and Planetary Science Conference, 535-553.

Barnes, J.J., Tartese, R., Anand, M., McCubbin, F.M., Franchi, I.A., Starkey, N.A., and Russell, S.S. (2014) The origin of water in the primitive Moon as revealed by the lunar highlands samples. Earth and Planetary Science Letters, 390, 244-252.

Bell, P.M., Mao, H.K., Roedder, E., and Weiblen, P.W. (1975) The problem of the origin of symplectites in olivine-bearing lunar rocks. Proceedings 6th Lunar Science Conference, 231-248.

Bence, A. E., Delano, J. W., Papike, J. J., and Cameron, K. L. (1974) Petrology of the highlands massifs at Taurus-Littrow: An analysis of the 2-4 mm soil fraction. Proc. 5th Lunar Sci. Conf. Geochim. Cosmochim. Acta Supp. 5, Vol. 1, 785-827.

Boardman, J. W., C. M. Pieters, R. O. Green, S. R. Lundeen, P. Varanasi, J. Nettles, N. Petro, P. Isaacson, S. Besse, and L. A. Taylor (2011), Measuring moonlight: An overview of the spatial properties, lunar coverage, selenolocation, and related Level 1B products of the Moon Mineralogy Mapper, *J. Geophys. Res.*, *116*, E00G14, doi:10.1029/2010je003730.

Bogard, D.D., Nyquist, L.E., Bansal, B.M., Wiesmann, H., and Shih, C.Y. (1975) 76535: an old lunar rock. Earth and Planetary Science Letters, 26(1), 69-80.

Borg L.E., Norman M., Nyquist L.E., Bogard D., Snyder G.A., Taylor L.A., and Lindstrom M. (1999) Isotopic studies of ferroan anorthosite 62236: A young lunar crustal rock from a light rare-earth element-depleted source. Geochimica et Cosmochimica Acta 63, 2679-2691.

Borg, L.E., Shearer, C.K., Asmerom, Y., and Papike, J.J. (2004) Prolonged KREEP magmatism on the Moon indicated by the youngest dated lunar igneous rock. Nature, 432, 209-211.

Borg L.E., Connelly J.N., Boyet, M., and Carlson R.W. (2011) Evidence that the Moon is either young or did not have a global magma ocean. Nature, 477, 70-72.

Borg L., Connelly J., Cassata W., Gaffney A.M., Carlson R., Papanastassiou D., Ramon E., Lindval R, and Bizarro M. (2013) Evidence for Widespread Magmatic Activity at 4.36 Ga in the Lunar Highlands from Young Ages Determined on Troctolite 76535. 44th Lunar and Planetary Science Conference, Abstract #1563.

Borg, L.E. Gaffney, A.M., and Shearer, C.K. (2014) Chronologic Evidence for a Young Moon. Geochimica et Cosmochimica Acta in review.

Boyce, J.W., Guan, Y., Treiman, A.H., Greenwood, J.P., Eiler, J.M., and Ma, C. (2013) Volatile components in the moon: Abundances and isotope ratios of Cl and H in lunar apatites.Proceedings of the 44th Lunar and Planetary Science Conference Lunar and Planetary Institute, Woodlands, TX.

Boyet M. and Carlson R.W. (2007) A highly depleted Moon or a non-magma origin for the lunar crust? Earth and Planetary Science Letters 262, 505–516.

Brandon A.D., Lapen T.L., Debaille V., Beard B.L., Rankenburg K., and Neal C.R. (2009) Re-evaluating $^{142}Nd/^{144}Nd$ in lunar mare basalts with implications for the early evolution and bulk Sm/Nd of the Moon. Geochimica et Cosmochimica Acta 73, 6421-6445.

Burns, R.G. (1970), Crystal field spectra and evidence of cation ordering in olivine minerals, American Mineralogist, 55, 1608-1632.

Caffee, M., Hohenberg, C.M., and Hudson, B. (1981) Troctolite 76535: a study in the preservation of early isotopic records. Proceedings 12th Lunar and Planetary Science Conference, 99-115.

Cahill, J.T.S., Lucey, P.G., and Wieczorek, M.A. (2009), Compositional variations of the lunar crust: Results from radiative transfer modeling of central peak spectra, Journal of Geophysical Research: Planets, 114(E9), E09001, doi:10.1029/2008JE003282.

Carlson R.W. and Lugmair G.W. (1979) Sm-Nd constraints on early lunar differentiation and the evolution of KREEP. Earth Planet. Sci. Lett., 45, no. 1, 123-132.

Carlson R.W. and Lugmair G.W. (1981a) Time and duration of lunar crust formation. Earth and Planetary Science Letters 52, 227-238.

Carlson R.W. and Lugmair G.W. (1981b) Sm-Nd age of lherzolite 67667: implications for the processes involved in lunar crustal formation. Earth and Planetary Science Letters 56, 1-8.

Carlson R.W. and Lugmair G.W. (1988) The age of ferroan anorthosite 60025: Oldest crust on a young Moon? Earth and Planetary Science Letters 90, 119-130.

Carlson R.W., Borg L.E., Gaffney A.M., and Boyet M. (2013) Rb-Sr, Sm-Nd, and Lu-Hf isotopic systematics of norite 77215: refining the age and duration of lunar crust formation. 44th Lunar Planetary Science Conference abstract # 1621.

Chao, E.C.T., Minkin, J.A., and Thompson, C.L. (1976) The petrology of 77215, a noritic impact ejecta breccia. Proceedings 7th Lunar Science Conference 7, 2287-2308.

Cheek, L.C. and Pieters, C.M. (2012) Variations in anorthosite purity at Tsiolkovsky crater on the Moon. 43rd Lunar Planetary Science Conference. abstract# 2624.

Compston W., Foster J.J., and Gray C.M. (1975) Rb-Sr ages of clasts within Boulder 1, Station 2, Apollo 17. The Moon, 14, 445-462.

Compston, W., Williams, I.S., and Meyer, C. (1984) U-Pb geochronology of zircons from lunar breccia 73217 using a sensitive high mass-resolution ion microprobe. J. Geophys. Res. Solid Earth, 89, S02, B525-B534.

Day, J.M.D., Walker, R.J., James, O.B., and Puchtel, I.S. (2010) Osmium isotope and highly siderophile element systematics of the lunar crust. Earth and Planetary Science Letters, 289(3-4), 595-605.

Dhingra, D., Pieters, C.M., Boardman, J.M., Head, J.W., Isaacson, P.J. and Taylor, L.A. (2011), Compositional diversity at Theophilus Crater: Understanding the geological context of Mg-spinel bearing central peaks, Geophysical Research Letters 38, 11201, doi:DOI: 10.1029/2011GL047314.

Domeneghetti M.C., McCallum I.S., Schwartz J.M., Camara F., Zema M., McCammon C. and Ganguly J. (2001) Complex cooling histories of lunar troctolite 76535 and Stillwater orthopyroxenite SC-936 abs#1151). Lunar Planetary Science XXX, Lunar Planetary Institute. Dowty, E., Prinz, M., and Keil, K. (1974) Ferroan anorthosite: A widespread and distinctive lunar lock type. Earth and Planetary Science Letters 24, no. 1, 15-25

Dowty, E., Keil, K., and Prinz, M. (1974) Igneous rocks from the Apollo 16 rake samples. Proc. 5th Lunar Sci. Conf. Geochim. Cosmochim. Acta, Supp. 5, 431-445.

Dymek, R.F., Albee, A.L., and Chodos, A.A. (1975) Comparative petrology of lunar cumulate rocks of possible primary origin: Dunite 72415, troctolite 76535, norite 78235, and anorthosite 62237. Proceedings 6th Lunar Science Conference, 301-341.

Dymek, R.F., Albee, A.L., and Chodos, A.A. (1976) Petrology and origin of Boulders #2 and #3, Apollo 17 Station 2. Proceedings 7th Lunar Science Conference, 7, 2335-2378.

Edmunson J., Nyquist L.E., and Borg L.E. (2007) Sm-Nd isotopic systematics of troctolite 76335. 38th Lunar Planetary Science Conference. abstract # 1962.

Edmunson, J., Borg, L.E., Nyquist, L.E., and Asmerom, Y. (2009) A combined Sm-Nd, Rb-Sr, and U-Pb isotopic study of Mg-suite norite 78238: Further evidence for early differentiation. Geochimica et Cosmochimica Acta 73, 514-527.

Elardo, S.M., Draper, D.S., and Shearer, C.K. (2011) Lunar Magma Ocean crystallization revisited: Bulk composition, early cumulate mineralogy, and the source regions of the highlands Mg-suite. Geochimica et Cosmochimica Acta 75, 3024-3045.

Elardo, S.M., McCubbin, F.M., and Shearer, C.K. (2012) Chromite symplectites in Mg-suite troctolite 76535 as evidence for infiltration metasomatism of a lunar layered intrusion. Geochimica et Cosmochimica Acta, 87, 154-177.

Elardo, S.M., Shearer Jr, C.K., Fagan, A.L., Borg, L.E., Gaffney, A.M., Burger, P.V., Neal, C. R., Fernandes, V.A., and McCubbin, F.M., (2014) The origin of young mare basalts inferred from lunar meteorites Northwest Africa 4734, 032, and LaPaz Icefield 02205. Meteoritics & Planetary Science, 49, 261-291.

Elkins-Tanton L.T., Van Orman J.A., Hager B.H., and Grove T.L. (2002) Reexamination of the lunar magma ocean cumulate overturn hypothesis: Melting or mixing is required. Earth and Planetary Science Letters 196:249-259.

Elkins-Tanton L.T., Chatterjee N., and Grove T.L. (2003) Experimental and petrological constraints on lunar differentiation from the Apollo 15 green picritic glasses. Meteoritics & Planetary Science 38:515-527.

Finnila, A.B., Hess, P.C., and Rutherford, M.J. (1994) Assimilation by lunar mare basalts: Melting of crustal material and dissolution of anorthite. Journal of Geophysical Research, 99, 14677–14690.

Frondel, J.W. (1975) Lunar Mineralogy. John Wiley & Sons, New York, NY.

Gaffney A.M., Borg L.E., Asmerom Y., Shearer C.K., and Burger P.V. (2011) Disturbance of isotope systematics during experimental shock and thermal metamorphism of a lunar basalt with implications for Martian meteorite chronology. Meteoritics & Planetary Science 46, 35-52.

Gaffney, A.M., and Borg, L.E. (2013) A young age for KREEP formation determined from Lu-Hf isotopic systematics of KREEP basalts and Mg-suite samples. 44^{th} Lunar Planet. Sci. Conf., Abstract #1714.

Garrick-Bethell, I., Weiss, B.P., Shuster, D.L., and Buz, J. (2009) Early lunar magnetism. Science 323(5912), 356-359.

Goodrich, C.A., Taylor, G.J., Keil, K., Kallemeyn, G.W., and Warren, P.H. (1986) Alkali norite, troctolites, and VHK mare basalts from Breccia 14304. Journal of Geophysical Research 91(B4), D305-D318.

Gooley, R., Brett, R., Warner, J., and Smyth, J.R. (1974) A lunar rock of deep crustal origin: Sample 76535. Geochimica et Cosmochimica Acta, 38(9), 1329-1339.

Grange T. L., Nemchim A.A., Pidgeon R.T., Muhling J.R., and Kennedy A.K. (2009) Thermal history recorded by the Apollo 17 impact melt breccia 73217. Geochimica et Cosmochimica Acta 73, 3093-3107.

Grange M.L., Nemchin A.A., Timms N., Pidgeon R.T., and Meyer C. (2011) Complex magmatic and impact history prior to 4.1 Ga recorded in zircon from Apollo 17 South Massif aphanitic breccia 73235. Geochimica et Cosmochimica Acta 75, 2213-2232.

Green, R.O., Pieters, C., Mouroulis, P., Eastwood, M., Boardman, J., Glavich, T., Isaacson, P., Annadurai, M., Besse, S., Barr, D., Buratti, B., Cate, D., Chatterjee, A., Clark, R., Cheek, L., Combe, J., Dhingra, D., Essandoh, V., Geier, S., Goswami, J. N., Green, R., Haemmerle, V., Head, J., Hovland, L., Hyman, S., Klima, R., Koch, T., Kramer, G., Kumar, A.S.K., Lee, K., Lundeen, S., Malaret, E., McCord, T., McLaughlin, S., Mustard, J., Nettles, J., Petro, N., Plourde, K., Racho, C., Rodriquez, J., Runyon, C., Sellar, G., Smith, C., Sobel, H., Staid, M., Sunshine, J., Taylor, L., Thaisen, K., Tompkins, S., Tseng, H., Vane, G., Varanasi, P., White, M., and Wilson, D. (2011) The Moon Mineralogy Mapper (M^3) imaging spectrometer for lunar science: Instrument description, calibration, on-orbit measurements, science data calibration and on-orbit validation. Journal of Geophysical Research 116, E00G19.

Greenwood, J.P., Itoh, S., Sakamoto, N., Warren, P., Taylor, L., and Yurimoto, H. (2011) Hydrogen isotope ratios in lunar rocks indicate delivery of cometary water to the Moon. Nature Geoscience 4, 79-82.

Griffin, W. L., Heier, K.S., and Amli, R. (1972) Whitlockite and apatite from lunar rock 14310 and from Odegarden, Norway. Earth and Planetary Science Letters 15, 53-58.

Gross, J. and Treiman, A. H., (2011) Unique spinel-rich lithology in lunar meteorite ALHA81005: Origin and possible connection to M^3 observations of the farside highlands. Journal of Geophysical Research.

Hagerty, J. J., Shearer, C. K., and Vaniman, D. T. (2006) Heat-producing elements in the lunar mantle: Constraints from ion microprobe analyses of lunar volcanic glasses. Geochimica et Cosmochimica Acta 70, 3457-3476, doi:10.1016/j.gca.2006.04.013.

Haggerty, S.E. (1975) Geochemistry of opaque oxides in troctolites and basalts from Taurus Littrow. Proceedings 6th Lunar Science Conference, 321-323.

Haskin, L.A., Shih, C.Y., Bansal, B.M., Rhodes, J.M., Wiesmann, H., and Nyquist, L.E. (1974) Chemical evidence for the origin of 76535 as a cumulate. Proceedings 5th Lunar Science Conference, 1213-1225.

Heiken, G.H., Vaniman, D.T., and French, B.M. (eds) (1991) Lunar Source Book: A users guide to the Moon. Cambridge University Press, Cambridge, UK.

Herbert, F. (1980) Time-dependent lunar density models. Proc. 11th Lunar Planet. Sci. Conf., 2015-2030.

Herzberg, C.T. (1978) The bearing of spinel cataclasites on the crust-mantle structure of the Moon. Proceedings 9th Lunar Planetary Science Conference, 319-336.

Hess, P.C. (1989) Origin of Igneous Rocks, 336 p. Harvard University Press, Cambridge, Massachusetts.

Hess, P.C. (1994) The petrogenesis of lunar troctolites. Journal of Geophysical Research E9, 19,083-19,093.

Hess, P.C., Rutherford, M.J., and Campbell, H.W. (1978) Ilmenite crystallization in non-mare basalt: Genesis of KREEP and high-Ti mare basalts. Proceedings 9th Lunar Science Conference, 705–724.

Hess P.C., and Parmentier E.M. (1995) A model for the thermal and chemical evolution of the Moon's interior: Implications for the onset of mare volcanism. Earth and Planetary Science Letters 134:501-514.

Hinthorne, J.R., Conrad, R.L., and Andersen, C.A. (1975) Lead-lead age and trace element abundances in lunar troctolite, 76535. 6th Lunar Science Conference, 373-375.

Hinthorne, J.R., Conrad, R.L., and Church, S.E. (1977) Lead-lead ages and rare earth element determinations in lunar norite 78235. Lunar Planet. Sci. Conf. abstracts, 444-446.

Holness, M.B., Stripp, G., Humphreys, M.C.S., Veksler, I.V., Nielsen, T.F.D., and Tegner, C. (2011) Silicate liquid immiscibility within the crystal mush: Late-stage magmatic microstructures in the Skaergaard intrusion, east Greenland. Journal of Petrology 52, 175-222.

Hughes, J.M., Jolliff, B.L., and Gunter, M.E. (2006) The atomic arrangement of merrillite from the Fra Mauro Formation, Apollo 14 lunar mission: The first structure of merrillite from the Moon. American Mineralogist 91, 1547-1552.

Hughes, J.M., Jolliff, B.L., and Rakovan, J. (2008) The crystal chemistry of whitlockite and merrillite and the dehydrogenation of whitlockite to merrillite. American Mineralogist 93, 1300-1305.

Huneke, J.C., and Wasserburg, G.J. (1975) Trapped ^{40}Ar in troctolite 76535 and evidence for enhanced ^{40}Ar- ^{39}Ar age plateaus. 6th Lunar Science Conference, 417-419.

Hunter, R.H. and Taylor, L.A. (1983) The magma ocean from the Fra Mauro shoreline: An overview of the Apollo 14 crust. Proceedings 13th Lunar and Planetary Science Conference, A591–A602.

Husain L. and Schaeffer O.A. (1975) Lunar evolution: The first 600 million years. Journal of Geophysical Research 2, 29-32.

Irving, A.J. (1977) Chemical variations and fractionation of KREEP basalt magmas. Proceedings 8th Lunar and Planetary Science Conference, 2433–2448.

Isaacson, P. J., and C. M. Pieters (2009) Northern Imbrium Noritic Anomaly, Journal of Geophysical Research, 114, 09007.

Isaacson, P. J., and C. M. Pieters (2010) Deconvlution of lunar olivine reflectance spectra: Implications for remote compositional assessment. Icraus, 210, no. 1, 8-13.

Isaacson, P.J., Pieters, C.M., Besse, S., Clark, R.N., Head, J.W., Klima, R.L., Mustard, J.F., Petro, N.E., Staid, M.I., Sunshine, J.M., Taylor, L.A., Thaisen, K.G., and Tompkins, S. (2011) Remote compositional analysis of lunar olivine-rich lithologies with Moon Mineralogy Mapper (M3) spectra. Journal of Geophysical Research 116, E00G11.

Ishihara, Y., Goossens, S., Matsumoto, K., Noda, H., Araki, H., Namiki, N., Hanada, H., Iwata, T. Tazawa, S. and Sasaki, S. (2009), Crustal thickness of the Moon: Implications for farside basin structures, Geophysical Research Letters 36, 19202.

Ishihara, Y., Morota, T., Nakamura, R., Goossens, S. and Sasaki, S. (2011), Anomalous Moscoviense basin: Single oblique impact or double impact origin?, Geophysical Research Letter 38(3), L03201, doi:10.1029/2010GL045887.

Jackson, E.D., Sutton, R.L., and Wilshire, H.G. (1975) Structure and Petrology of a Cumulus Norite Boulder Sampled by Apollo-17 in Taurus-Littrow Valley, Moon. Geological Society of America Bulletin 86, 433-442.

James, O.B. (1980) Rocks of the early lunar crust. Proceedings 11th Lunar and Planetary Science Conference, 365-393.

James, O. B., and McGee, J. J. (1979) Consortium breccia 73255: Genesis and history of two coarse-grained "norite" clasts. Proc. 10th Lunar Planet. Sci. Conf. 713-743.

James, O.B. and Flohr, M.K. (1983) Subdivision of the Mg-suite noritic rocks into Mg-gabbronorites and Mg-norites. Journal of Geophysical Research 88, Suppl., A603-A614.

James, O.B., Lindstrom, M.M., and Flohr, M.K. (1987) Petrology and geochemistry of alkali abbronorites from lunar breccia 67975. Proceedings 17th Lunar Science Conference, E314–E330.

Jolliff, B.L., Haskin, L.A., Colson, R.O., and Wadhwa, M. (1993) Partitioning in REE-saturating minerals - theory, experiment, and modeling of whitlockite, apatite, and evolution of lunar residual magmas. Geochimica et Cosmochimica Acta 57, 4069-4094.

Jolliff, B.L., Gillis, J.J., Haskin, L.A., Korotev, R.L., and Wieczorek, M.A. (2000) Major Lunar Crustal Terranes: Surface Expressions and Crust-Mantle Origins, Journal of Geophysical Research, v. 105, p. 4197-4216, doi: 10.1029/1999JE001103.

Jolliff, B.L., Hughes, J.M., Freeman, J.J., and Zeigler, R.A., (2006) Crystal chemistry of lunar merrillite and comparison to other meteoritic and planetary suites of whitlockite and merrillite. American Mineralogist 91, 1583-1595.

Jones, J.H. (1995) Experimental trace element partitioning. In: Rock Physics and Phase Relations. A Handbook of Physical Constants. Ahrens, T.J. (ed). American Geophysical Union, 73-104.

Jones, J.H. and Delano, J.W. (1989) A three component model for the bulk composition of the moon. Geochimica et Cosmochimica Acta, 53, 513–527.

Karner, J., Papike, J.J., and Shearer, C.K. (2003) Olivine from planetary basalts: chemical signatures that indicate planetary parentage and those that record igneous setting and process. American Mineralogist 88, 806-816.

Klima, R.L., Pieters, C.M., and Dyar, M.D. (2007) Spectroscopy of syntthetic Mg-Fe pyroxenes I: Spin-allowed and spin-forbidden crystal field bands in the visible and near-infrared. Metor. Planet. Sci., 42, no. 2, 235-253.

Klima, R.L., Cahill, J., Hagerty, J., and Lawrence, D. (2013), Remote detection of magmatic water in Bullialdus Crater on the Moon, Nature Geoscience 6(9), 737-741, doi:10.1038/ngeo1909.

Klima, R. L., M. D. Dyar, and C. M. Pieters (2011a), Near-infrared spectra of clinopyroxenes: Effects of calcium content and crystal structure, *Meteoritics & Planetary Science*, *46*(3), 379-395, doi:10.1111/j.

Klima, R.L., Pieters, C.M., Boardman, J.W., Green, R.O., Head, J.W., III, Isaacson, P.J., Mustard, J.F., Nettles, J.W., Petro, N.E., Staid, M.I., Sunshine, J.M., Taylor, L.A., and Tompkins, S. (2011b) New insights into lunar petrology: Distribution and composition of prominent low-Ca pyroxene exposures as observed by the Moon Mineralogy Mapper (M3). Journal of Geophysical Research 116.

Korotev, R.L., Jolliff, B.L., Zeigler, R.A., Gillis, J.J., and Haskin, L.A. (2003) Feldspathic lunar meteorites and their implications for compositional remote sensing of the lunar surface and the composition of the lunar crust. Geochim. Cosmochim. Acta, 67, no. 24, 4895-4923.

Korotev, R.L. (2005) Lunar geochemistry as told by lunar meteorites. Chem Erde-Geochem 65, 297-346.

Korotev, R.L., Zeigler, R.A., Jolliff, B.L., Irving, A.J., and Bunch, T.E. (2009) Compositional and lithological diversity among brecciated lunar meteorites of intermediate iron concentration. Meteor. Plant. Sci., 44, Nr. 9, 1287-1322.

Kurat, G. and Bandstatter, F. (1983) Meteorite ALHA81005- Petrology of a new lunar highland sample. Geophysical Research Letters 10, 795-798, doi:10.1029/GL010i009p00795.

Kushiro, I. and Yoder, H. S., Jr. (1966) Anorthite-forsterite and anorthite-enstatite reactions and their bearing on the basalt-eclogite transformation. Journal of Petrology 7, 337-362.

Lal, D., Chauhan, P.,. Shah, R.D., Bhattacharya, S., Ajai, S. and Kiran Kumar, A.S. (2012), Detection of Mg spinel lithologies on central peak of crater Theophilus using Moon Mineralogy Mapper (M3) data from Chandrayaan-1, Journal of Earth System Science, 121(3), 847-853, doi:10.1007/s12040-012-0193-7.

Lally, J.S., Christie, J.M., Nord, G.L., and Heuer, A.H. (1976) Deformation, recovery, and recrystallization of lunar dunite 72417. Proceedings 7th Lunar Science Conference, 1845-1863.

Laneuville, M., Wieczorek, M.A., Breuer, D., and Tosi, N. (2013) Asymmetric thermal evolution of the Moon. Journal of Geophysical Research 118, 1435–1452, doi:10.1002/ jgre.20103,2013.

Laul, J.C. and Schmitt, R.A. (1975) Dunite 72415: A chemical study and interpretation. Proceedings 6th Lunar Science Conference, 1231-1254.

Lawrence, D.J., Elphic, R.C., Feldman, W.C., Prettyman, T.H., Gasnault, O., and Maurice, S. (2003), Small-area thorium features on the lunar surface, Journal of Geophysical Research, 108(E9), 5102, doi:1029/2003JE002050.

Leich D.A., Kahl S.B., Kirschbaum A.R., Niemeyer S. and Phinney D. (1975a) Rare gas constraints on the history of Boulder 1, Station 2, Apollo 17. The Moon 14, 407-444.

Lindstrom M.M. and Salpas P.A. (1983) Geochemical studies of feldspathic fragmental breccias and the nature of North Ray crater ejecta. Proceedings 13th Lunar and Planetary Science Conference, A671-A683.

Lindstrom, M.M., Knapp, S.A., Shervais, J.W., and Taylor, L.A. (1984) Magnesian anorthosites and associated troctolites and dunite in Apollo 14 breccias. Journal of Geophysical Research 89, Suppl. 1(B), C41-C49.

Lindstrom, M.M., Marvin, U.B., and Mittlefehldt, D.W. (1989) Apollo 15 Mg- and Fe-norites: a redefinition of the Mg-suite differentiation trend. 19th Lunar and Planetary Science Conference, 245-254.

Lindstrom, M.M. and Lindstrom D.J. (1986) Lunar Granulites and Their Precursor Anorthositic Norites of the Early Lunar Crust, Journal of Geophysical Research, v. 91(B4), p. D263-D276, doi: 10.1029/JB091iB04p0D263.

Liu, Y., Patchen, A.D., and Taylor, L.A., (2011) Lunar highland breccias MIL 090034/36/70/75: A significant KREEP component. 42nd Lunar and Planetary Science Conference, Abstract #1261.

Longhi, J. (1981) Preliminary modeling of high-pressure partial melting: Implications for early lunar differentiation. Proceedings 12th Lunar and Planetary Science Conference, 1001–1018.

Longhi, J. and Boudreau, A.E. (1979) Complex igneous processes and the formation of the primitive lunar crustal rocks. Proceedings 10th Lunar Planetary Science Conference 2085-2105.

Longhi, J., Durand, S.R., and Walker, D., (2010) The pattern of Ni and Co abundances in lunar olivines. Geochimica et Cosmochimica Acta 74, 784-798.

Lucey, P.G., and J. T. S. Cahill (2009), The Composition of the Lunar Surface Relative to Lunar Samples. 40th Lunar and Planetary Science Conference Abstract #2424.

Lugmair, G.W., Marti, K., Kurtz, J.P., and Scheinin, N.B. (1976) History and genesis of lunar troctolite 76535 or: How old is old? Proceedings 7th Lunar Science Conference, 2009-2033.

Ma, M.-S., Schmitt, R.A., Taylor, G.J., Warner, R.D., and Keil, K. (1981) Chemical and petrographic study of spinel troctolite in 67435: Implications for the origin of Mg-rich plutonic rocks. 12th Lunar and Planetary Science Conference, 640-642.

Marti, K., Aeschlimann, U., Eberhardt, P., Geiss, J., Grögler, N., Jost, D. T., Laul, J. C., Ma, M.-S., Schmitt, R. A., and Taylor, G. J. (1983) Pieces of the ancient lunar crust: Ages and composition of clasts in consortium breccis 67915. Journal Geophysical Research 88, Supp. 1, B165-B175.

Marvin, U. B., and Warren, P. H. (1980) A pristine eucrite-like gabbro from Descartes and its exotic kindred. Proc. 11th Lunar Planet. Sci. Conf. 507-521.

Marvin, U.B., Carey, J.W., and Lindstrom, M.M. (1989) Cordierite-Spinel Troctolite, a New Magnesium-Rich Lithology from the Lunar Highlands. Science 243(4893), 925-928.

Matsunaga, T., Ohtake, M., Haruyama, J., Ogawa, Y., Nakamura, R., Yokota, Y., Morota, C., Honda, C., Torii, M., Abe, M., Nimura, T., Hiroi, T., Arai, T., Saiki, K., Takeda, H., Hirata, N., Kodama, T., Sugihara, T., Demura, H., Asada, N., Terazono, J., and Otake, H. (2008) Discoveries on the lithology of lunar crater central peaks by SELENE Spectral Profiler, Geophysical Research Letters, 35, 23201.

McCallum, I.S. (1983) Formation of Mg-rich pristine rocks by crustal metasomatism. Lunar and Planetary Science XIV, 473–474.

McCallum, I.S. and Mathez, E.A., (1975) Petrology of noritic cumulates and a partial melting model for genesis of the Fra Mauro basalts. Proceedings Lunar Science Conference, 395-414.

McCallum, I.S. and OBrien, H.E., (1996) Stratigraphy of the lunar highland crust: Depths of burial of lunar samples from cooling-rate studies. American Mineralogist 81, 1166-1175.

McCallum, I.S., Raedeke, L.D., and Mathez, E.A. (1980) Investigations of the Stillwater Complex .1. Stratigraphy and Structure of the Banded Zone. American Journal of Science, 280, 59-87.

McCallum, I.S., and Schwartz, J.M. (2001) Lunar Mg-suite: thermobarometry and petrogenesis of parental magmas. Journal of Geophysical Research, 106(E11), 27,969-27,983.

McCallum, I.S., Domeneghetti, M.C., Schwartz, J.M., Mullen, E.K., Zema, M., Camara, F., McCammon, C.A., and Ganguly, J. (2006) Cooling history of lunar Mg-suite gabbronorite 76255, troctolite 76535 and Stillwater pyroxenite SC-936: the record in exsolution and ordering in pyroxenes. Geochimica et Cosmochimica Acta, 70(24), 6068-6078.

McCubbin, F.M., Vander Kaaden, K. E., Klima, R.L., Tartèse, R., Liu, Y., Mortimer, J., Barnes, J.J., , Shearer, C.K., Treiman, A.H., Lawrence, D. J., Elardo, S. M., Boyce, J.W., Anand, M. (2014) Volatiles (H, C, N, F, S, Cl) in the lunar crust and regolith: Distribution, processes, sources, and significance. American Mineralogist. This Volume.

McCubbin, F.M., Steele, A., Hauri, E.H., Nekvasil, H., Yamashita, S., and Hemley, R.J., (2010a) Nominally hydrous magmatism on the Moon. Proceedings of the National Academy of Science 107, 11223-11228.

McCubbin, F. M., Steele, A., Nekvasil, H., Schnieders, A., Rose, T., Fries, M., Carpenter, P. K., and Jolliff, B. L., (2010b) Detection of structurally bound hydroxyl in fluorapatite from Apollo mare basalt 15058,128 using TOF-SIMS. American Mineralogist 95, 1141-1150.

McCubbin, F. M., Jolliff, B. L., Nekvasil, H., Carpenter, P. K., Zeigler, R. A., Steele, A., Elardo, S. M., and Lindsley, D. H., (2011) Fluorine and chlorine abundances in lunar apatite: Implications for heterogeneous distributions of magmatic volatiles in the lunar interior. Geochimica et Cosmochimica Acta 75, 5073-5093.

Meyer, C., Williams I.S. and Compston W. (1989) Zircon containing rock fragments within Apollo 14 breccias indicate serial magmatism from 4350 to 4000 million years (abs). In Workshop on Moon in Transition: Apollo 14, KREEP, and evolved lunar rocks. LPI Technical Report. 89-03, 75-78. Lunar Planetary Inst.

Morris, R. W., Taylor, G. J., Newsome, H. E., Keil, K., and Garcia, S. R., (1990) Highly evolved and ultramafic lithologies from Apollo 14 soils. Proc. 12th Lunar Planet. Sci. Conf. 61-75

Morse, S.A. (1982) Adcumulus growth of anorthosite at the base of the lunar crust. Journal of Geophysical Research, 87, A10–A18.

Mustard, J.F., Pieters, C.M., Isaacson, P.J., Head, J.W., Besse, S., Clark, R.N., Klima, R.L., Petro, N.E., Staid, M.I., Sunshine, J.M., Runyon, C.J., and Tompkins, S. (2011) Compositional diversity and geologic insights of the Aristarchus crater from Moon Mineralogy Mapper data. Journal of Geophysical Research 116.

Nakumura N., Tatsumoto M., Nunes P.D., Unruh D.M., Schwab A.P., and Wildeman T.R. (1976) 4.4 b.y.-old clast in Boulder 7, Apollo 17: A comprehensive chronological study by U-Pb, Rb-Sr, and Sm-Nd methods. Proceedings 7th Lunar Science Conference, 2309-2033.

Nakumura N. and Tatsumoto M. (1977) The history of the Apollo 17 station 7 boulder. Proc. 8th Lunar Planet. Sci Conf., Vol. 2, 2301-2314.

Neal, C., Taylor, L., and Patchen, A. (1990) The dichotomy between primitive highland cumulates and evolved interstitial whitlockites: The process of "REEP-fraction" metasomatism. Proceedings 21st Lunar and Planetary Science Conference,445-446.

Neal, C.R. and Taylor, L.A. (1991) Evidence for metasomatism of the lunar highlands and the origin of whitlockite. Geochimica et Cosmochimica Acta 55, 2965-2980.

Nehru, C.E., Warner, R.D., Keil, K., and Taylor, G.J. (1978) Metamorphism of brecciated ANT rocks: anorthositic troctolite 72559 and norite 78527. Proceedings 9th Lunar and Planetary Science Conference, 773-788.

Nemchin A., Timms N., Pidgeon R., Geisler T., Reddy S. and Meyer C. (2009a) Timing of crystallisation of the lunar magma ocean constrained by the oldest zircon. Nature Geoscience 2(2), 133–136.

Nemchin A.A., Pidgeon R.T., Healy D., Grange M.L., Whithouse M.J., and Vaughan J. (2009b) The comparative behavior of apatite-zircon U-Pb systems in Apollo 14 breccias: Implications for the thermal history of the Fra Mauro formation. Meteoritics & Planetary Science 44, 1717-1734.

Nemchin, A.A., Whitehouse, M.J., Grange, M.L., and Muhling, J.R. (2011) On the elusive isotopic composition of lunar Pb. Geochim. Cosmochim. Acta, 75, 2940-2964.

Nord, G.L. (1976) 76535: Thermal history deduced from pyroxene precipitation in anorthite. Proc. 7th. Lunar Sci. Conf., 1875-1888.

Norman, M.D. (1981) Petrology of suevitic lunar breccia 67016. Proceedings of the 12th Lunar and Planetary Science Conference 12B, 235-252.

Norman, M.D. and Ryder, G. (1979) A summary of the petrology and geochemistry of pristine highlands rocks. Proceedings 10th Lunar and Planetary Science Conference, 531–559.

Norman, M.D. and Ryder, G. (1980) Geochemical constraints on the igneous evolution of the lunar crust. Proceedings 11th Lunar and Planetary Science Conference, 317-331.

Norman, M.D., Keil, K., Griffin, WL., and Ryan, C.G. (1995) Fragments of Ancient Lunar Crust: Petrology and Geochemistry of Ferroan Noritic Anorthosites from the Descartes Region of the Moon. Geochimica et Cosmochimica Acta 59, 831-847.

Norman, M.D., Borg, L.E., Nyquist, L.E., and Bogard, D.D. (2003) Chronology, geochmeistry, and patrology of a ferroan noritic anorthosite clast from Descartes breccia 67215: Clues to the age, origin, structure, and impact history of the lunar crust. Meteor. Planet. Sci. 38, Nr. 4, 645-661.

Nyquist L.E. and Shih C.-Y. (1992) The isotopic record of lunar volcanism. Geochimica et Cosmochimica Acta 56, 2213-2234.

Nyquist, L.E., Reimold, W.U., Bogard, D.D., Wooden, J.L., Bansal, B.M., Wiesmann, H., and Shih, C.-Y. (1981) A comparative Rb-Sr, Sm-Nd and K-Ar study of shocked norite 78236: Evidence of slow cooling in the lunar crust? Proceedings 12th Lunar and Planetary Science Conference, 67-97.

Nyquist, L.E., Wiesmann, H., Bansal, B., Shih, C.-Y., Keith, J.E., and Harper, C.L. (1995) ^{146}Sm-^{142}Nd formation interval for the lunar mantle. Geochim. Cosmochim. Acta, 59, no. 13, 2817-2837.

Nyquist L.E., Bogard D.D., and Shih C.-Y. (2001) "Radiometric chronology of the Moon and Mars." The Century of Space Science, Chap. 55, pp. 1325-1376 Kluwer Academic Publishers.

Nyquist L.E., Shih C.-Y., and Reese Y.D. (2012) Redetermination of the Sm-Nd age and initial ε_{Nd} of lunar troctolite 76535: Implications for lunar crustal development. 43rd Lunar Planetary Science Conference abstract #2416.

Ohtake, M., H. Takeda, T. Matsunaga, Y. Yokota, J. Haruyama, T. Morota, S. Yamamoto, Y. Ogawa, T. Hiroi, Y. Karouji, K. Saiki, P.G. Lucey, (2012) Asymmetric crustal growth on the Moon indicated by primitive farside highland materials, Nature Geoscience, DOI: 10.1038.

O'Keefe, J.D. and Ahrens, T.J. (1977) Impact-inducing energy partitioning, melting, and vaporization on terrestrial planets. Proceedings 8th Lunar and Planetary Science Conference, 3357–3374.

O'Neill, H.St.C. (1991) The origin of the moon and the early history of the Earth – a chemical model, Part 1: the moon. Geochimica et Cosmochimica Acta 55, 1135–1157.

Papanastassiou D.A. and Wasserburg G.J. (1975) Rb-Sr study of lunar dunite and evidence for early lunar differentiation. Proceedings 6th Lunar Science Conference 1467-1490.

Papanastassiou, D.A. and Wasserburg, G.J., (1976) Rb-Sr age of troctolite 76535. Proceedings 7th Lunar Science Conference, 2035-2054.

Papike, J.J. (1996) Pyroxene as a recorder of cumulate formational processes in asteroids, Moon, Mars, Earth: Reading the record with the ion microprobe. American Mineralogist, 81, 525–544.

Papike, J.J., Fowler, G.W., and Shearer, C.K. (1994) Orthopyroxene as a recorder of lunar crust evolution: an ion microprobe investigation of Mg-suite norites. American Mineralogist 79, 796-800.

Papike, J.J., Fowler, G.W., Shearer, C.K., and Layne, G.D. (1996) Ion microprobe investigation of plagioclase and orthopyroxene from lunar Mg suite norites: Implications for calculating parental melt REE concentrations and for assessing post-crystallization REE redistribution. Geochimica et Cosmochimica Acta, 60, 3967–3978.

Papike, J.J., Fowler, G.W., and Shearer, C.K. (1997) Evolution of the lunar crust: SIMS study of plagioclase from ferroan anorthosites. Geochimica et Cosmochimica Acta 61, 2343–2350.

Papike, J.J., Fowler, G.W., Adcock, C.T., and Shearer, C.K. (1999) Systematics of Ni and Co in olivine from planetary melt systems: Lunar mare basalts. American Mineralogist 84, 392-399.

Papike, J.J., Ryder, G., and Shearer, C.K. (1998) Lunar samples. Reviews in Mineralogy, 36, 5-1 - 5-234.

Parmentier E.M., Zhong S., and Zuber M.T. (2002) Gravitational differentiation due to initial chemical stratification: origin of lunar asymmetry by the creep of dense KREEP? Earth and Planetary Science Letters 201, 473-480.

Petro, N.E., and Klima, R. (2013), Moon Mineralogy Mapper Perspective On The Composition Of The Sculptured Hills: Implications For The Origin Of The Apollo 17 Station 8 Boulder And Guidance For Future Lunar Rovers, in Annual Meeting of the Lunar Exploration Analysis Group, edited, p. 7036, LPI, Columbia, MD.

Petro, N.E., J. Sunshine, C. Pieters, R. Klima, J. Boardman, S. Besse, J. Head, P. Isaacson, L. Taylor, and S. Tompkins (2010), Lower Crustal Materials Exposed in the Apollo Basin Revealed Using Moon Mineralogy Mapper (M3) Data. 41st Lunar and Planetary Science Conference. Abstract #1802.

Pidgeon R.T. Nemchin A. A., van Bronswijk W., Geisler T., Meyer C., Compston W. and Williams I. S. (2007) Complex history of a zircon aggregate from lunar breccia 73235. Geochimica et Cosmochimica Acta 71, 1370–1381.

Pidgeon, R.T., Nemchin, A.A., and Meyer, C. (2010) The contribution of the sensitive high-resolution ion microprobe to lunar geochronology. Precambrian Research, 183, no. 1, 44-49.

Pieters, C.M. (1993), Compositional diversity and stratigraphy of the lunar crust derived from reflectance spectrscopy, in Remote Geochemical Analysis: Elemental and Mineralogical Composition, edited by C. M. Pieters and P. A. J. Englert, pp. 309-339, Cambridge University Press, Cambridge.

Pieters, C.M., Besse, S., Boardman, J., Buratti, B., Cheek, L., Clark, R.N., Combe, J.P., Dhingra, D., Goswami, J.N., Green, R.O., Head, J.W., Isaacson, P., Klima, R., Kramer, G., Lundeen, S., Malaret, E., McCord, T., Mustard, J., Nettles, J., Petro, N., Runyon, C., Staid, M., Sunshine, J., Taylor, L.A., Thaisen, K., Tompkins, S., and Whitten, J. (2011) Mg-spinel lithology: A new rock type on the lunar farside. Journal of Geophysical Research 116.

Pieters, C.M, Donaldson Hanna, K., Cheek, L., Dhingra, D., Prissel, T., Jackson, C., Moriarty, D. Parman, S., and Taylor L.A. (2014) The Distribution and Origin of Mg-Spinel on the Moon. Am. Mineral., Special Issue on the Second Conference on the Lunar Highlands Crust, In Press.

Premo, W.R., and Tatsumoto, M. (1991) U-Th-Pb isotopic systematics of lunar norite 78235. Proc. 21st Lunar Planet. Sci. Conf., 89-100.

Premo, W.R., and Tatsumoto, M. (1992a) U-Th-Pb, Rb-Sr, and Sm-Nd isotopic systematics of lunar troctolitic cumulate 76535: Implications on the age and origin of this early lunar, deep-seated cumulate. Proceedings 22nd Lunar and Planetary Science Conference, 381-397.

Premo W.R. and Tatsumoto M. (1992b) U-Pb isotopes in dunite 72415 (abs). Lunar Planetary Science XXIII, 1103-1104. Lunar Planetary Institute, Houston.

Premo W.R. and Tatsumoto M. (1992c) Isotopic ages and characteristics of ancient (pre-Serenitatis) crustal rocks at Apollo 17. Workshop on Geology of the Apollo 17 landing site. 45-48.

Prinz, M., Dowty, E., Keil, K., and Bunch, T.E. (1973) Spinel Troctolite and Anorthosite in Apollo 16 Samples. Science 179(4068), 74-76.

Raedeke, L.D., and McCallum, I.S. (1980) A comparison of the fractionation trends in the lunar crust and the Stillwater complex. Proceeding of the Conference on the Lunar Highlands Crust, 133-153.

Raedeke, L.D., and McCallum, I.S. (1984) Investigations in the Stillwater Complex .2. Petrology and Petrogenesis of the Ultramafic Series. Journal of Petrology 25(2), 395-420.

Rankenburg K., Brandon A.D., and Neal C.R. (2006) Neodymium isotope evidence for a chondritic composition of the Moon. Science 312, 1369-1372.

Ringwood, A.E. (1976) Limits on the bulk composition of the Moon. Icarus, 28, no. 3, 325-349.

Roedder, E. and Weiblen, P.W. (1974) Petrology of clasts in lunar breccia 67915. Proceedings 5th Lunar Science Conference 303-318.

Ryder, G. (1983) Nickel in olivines and parent magmas of lunar pristine rocks. Workshop on Pristine Highlands Rocks and the early History of the Moon, 66-68.

Ryder, G. (1985) Catalog of Apollo 15 rocks. Curatorial Publication 20787, 3 vols., NASA Johnson Space Center, Houston, TX.

Ryder, G. (1991) Lunar ferroan anorthosites and mare basalt sources: the mixed connection. Geophysical Research Letters, 18, 2065–2068.

Ryder, G. (1992) Chemical variation and zoning of olivine in lunar dunite 72415: Near-surface accumulation. Proceedings 22nd Lunar Science Conference 22, 373-380.

Ryder, G. and Bower, J.F. (1977) Petrology of the Apollo 15 black-and-white rocks 15445 and 15455: Fragments of the Imbrium impact melt sheet? Proceedings 8th Lunar Science Conference, 1985-1923.

Ryder, G., and Norman, M. D. (1979) A summary of the petrology and geochemistry of pristine highlands rocks. Proc. 10th Lunar Planet. Sci. Conf. 531-559.

Ryder, G., Norman, M.D., and Taylor, G.J. (1997) The complex stratigraphy of the highland crust in the Serenitatis region of the Moon inferred from mineral fragment chemistry. Geochimica et Cosmochimica Acta 61, 1083-1105.

Sharp, Z.D., McCubbin, F.M., and Shearer Jr, C.K. (2013) A hydrogen-based oxidation mechanism relevant to planetary formation. Earth and Planetary Science Letters 380, 88-97.

Sharp, Z.D., Shearer, C.K., McKeegan, K.D., Barnes, J.D., and Wang, Y.Q. (2010) The chlorine isotope composition of the Moon and implications for an anhydrous mantle. Science 329, 1050-1053.

Shearer, C.K. and Floss, C. (1999) Evolution of the Moon's mantle and crust as reflected in trace element microbeam studies of lunar magmatism. In R. Canup and K. Righter, Eds., Origin of the Earth and Moon. University of Arizona Press, Tuscon, in press.

Shearer, C.K., and Papike, J.J. (1993) Basaltic magmatism on the Moon: A perspective from volcanic picritic glass beads. Geochimica et Cosmochimica Acta, 57, 4785–4812.

Shearer, C.K., and Papike, J.J. (1999) Magmatic evolution of the Moon. American Mineralogist, 84, 1469-1494.

Shearer, C.K., and Papike, J.J. (2005) Early crustal building processes on the Moon: models for the petrogenesis of the Mg-suite. Geochimica et Cosmochimica Acta, 69(13), 3445-3461.

Shearer, C.K., Papike, J.J., Galbreath, K.C., and Shimizu, N. (1991) Exploring the lunar mantle with secondary ion mass spectrometry: A comparison of lunar picritic glass beads from the Apollo 14 and Apollo 17 sites. Earth and Planetary Science Letters 102, 134–147.

Shearer, C.K., Hess, P.C., Wieczorek, M.A., Pritchard, M.E., Parmentier, E.M., Borg, L.E., Longhi, J., Elkins-Tanton, L.T., Neal, C.R., Antonenko, I., Canup, R.M., Halliday, A.N., Grove, T.L., Hager, B.H., Lee, D-C., and Wiechert, U. (2006) Chapter 3. Magmatic and thermal history of the Moon. In New Views of the Moon (eds. B. Jolliff, M. Wieczorek, C.K. Shearer, C. Neal). Reviews in Mineralogy and Geochemistry. RiMG 60, 365-518.

Shearer, C.K., Burger, P.V., Guan, Y.B., Papike, J.J., and Sutton, S.R. (2011) Vapor element transport in the lunar crust. Open system transport of elements in the shallow lunar crust by anhydrous, isotopically light S-rich vapor. 42nd Lunar and Planetary Science Conference, Abstract #1141.

Shearer, C.K., Borg, L.E., Burger, P.V., Connelly, J.N., and Bizzaro, M. (2012a) Timing and Duration of the Mg-Suite Episode of Lunar Crustal Building. Part 1: Petrography and Mineralogy of a Norite Clast in 15445. 43rd Lunar and Planetary Science Conference, Abstract #1659.

Shearer, C.K., Burger, P.V., Guan, Y., Papike, J.J., Sutton, S.R., and Atudorei, N.V. (2012b) Origin of sulfide replacement textures in lunar breccias. Implications for vapor element transport in the lunar crust. Geochimica et Cosmochimica Acta 83, 138-158.

Shearer, C.K., Burger, P.V, Marks, N.E., Borg, L.E., Gaffney, A.M. (2013) Petrology and chronology of early lunar crust building 1. Comprehensive examination of a ferroan anothosite clast in 60016. 44th Lunar Planet Sci. Conf., Abstract #1689

Shervais, J.W. and McGee, J.J. (1998) Ion and electron microprobe study of troctolites, norite, and anorthosites from Apollo 14: evidence for urKREEP assimilation during petrogenesis of Apollo 14 Mg-suite rocks. Geochimica et Cosmochimica Acta 62, 3009-3023.

Shervais, J.W. and McGee, J.J. (1999) Petrology of the Western Highland Province: Ancient crust formation at the Apollo 14 site. Journal of Geophysical Research-Planets 104, 5891-5920

Shervais, J.W., Taylor, L.A., Laul, J.C., and Smith, M.R., (1984) Pristine highland clasts in consortium breccia 14305: petrology and geochemistry. Journal of Geophysical Research 89, Suppl. 1, C25-C40.

Shih, C.Y., Nyquist, L.E., Dasch, E.J., Bogard, D.D., Bansal, B.M., and Wiesmann, H. (1993) Ages of pristine noritic clasts from lunar breccias 15445 and 15455. Geochimica et Cosmochimica Acta 57, 915-931.

Shirai, N., Ebihara, M., Sekimoto, A., Yamaguchi, A., Nyquist, L., Shih, C.-Y., Park, J., and Nagao, K. (2012) Geochemistry of lunar highland meteorites MIL 090034, 090036 and 090070. 43rd Lunar and Planetary Science Conference, Abstract #2003.

Shirley, D.N. (1983) A partially molten magma ocean model. Journal of Geophysical Research, 88, A519–A527.

Smith, J.V. (1982) Heterogeneous growth of meteorites and planets, especially the Earth and Moon. Journal of Geology, 90, 1–48.

Smith, J.V. and Steele, I.M. (1976) Lunar mineralogy: Heavenly detective story part 2. American Mineralogist 61, 1059-1116.

Snee, L.W., and Ahrens, T.J. (1975) Shock-induced deformation features in terrestrial peridot and lunar dunite. Proceedings 6th Lunar Science Conference, 833-842.

Snyder, G.A., Neal, C.R., Taylor, L.A., and Halliday, A.N. (1995) Processes involved in the formation of the magnesian-suite plutonic rocks from the highlands of the Earth's Moon. Journal of Geophysical Research-Planets, 100(E5), 9365-9388.

Snyder, G.A., Borg, L.E., Nyquist, L.E., and Taylor, L.A., (2000) Chronology and isotopic constraints on lunar evolution, in Canup, R.M., and Righter, K., eds., Origin of the Earth and Moon: Tucson, University of Arizona Press, p. 361–395.

Spera, F.J. (1992) Lunar magma transport phenomena. Geochimica et Cosmochimica Acta, 56, 2253–2266.

Sprung, P., Kleine, T., and Scherer, E.E. (2013) Isotopic evidence for chrondritic Lu/Hf and Sm/Nd of the Moon. Earth Planet. Sci. Lett., 380, 77-87.

Spudis, P.D. (1998) The once and future Moon. Smithsonian Institution Press, Washington D.C., 320 p.

Steele, I.M., (1975) Mineralogy of Lunar Norite 78235: 2nd Lunar Occurrence of P21ca Pyroxene from Apollo-17 Soils. American Mineralogist 60, 1086-1091.

Stegman, D.R., Jellinek, A.M., Zatman, S.A., Baumgardner, J.R., Richards, M.A. (2003) An early lunar core dynamo driven by thermomechanical mantle convection. Nature (London) 421:143-146

Sunshine, J. M., Pieters, C. M., and S. F. Pratt (1990), Deconvolution of mineral absorption bands - An improved approach,. Journal of Geophysical Research 95, 6955-6966.

Takeda, H., Yamaguchi, A., Bogard, D.D., Karouji, Y., Ebihara, M., Ohtake, M., Saiki, K., and Arai, T., (2006) Magnesian anorthosites and a deep crustal rock from the farside crust of the moon. Earth and Planetary Science Letters 247, 171-184.

Takeda H., Arai T., Yamaguchi A., Otuki M., and Ishii T. 2007. Mineralogy of Dhofar 309, 489, and Yamato-86032 and varieties of lithologies of the lunar farside crust. 38th Lunar and Planetary Science Conference. Abstract #1607.

Takeda H., Arai T., Yamaguchi A., Otsuki M., and Ohtake M. 2008. Granulitic lithologies in Dhofar 307 lunar meteorite and magnesian, Th-poor terrane of the northern farside crust. 39th Lunar and Planetary Science Conference, abstract #1574.

Tartèse, R., Anand, M., Barnes, J.J., Starkey, N.A., Franchi, I.A., and Sano, Y. (2013) The abundance, distribution, and isotopic composition of Hydrogen in the Moon as revealed by basaltic lunar samples: implications for the volatile inventory of the Moon. Geochimica et Cosmochimica Acta, 122, 58-74.

Tartèse, R., Anand, M., McCubbin, F.M., Elardo, S.M., Shearer Jr, C.K., and Franchi, I.A. (2014) Apatites in lunar KREEP basalts: The missing link to understanding the H isotope systematics of the Moon. Geology, 42, 363-366.

Taylor, L.A., Patchen, A., Mayne, R.G., and Taylor, D.-H. (2004) The most reduced rock from the Moon, Apollo 14 basalt 14053: Its unique fearures and their origin. Am. Mineral., 89, no. 11-12, 1617-1624.

Taylor, S.R., Norman, M.D., and Esat, T.M. (1993) The Mg-suite and the highland crust: An unsolved enigma. Proceedings 24th Lunar and Planetary Science Conference 1413-1414.

Tompkins, S.,and Pieters, C. (1999) Mineralogy of the lunar crust: Results from Clementine, Met. & Planet. Sci., 34, 25-41.

Treiman, A.H., Maloy, A.K., Shearer, C.K., and Gross, J. (2010) Magnesian Anorthositic Granulites in Lunar Meteorites Allan Hills A81005 and Dhofar 309: Geochemistry and Global Significance, Meteoritics & Planetary Science, v. 45(2), p. 163-180, doi: 10.1111/j.1945-5100.2010.01014.x.

Vaughan, W.M., Head, J.W., Wilson, L. and Hess, P.C. (2013) Geology and petrology of enormous volumes of impact melt on the Moon: A case study of the Orientale basin impact melt sea. Icarus 223, 749-765.

Wanke, H. and Dreibus, G. (1986) Geochemical evidence for the formation of the moon by impact-induced fussion of the proto-Earth. In Origins of the Moon (eds. Hartmann, Phillips, and Taylor) 649–672.

Warner, J.L., Simonds, C.H., and Phinney, W.C. (1976a) Genetic distinction between anorthosites and Mg-rich plutonic rocks: New data from 76255. Proceedings 7th Lunar Science Conference, 915-917.

Warner, J.L., Simonds, C.H., and Phinney, W.C., (1976b) Warner, J.L., Simonds, C.H., and Phinney, W.C., (1976b) Apollo 17, Station 6 boulder sample 76225: Absolute petrology of breccia matric and igneous clasts. Proc. 7th Lunar Sci. Conf. 2233-2250.

Warner, J.L., Phinney, W.C., Bickel, C.E., and Simonds, C.H. (1977) Feldspathic granulitic impactities and pre-final bombardment lunar evolution. Proc. 8th Lunar Planet. Sci. Conf., 2051-2066.

Warner, R. D., Taylor, G. J., and Keil, K. (1980) Petrology of 60035: Evolution of a polymict ANT breccia. Proc. Conf. Lunar Highlands Crust. Papike, J. J., and Merrill, R. B. (eds) 377-394.

Warner, R. D., Taylor, G. J., Mansker, W. L., and Keil, K. (1978) Clast assemblages of possible deep-seated (77517) and immiscible-melt (77538) origins in Apollo 17 breccias. Proc. 9^{th} Lunar Planet. Sci. Conf. 941-958.

Warren, P.H. (1983) Al-Sm-Eu-Sr systematics of eucrites and Moon rocks: Implications for planetary bulk compositions. Geochimica et Cosmochimica Acta 47, 1559–1571.

Warren, P.H., (1986) Anorthosite assimilation and the origin of the Mg/Fe-related bimodality of pristine Moon rocks: support for the magmasphere hypothesis. Journal of Geophysical Research 91, D331-D343.

Warren, P.H., (1993) A Concise Compilation of Petrologic Information on Possibly Pristine Nonmare Moon Rocks. American Mineralogist 78, 360-376.

Warren, P.H. and Kallemeyn, G.W. (1993) The ferroan-anorthositic suite, the extent of primordial lunar melting, and the bulk composition of the moon. Journal of Geophyical Research, 98, 5445–5455.

Warren, P.H. and Wasson, J.T. (1977) Pristine nonmare rocks and the nature of the lunar crust. Proceedings 8^{th} Lunar Science Conference, 2215-2235.

Warren, P.H. and Wasson, J.T. (1978) Compositional-petrographic investigation of pristine nonmare rocks. Proc. 9^{th} Lunar Planet. Sci. Conf. 185-217.

Warren, P. H., and Wasson, J. T. (1979) The compositional-petrographic search for pristine nonmare rocks: Third foray. Proc. 10^{th} Lunar Planet Sci. Conf. 583-610.

Warren, P.H. and Wasson, J.T. (1980) Further foraging for pristine nonmare rocks: Correlations between geochemistry and longitude. Proc. 11^{th} Lunar Planet. Sci. Conf. 431-470.

Warren, P. H., Taylor, G. J., Keil, K., Marshall, C., and Wasson, J. T. (1981) Foraging westward for pristine nonmare rocks: Complications for petrogenetic models. Proc. 12^{th} Lunar Planet. Sci. Conf. 21-40.

Warren, P. H., Taylor, G. J., and Keil, K. (1983a) Sixth foray for pristine nonmare rocks and an assessment of the diversity of lunar anorthosites. J. Geophys. Res. 88, Supp. 2, A615-A630.

Warren, P. H., Taylor, G. J., and Keil, K. (1983b) Seventh foray: Whitlockite-rich lithologies, a diopside-bearing troctolitic anorthosite, ferroan anorthosites, and KREEP. J. Geophys. Res. Vol. 88, Supp. 1, B151-B164.

Warren , P. H., Shirley, D. N., and Kallemeyn, G. W. (1986) A potpourri of pristine Moon rocks, including a VHK mare basalt and a unique, augite-rich Apollo 17 anorthosite. J. Geophys. Res. Vol. 91, No. B4, D319-D330.

Warren, P. H., Jerde, E. A., Kallemeyn, G. W. (1987) Pristine Moon rocks: A “large” felsite and a metal-rich ferroan anorthosite. J. Geophys. Res. Vol. 92, No. B4, E303-E313.

Warren, P.H., Jerde, E.A., and Kallemeyn, G.W., (1990) Pristine Moon rocks: An alkali anorthosite with coarse augite exsolution from plagioclase, a magnesian harzburgite, and other oddities. Proceedings 20^{th} Lunar Science Conference, 31-59.

Wieczorek M.A., and Phillips R.J. (2000), The “Procellarum KREEP Terrane”: Implications for mare volcanism and lunar evolution, Journal of Geophysical Research 105, 20,417–20,430, doi:10.1029/1999JE001092.

Wieczorek, M.A., Jolliff, B.L., Khan, A., Pritchard, M.E., Weiss, B.P., Williams, J.G., Hood, L.L., Righter, K., Neal, C.R., Shearer, C.K., McCallum, I.S., Tompkins, S., Hawke, B.R., Peterson, C., Gillis, J.J., and Bussey, B. (2006) Chapter 3. The Constitution and Structure of the Lunar Interior. In New Views of the Moon. 221 – 364, 772 pages. ISBN 0-939950-72-3; ISBN13 978-0-939950-72-0.

Wieczorek, M.A., Neumann, G.A., Nimmo, F., Kiefer, W.S., Taylor, G.J., Melosh, H.J., Phillips, R.J., Solomon, S.C., Andrews-Hanna, J.C., Asmar, S.W., Konopliv, A.S., Lemoine, F. G., Smith, D E., Watkins, M.M., Williams, J.G., and Zuber, M.T., (2012) The Crust of the Moon as Seen by GRAIL. Science. doi:10.1126/science.1231530.

Wood, J.A. (1975) Lunar petrogenesis in a well-stirred magma ocean. Proceedings 6th Lunar Science Conference, 1087–1102.

Yamamoto, S., Nakamura, R., Matsunaga, T., Ogawa, Y., Ishihara, Y., Morota, T., Hirata, N., Ohtake, M., Hiroi, T., Yokota, Y., and Haruyama, J., (2010) Possible mantle origin of olivine around lunar impact basins detected by SELENE. Nature Geoscience 3, 533-536.

Yamamoto, S., Nakamura, R., Matsunaga, T., Ogawa, Y., Ishihara, Y., Morota, T., Hirata, N., Ohtake, M., Hiroi, T., Yokota, Y., and Haruyama, J., (2011) Olivine-rich exposures in the South Pole-Aitken Basin. Icarus 218, 331-344.

Yamamoto, S., Nakamura, R., Matsunaga, T., Ogawa, Y., Ishihara, Y., Morota, T., Hirata, N., Ohtake, M., Hiroi, T., Yokota, Y., and Haruyama, J. (2013) A new type of pyroclastic deposit on the Moon containing Fe-spinel and chromite, Geophysical Research Letters, doi: 10.1002/grl.50784.

Zeigler, R.A., Korotev, R.L., Jolliff, B.L., and Haskin, L.A., (2005) Petrography and geochemistry of the LaPaz Icefield basaltic lunar meteorite and source crater pairing with Northwest Africa 032. Meteoritics & Planetary Science 40, 1073-1101.

Zeigler, R. A., Jolliff, B. L., Korotev, R. L., and Carpenter, P. K. (2008) Determination of Sr concentrations in lunar plagioclase by electron microprobe analysis. Geochim. Cosmochim. Acta, 72, 12S, A1072.

Zhong S, Parmentier EM, Zuber MT (2000) A dynamic origin for the global asymmetry of lunar mare basalts. Earth and Planetary Science Letters 177, 131-140.

TABLES

Table 1: List of ultramafic samples in the Apollo sample collection considered members of the Mg-suite.

Sample	Lithology	Mass (g)	Max. Grain Size (mm)	Pristinity Index	Olivine Mg#	OPX Mg#	Plag. An#	Modal % Olivine	Modal % Pyroxene	Modal % Plag.	Comments and Notable Features	Main Ref.
12033,503	Harzburgite	0.1	3	8	89	91	-	45	55	-		[1]
14161,212,1	Peridotite	<0.1	0.2	7	82	84	-	35	65	-		[2]
14161,212,4	Dunite	<0.1	?	5	83	-	-	-	-	-		[2]
14304c121	Dunite?	0.1	1.7	6	89	-	-	100	-	-		[3]
14305c389	Pyroxenite?	<0.1	2.8	7	90	91	-	2	98	-	Single grain of OPX with olivine inclusions.	[4]
14321c1141	Dunite	0.1	3	6	89	-	-	100	-	-		[5]
72415-8	Dunite	55.2	10	9	87	87	94	93	3	4	Chromite symplectites, apatite veining.	[6]

References: [1] Warren et al., 1990 [2] Morris et al., 1990 [3] Warren 1987 [4] Shervais et al., 1984 [5] Lindstrom et al., 1984 [6] Ryder 1992

Table 2: List of troctolites in the Apollo sample collection considered members of the Mg-suite.

Sample	Mass (g)	Max Grain Size (mm)	Pristinity Index	Olivine Mg#	OPX Mg#	Plag. An#	Modal % Olivine	Modal % Pyroxene	Modal % Plag.	Comments and Notable Features	Main Ref.
14172c11	0.7	2	7	87	-	94	35	-	60		[1]
14179c6	0.7	1.7	6	87	-	94	40	-	60		[2]
14303c194	2	1.5	6	88	-	95	30	-	70		[1]
14304c95"a"	0.9	>1.1	7	87	-	94	45	-	55		[3]
14321c1020	9.2	3	7	86	89	95	24	<1	75		[2]
14321c1024	0.7	1	7	80	-	95	15	-	85		[2]
15455c106	3	2	7	83	85	95	22	11	67		[4]
60035c21	0.7	2	6	88	89	96	-	-	57		[5]
73146	3	2	7	86	88	95	15	<1	85		[4]
73235c127	0.7	1.3	5	83	86	96	24	7	67		[4]
76255c57	2	1	8	89	91	96	-	-	77		[6]
76335	465	4	8	87	88	96	21	-	79	Likely a crushed version of 76535.	[7]
76535	155	10	9	88	86	96	35	5	60	Chromite symplectites and veins, sulfide alteration.	[8]
76536	10.3	1	7	83	86	-	-	-	67	Likely a crushed version of 76535.	[4]

References: [1] Warren and Wasson 1980 [2] Warren et al., 1981 [3] Goodrich et al. 1986 [4] Warren and Wasson 1979 [5] Warner et al., 1980 [6] Warner et al., 1976b [7] Warren and Wasson, 1978 [8] Dymek et al., 1975

Table 3: List of spinel troctolites in the Apollo sample collection considered members of the Mg-suite.

Sample	Mass (g)	Max Grain Size (mm)	Pristinity Index	Olivine Mg#	OPX Mg#	Plag. An#	Modal % Olivine	Modal % Pyroxene	Modal % Plag.	Comments and Notable Features	Main Ref.
12071c10	1.3	3	6	>78	-	97	-	-	70		[1]
14304c109"q"	0.0	0.7	6	87	-	94	-	-	-		[2]
15295,101	-	<0.9	-	91	-	93	11	-	75	Clast contains 8% modal corderite.	[3]
15445c71"A"	1.5	>2	5	92	-	92?	-	-	35		[4]
15445G	4	?	-	90	-	-	-	-	50		[5]
15445H	2?	?	-	92	91	96	44	3	15		[6]
65785c4	0.3	5	8	83	84	96	30	<1	65	Contains a single large spinel grain.	[7]
67435c77	0.1	3	8	92	-	97	50	-	35		[8]
72435	-	?	-	73	70	96	20	1	70	72435,8 contains a grain of corderite.	[9]
73263 (part.)	-	?	-	90	90	96	-	-	70		[10]
76503 (part.)	-	?	-	90	90	96	-	-	70		[10]
77517c disagg	-	?	-	90	90	97	-	-	-		[11]

References: [1] Warren 1990 [2] Goodrich et al., 1986 [3] Marvin et al., 1989 [4] Ryder 1985 [5] Ryder and Norman 1979 [6] Baker and Herzberg 1980 [7] Dowty et al., 1974 [8] Ma et al., 1981 [9] Dymek et al., 1976 [10] Bence et al., 1974 [11] Warner et al., 1978

Table 4: List of norites in the Apollo sample collection considered members of the Mg-suite.

Sample	Mass (g)	Max Grain Size (mm)	Pristinity Index	Olivine Mg#	OPX Mg#	Plag. An#	Modal % Olivine	Modal % Pyroxene	Modal % Plag.	Comments and Notable Features	Main Ref.
14318c146	1.2	1.9	6	71	73	87	12	35	55		[1]
14318c150	0.5	1	6	74	78	83	5-10	25	65		[2]
15360,11	0.7	2.9	9	-	78	93	-	35	65		[3]
15361	0.9	1.8	8	-	84	94	-	60	40		[3]
15445c17"B"	10	>1	8	-	82	95	-	35-40	60-65	Different regions of clast B produce different ages.	[4]
15455c228	200	5	9	-	83	93	-	30	70		[4]
72255c42	10	4	8	-	75	93	-	60	40		[5]
77035c130	100	>2.5	7	-	79	93	-	40	60		[6]
77075/77215	840	2	8	-	71	91	-	42	54	OPX is inverted pigeonite, contains CPX exsolution lamellae.	[7]
78235/78255	395	10	8	-	81	93	-	50	50	Texturally nearly pristine.	[8]
78527	5.2	2	4	77	80	93	2	46	52		[1]

References: [1] Warren et al., 1983a [2] Warren et al., 1986 [3] Warren et al., 1990 [4] Shih et al., 1993 [5] Ryder and Norman 1979 [6] Warren and Wasson 1979 [7] Chao et al., 1976 [8] Dymek et al., 1975

Table 5: List of gabbronorites in the Apollo sample collection considered members of the Mg-suite.

Sample	Mass (g)	Max Grain Size (mm)	Pristinity Index	Olivine Mg#	OPX Mg#	Plag. An#	Modal % Olivine	Modal % Pyroxene	Modal % Plag.	Comments and Notable Features	Main Ref.
14161,7044	<0.1	?	6	-	64	88	-	42	49		[1]
14161,7350	<0.1	?	6	-	-	96	7	2	90	Also reffered to as a troctolitic anorthosite.	[1]
14304c114"h"	<0.1	1.1	6	68	-	89	-	-	40		[2]
14311c220	0.2	0.5	5	-	60	85	-	13	75		[3]
61224,6	0.3	3	8	-	67	83	-	63	34		[4]
67667	7.9	2	7	71	78	91	58	20	21	Also reffered to as a feldspathic lherzolite.	[5]
67915c163	0.2	1	6	32	40	67	-	25-30	40-45	Pyroxene-sulfide reaction features in olivine. Na-rich.	[6]
73255c27,45	0.9	1.8	7	-	74	89	-	45	53		[7]
76255c72	0.1	2	7	-	67	86	-	61	39	Pyroxenes contain exsolution lamellae, sulfide veining.	[8]
76255c82	300	0.5?	6	-	65	87	-	61	39		[8]

References: [1] Jolliff et al., 1993 [2] Goodrich et al., 1986 [3] Warren et al., 1983b [4] Marvin and Warren 1980 [5] Warren and Wasson 1979 [6] Marti et al., 198 [7] James and McGee 1979 [8] Warner et al., 1976b

FIGURE CAPTIONS

Figure 1. A plot of Mg# in mafic silicates (olivine or OPX) vs. An in plagioclase for Mg-suite, Alkali-suite, and Ferroan Anorthosite lithologies after Warner et al. (1976a). Data from Papike et al. (1998) and references therein.

Figure 2. Backscattered electron (BSE) and qualitative Kα X-ray maps (Mg, Fe, Cr, Al, and Ca) of selected Mg-suite lithologies. (a) dunite (72415), (b) troctolite (76535), (c) norite (78235), (d) norite clast in breccia (77215), (e) shocked norite clast (15445), (f) gabbronorite clast (76255), (g) spinel troctolite clast (72435) and (h) cordierite-spinel troctolite clast (72435). Relative concentration color scale is shown in (a). The color contrast for each map has been adjusted to best shown compositional features, therefore similar colors do not necessarily correspond to similar concentrations in different maps.

Figure 3. Range in major element chemistry of mineral phases exhibited by the Mg-suite. (a) Pyroxene. (b) Olivine. (c) Plagioclase.

Figure 4. Plot of Cr in ppm vs. Mg# in olivine from Mg-suite lithologies and mare basalts, after Elardo et al. (2011) and references therein.

Figure 5. Plot of Ni vs. Co in ppm in olivine in Mg-suite lithologies, ferroan anorthosites, and mare basalts after Shearer and Papike (2005), Elardo et al. (2014), and references therein.

Figure 6. Plot of Y vs Ba in ppm for plagioclase in the Mg-suite, FANs, mare basalts, and KREEP basalts. Data are from Papike et al. (1996), Shervais and McGee (1998; 1999), and Shearer and Papike (2005).

This is a preprint, the final version is subject to change, of the American Mineralogist (MSA)
Cite as Authors (Year) Title. American Mineralogist, in press.
(DOI will not work until issue is live.) DOI: http://dx.doi.org/10.2138/am-2015-4817 8/6

Figure 7. Plot of Cr# vs. Mg# for spinels in Mg-suites lithologies after Elardo et al. (2012) and references therein.

Figure 8. Ce versus Cl abundances of apatites in mare basalts, KREEP basalts, and Mg-suite rocks. The data used for generating this plot are from previously published literature (Jolliff et al., 1993; McCubbin et al., 2010b; McCubbin et al., 2011; Tartese et al., 2013; Barnes et al., 2014; Elardo et al., 2014; Tartese et al., 2014).

Figure 9. REE patterns of Mg-suite rocks. a. Olivine-bearing lithologies compared to that range observed in FANs (yellow field). b. Olivine-absent lithologies compared to that range observed in KREEP basalts (gray field) and urKREEP.

Figure 10. Range observed in a series of whole rock geochemical parameters for the Mg-suite. Mg-suite lithologies with olivine are filled data points, whereas Mg-suite lithologies with minor or no olivine are open data points. Fields are shown for mare basalts, FANs, KREEP basalts, and quartz-monzodiorites (QMD). (a) Mg/(Mg+Fe) versus Ti/Sm. (b) Mg/(Mg+Fe) versus Sc/Sm. (c) Mg/(Mg+Fe) versus Th. (d) Mg/(Mg+Fe) versus Cr. (e) Mg/(Mg+Fe) versus Ni. (f) Co versus Ni.

Figure 11. BSE image and qualitative X-ray maps of orthopyroxene (Opx)-clinopyroxene (Cpx)-chromite symplectites in troctolite 76535. X-ray maps are for Mg, Ca, and Cr.

Figure 12. BSE images of troilite (Tro) and high-Ca pyroxene (Cpx) intergrowths observed in troctolite 76535.

Figure 13. Troilite + orthopyroxene replacement of olivine in gabbronorite clast (67915). BSE image and S, Mg, and Ca x-ray maps. Cpx = high-Ca pyroxene, Pl = plagioclase, OTP = olivine + troilite + orthopyroxene intergrowths, Chr = chromite, and M = merrillite.

Figure 14. Apatite veins in Apollo 17 dunite (72415). Ol=olivine, and Ap=apatite. BSE image and P, Ca, and Mg qualitative X-ray maps.

Figure 15. (a) Exsolution exhibited by pyroxene in a Mg-suite intrusion emplaced in the shallow crust (1-2 km). (b) Corrected (for beam overlap) microprobe traverse across exsolution lamellae that was used to calculate emplacement depth.

Figure 16. Distribution of Mg-suite rocks on the Moon as detected by near-infrared remote sensing. A Lunar Reconnaissance Orbiter Camera Wide Angle Camera mosaic, centered on the nearside showing the latitude range from 70º to -70º. The outlines of two of the geochemical terranes (Jolliff et al., 2000) are indicated. The Procellarum KREEP Terrane (PKT) is defined as containing Th abundances greater than ~3.5 ppm and the South Pole-Aitken Terrane (SPA) is defined on the basis of topography and enhancements in Th and Fe. Feldspathic Highlands Terrane (FHT) is defined by low thorium (0.37 ± 0.11 ppm) and Fe (4.4 ± 0.5% FeO) abundances. The locations of the six Apollo landing sites (stars with appropriate mission number) are identified, as are specific areas described in the text. Symbols for location, potential rock-type, and references are in the figure.

Figure 17. Generalized chronological relationships between Mg-suite and other lunar events (modified after Spudis, 1998).

Figure 18. Chronology of Mg-suite rocks compared to other highlands lithologies and model ages for mantle sources for mare basalts (Nyquist and Shih, 1992; Nyquist et al., 2001; Snyder et al., 1995, 2000; Papike et al., 1998; Shearer et al., 2005, 2006; Borg et al., 2013).

Figure 19. Potential models for the formation of the Mg-suite. (a) Impact formation through crystallization of melt sheets. (b) Co-crystallization of Mg-suite and FANs from the LMO. (c) Mobilization of urKREEP and emplacement into the lunar crust. (d) Assimilation of urKREEP ± FANs by Mg-rich magmas derived from early LMO cumulates. (e) Hybridization of early LMO cumulates by KREEP as a result of overturn of cumulate pile. (f) Hybridization and melting of early LMO cumulates at the base of the lunar crust. Models are discussed in detail in the text.

FIGURES

Figure 1.

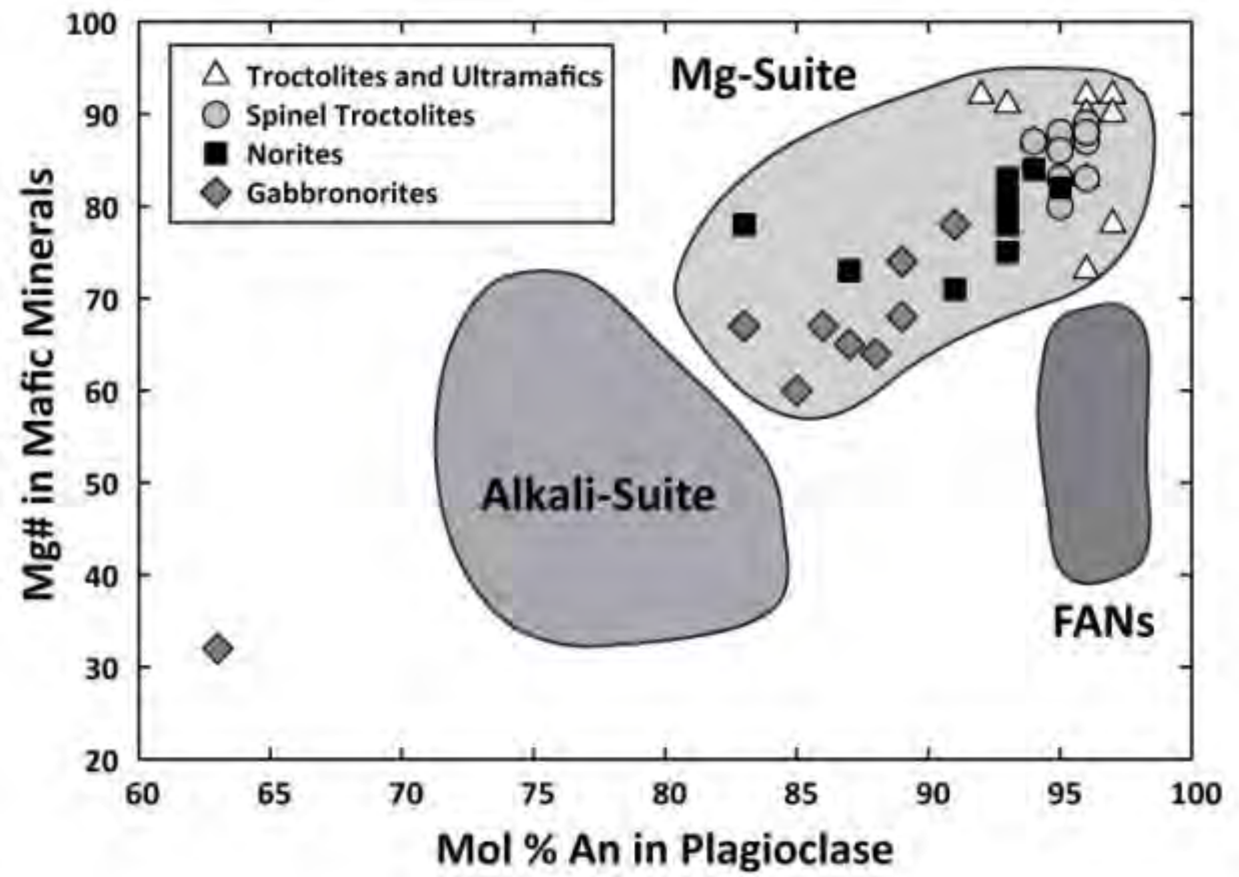

2339 Figure 2.

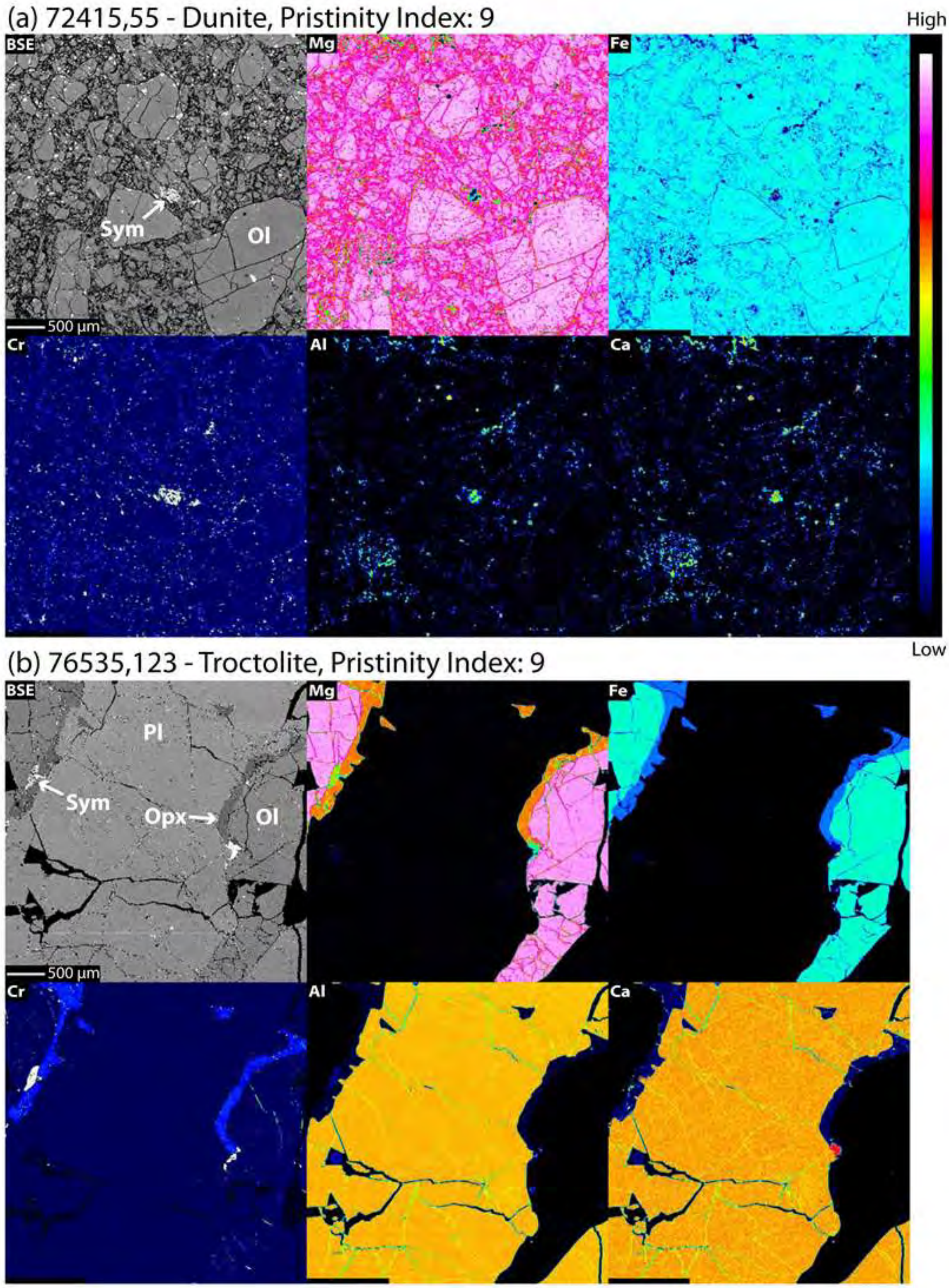

2340

(c) 78235,46 - Norite, Pristinity Index: 8

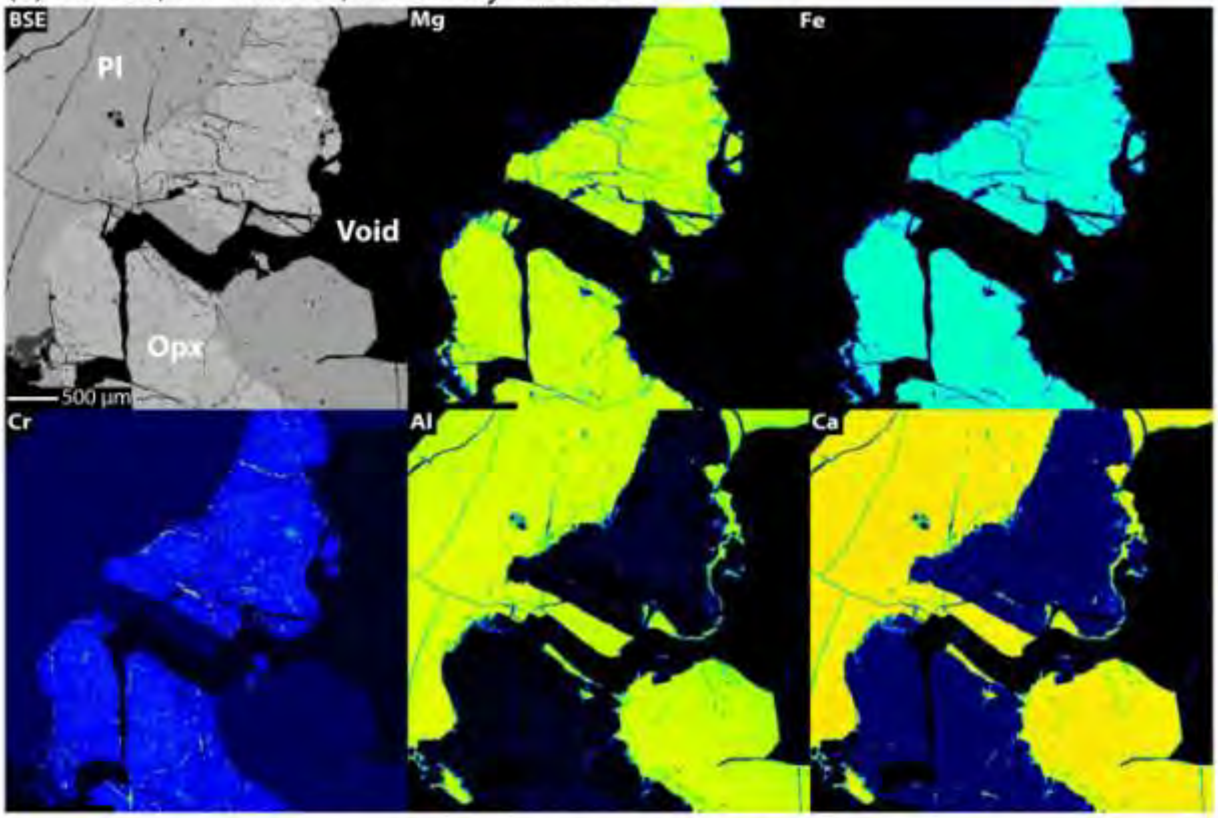

(d) 77215,201 - Norite Clast, Pristinity Index: 8

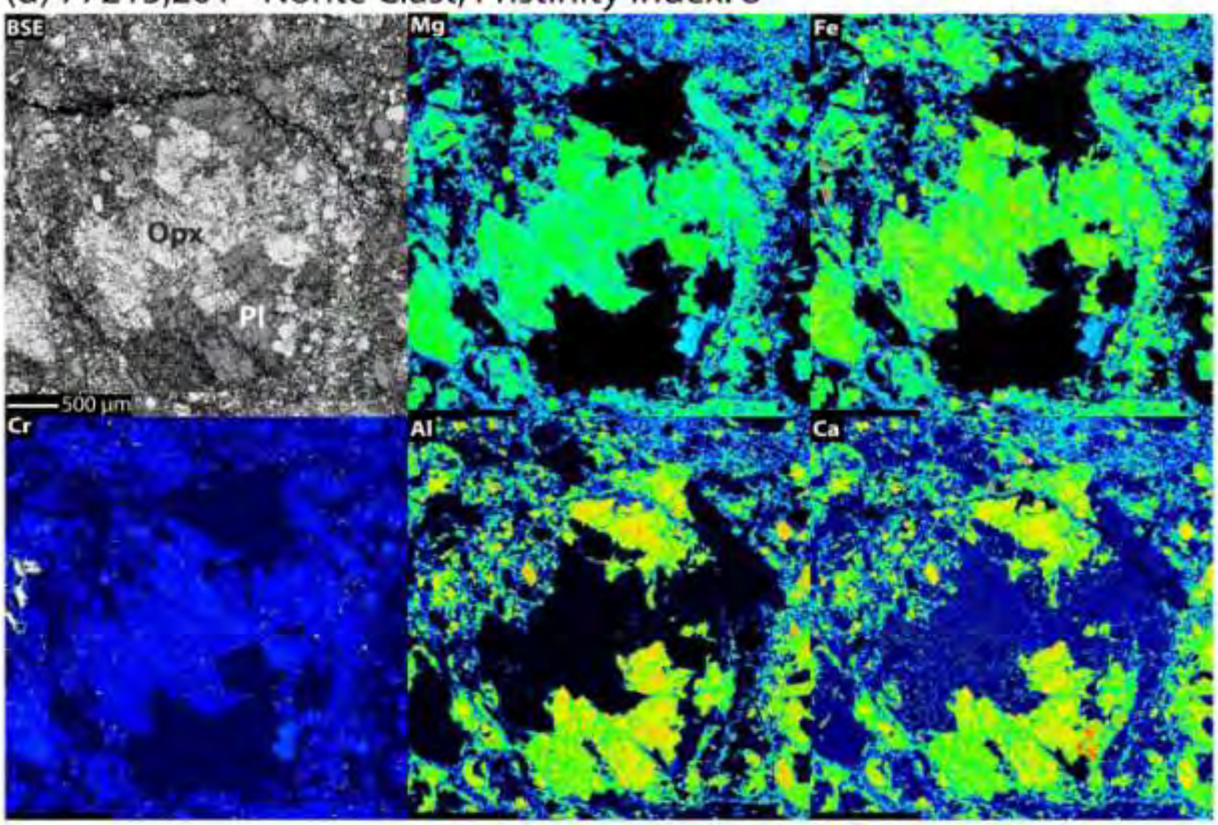

(e) 15445,292 - Shocked Norite "Clast B", Pristinity Index: 8

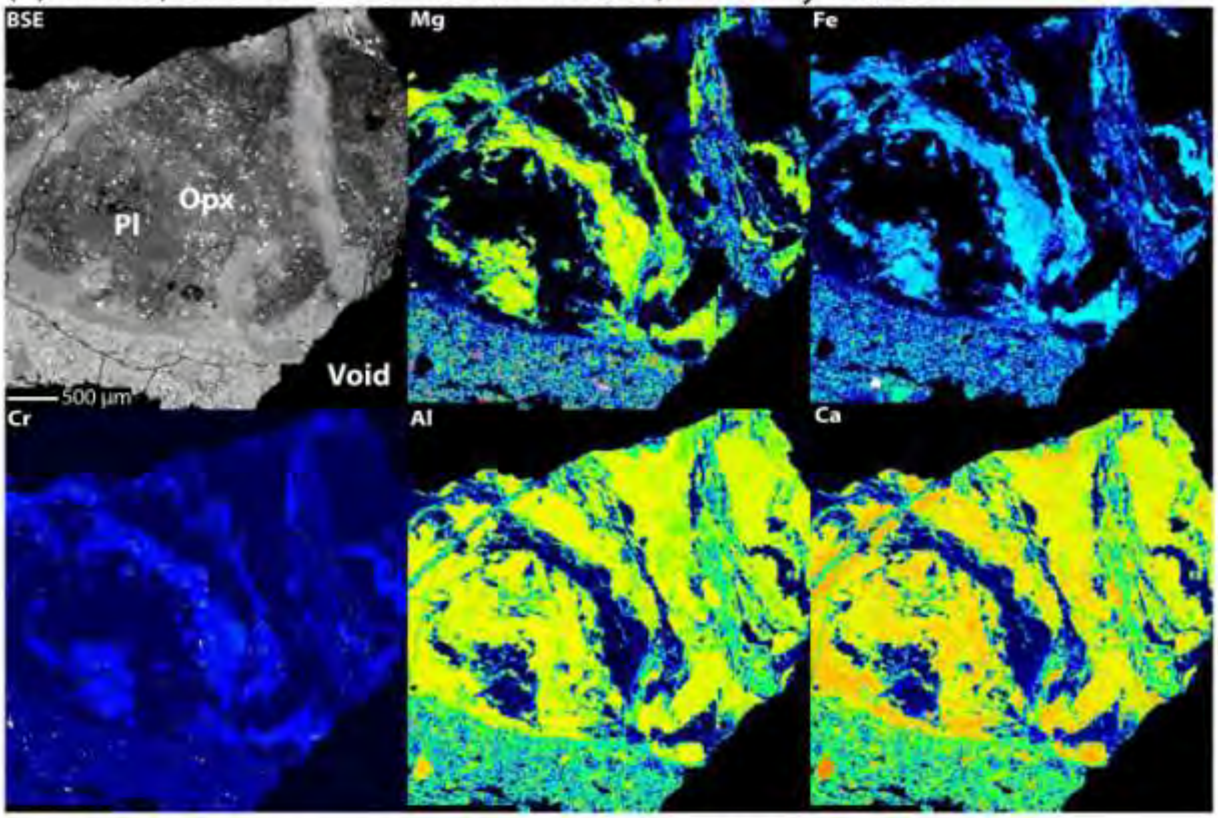

(f) 76255,72 - Gabbronorite Clast, Pristinity Index: 7

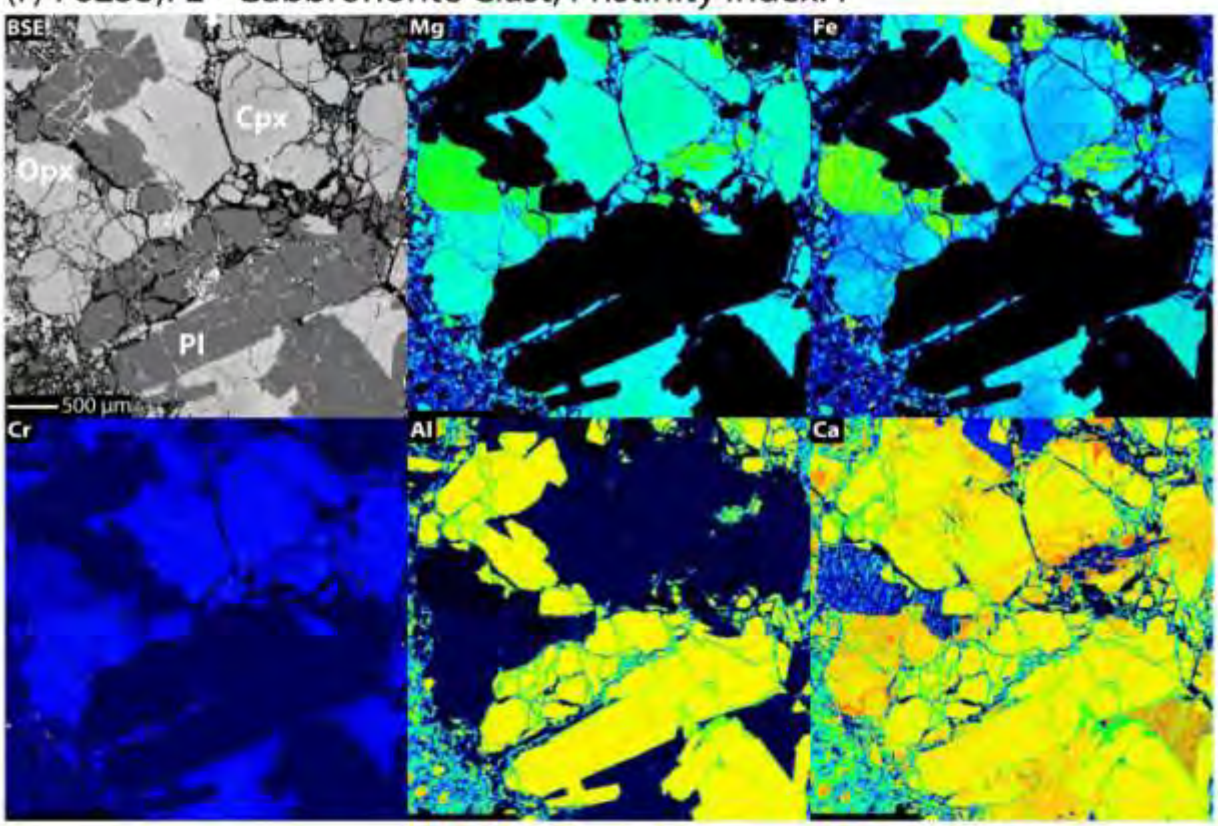

(g) 72435,30 - Spinel Troctolite Clast, Pristinity Index: Unassessed

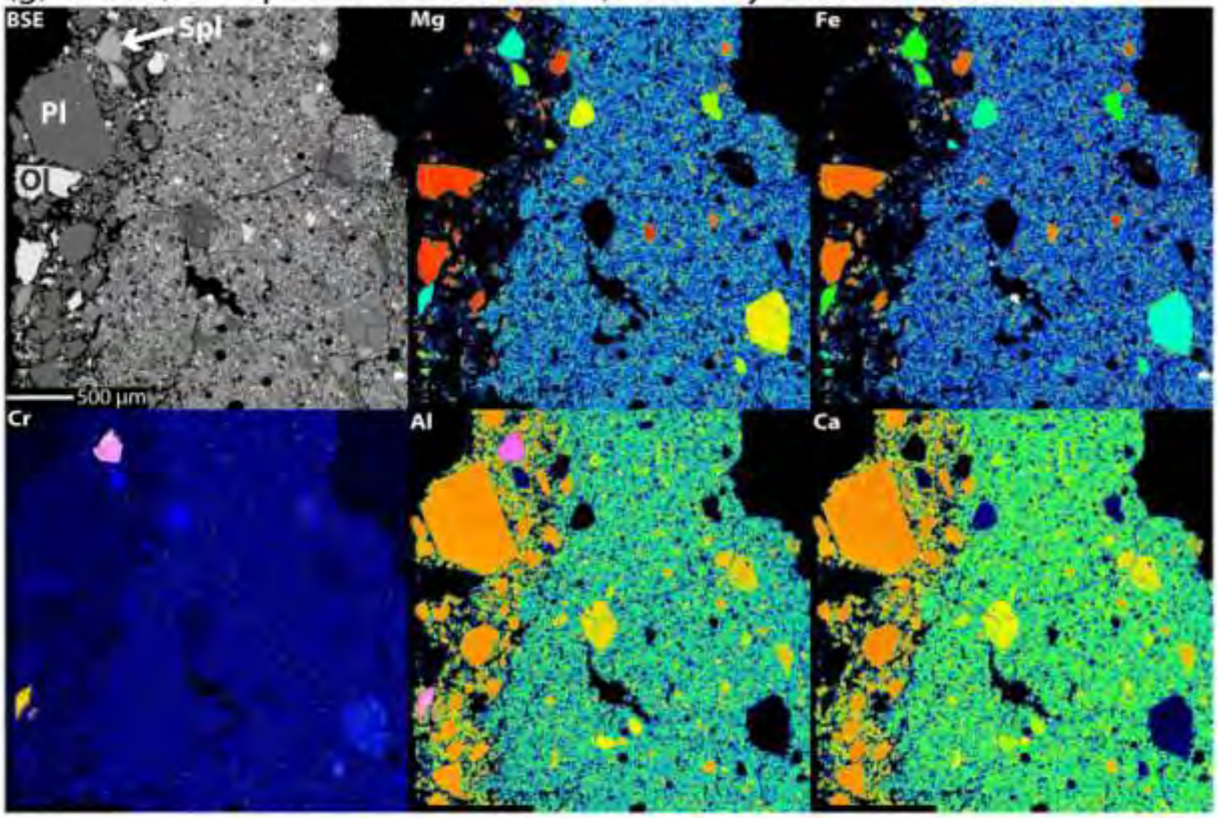

(h) 72435,8 - Corderite-Spinel Troctolite Clast, Pristinity Index: Unassessed

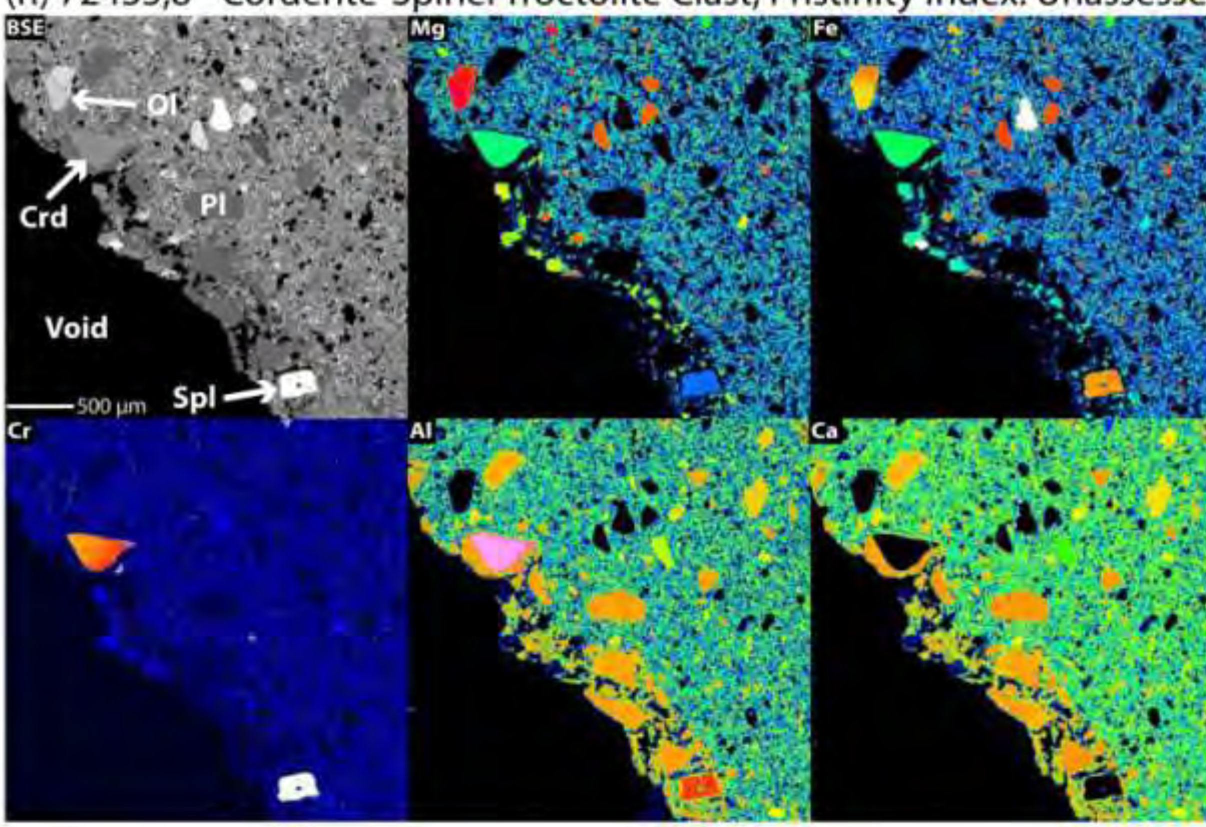

Figure 3.

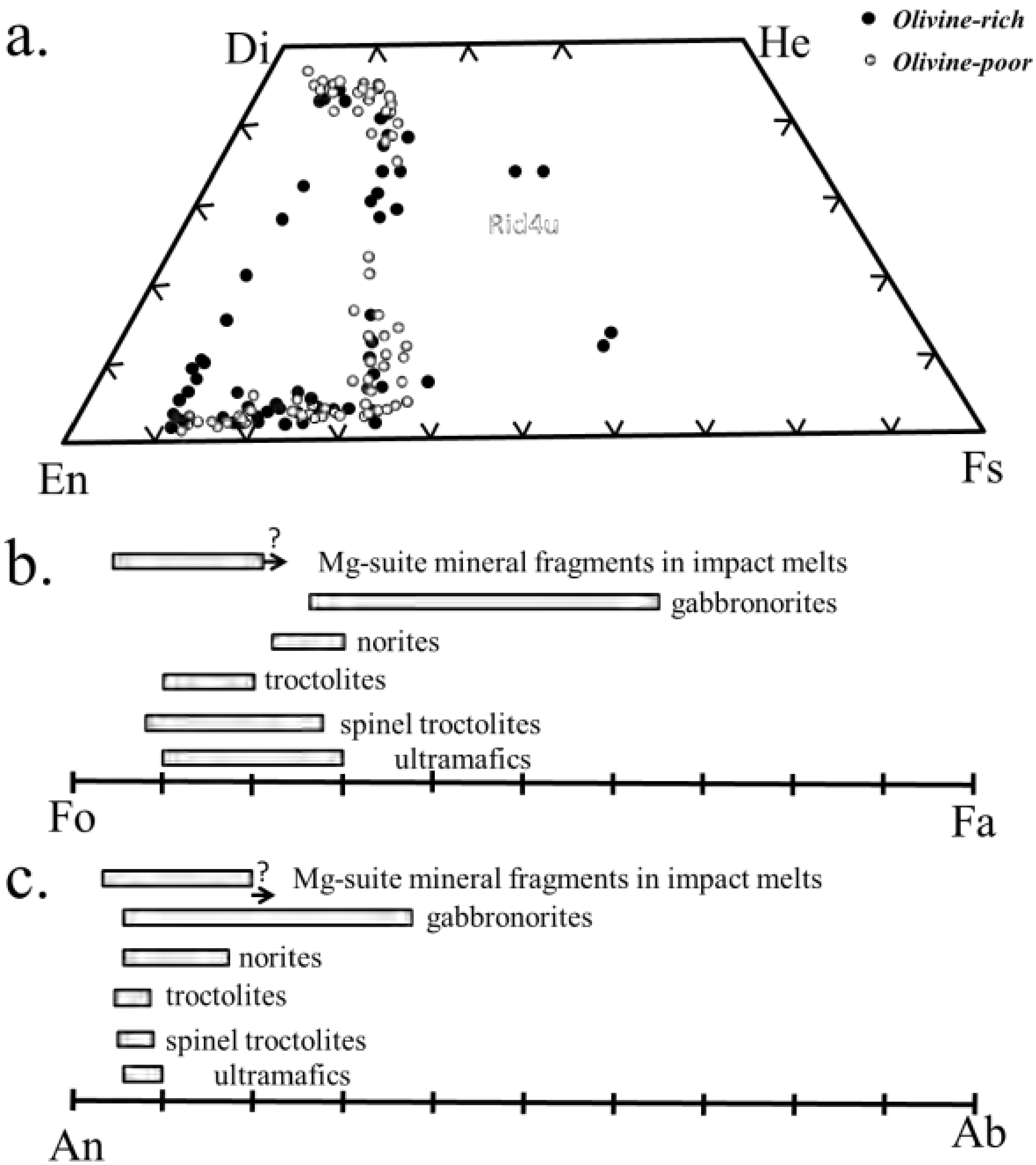
a.
Di
He
En
Fs
Olivine-rich
Olivine-poor
b.
Mg-suite mineral fragments in impact melts
gabbronorites
norites
troctolites
spinel troctolites
ultramafics
Fo
Fa
c.
Mg-suite mineral fragments in impact melts
gabbronorites
norites
troctolites
spinel troctolites
ultramafics
An
Ab

Figure 4.

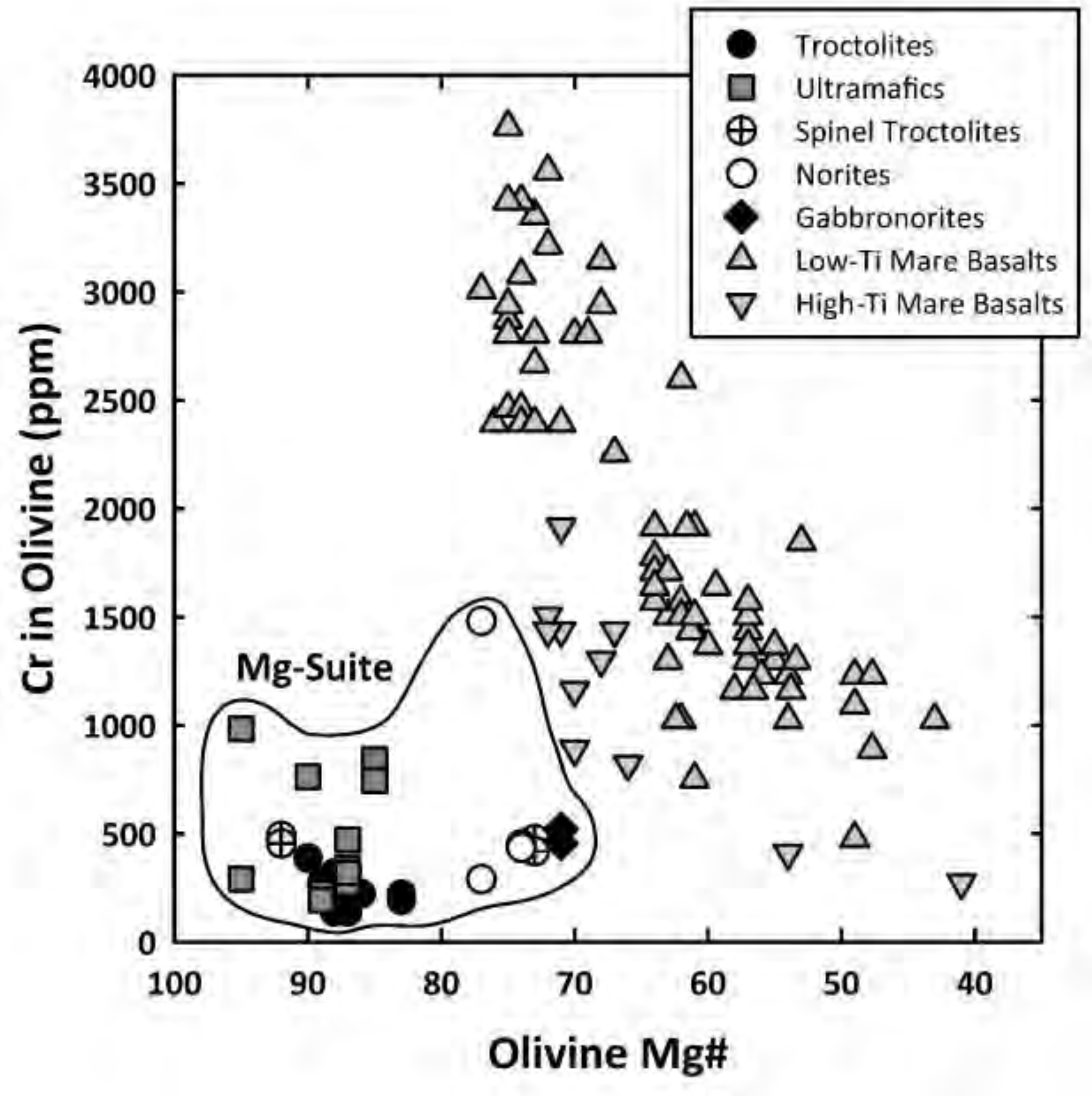
Troctolites
Ultramafics
Spinel Troctolites
Norites
Gabbronorites
Low-Ti Mare Basalts
High-Ti Mare Basalts
Mg-Suite
Cr in Olivine (ppm)
4000
3500
3000
2500
2000
1500
1000
500
0
100
90
80
70
60
50
40
Olivine Mg#

Figure 5.

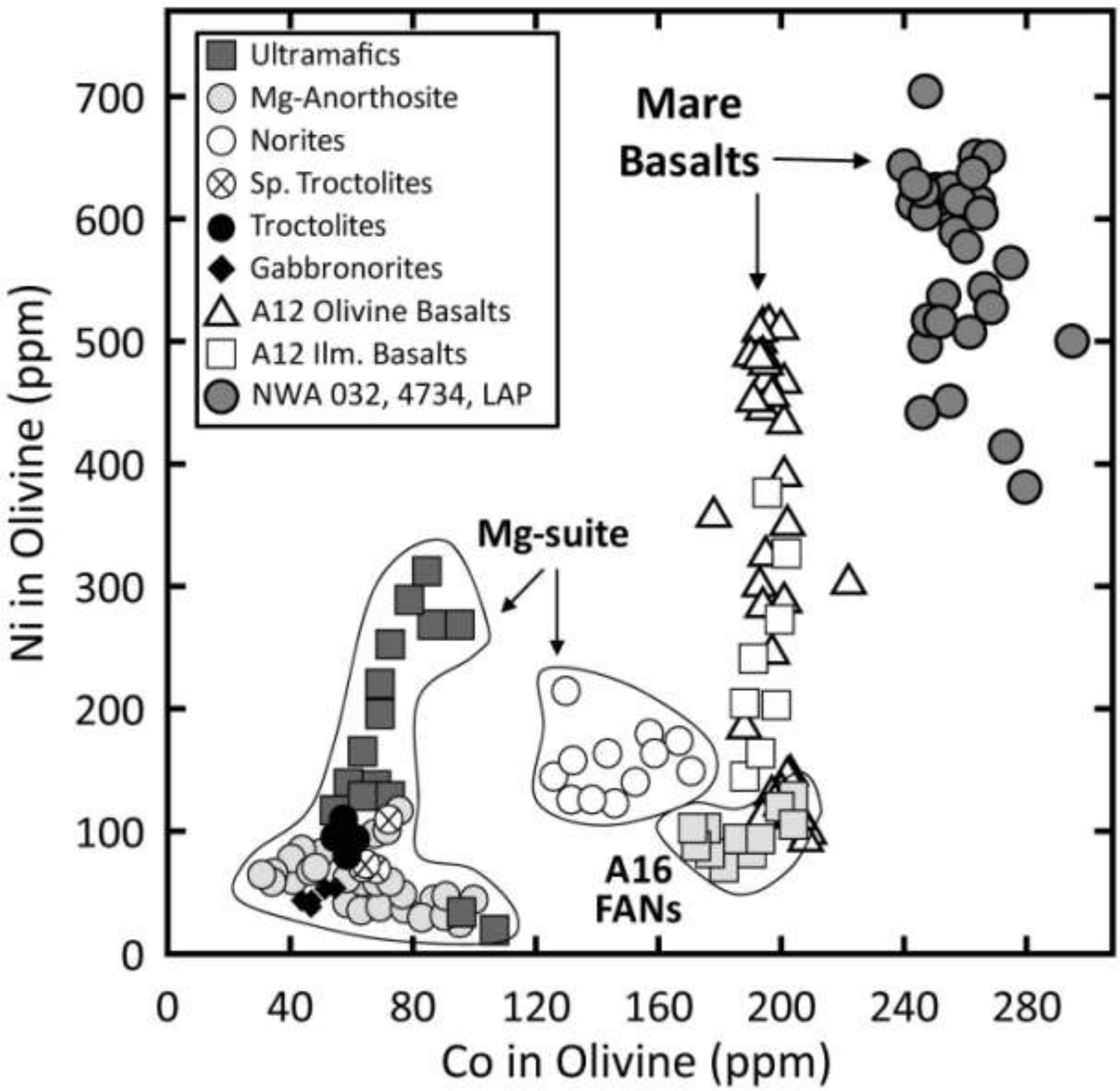
Ultramafics
Mg-Anorthosite
Norites
Sp. Troctolites
Troctolites
Gabbronorites
A12 Olivine Basalts
A12 Ilm. Basalts
NWA 032, 4734, LAP
Mare Basalts
Mg-suite
A16 FANs
Ni in Olivine (ppm)
Co in Olivine (ppm)
0
100
200
300
400
500
600
700
0
40
80
120
160
200
240
280

2360 Figure 6.

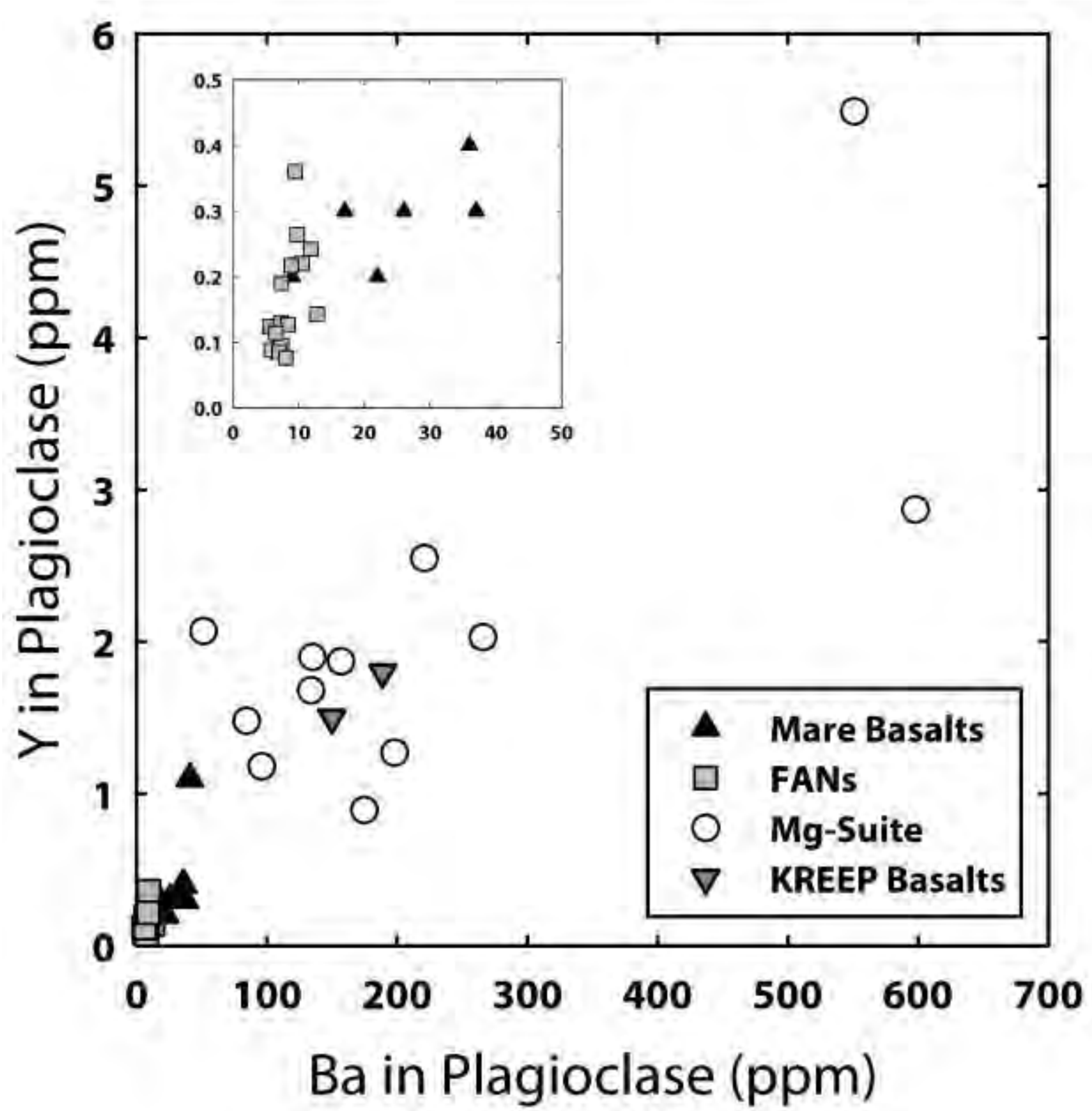

2361

2362

2363

2364

2365

2366

Figure 7.

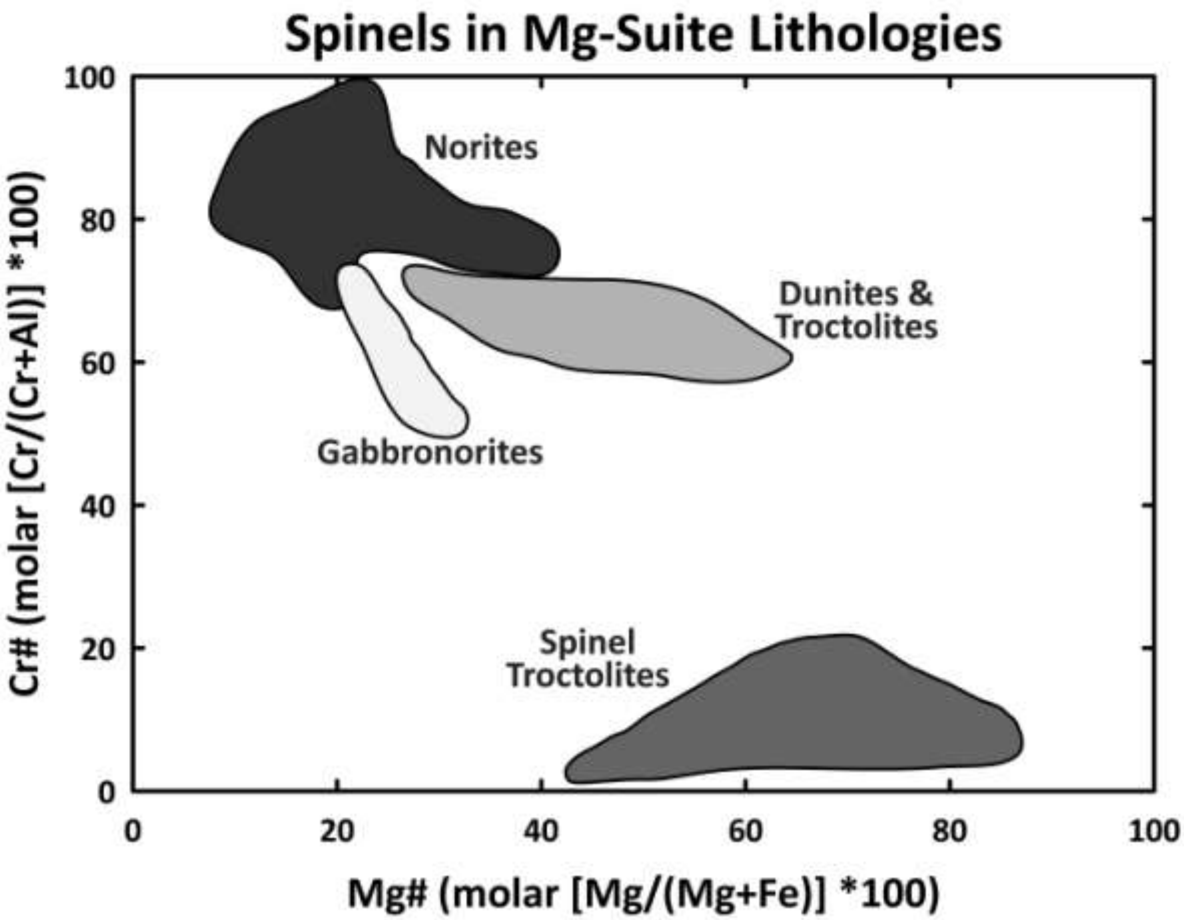
Spinels in Mg-Suite Lithologies
Norites
Dunites &
Troctolites
Gabbronorites
Spinel
Troctolites
Cr# (molar [Cr/(Cr+Al)] *100)
Mg# (molar [Mg/(Mg+Fe)] *100)
0
20
40
60
80
100

Figure 8.

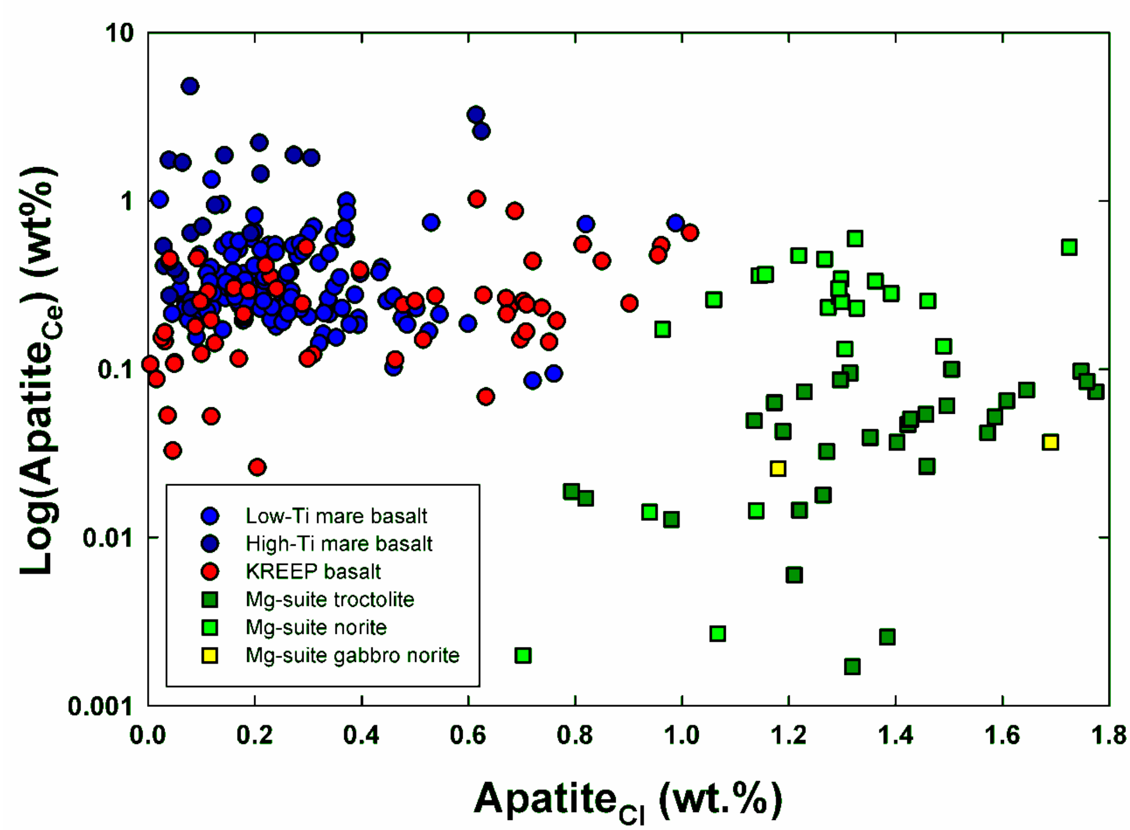
Log(Apatite$_{Ce}$) (wt%)
10
1
0.1
0.01
0.001
0.0
0.2
0.4
0.6
0.8
1.0
1.2
1.4
1.6
1.8
Apatite$_{Cl}$ (wt.%)
Low-Ti mare basalt
High-Ti mare basalt
KREEP basalt
Mg-suite troctolite
Mg-suite norite
Mg-suite gabbro norite

Figure 9.

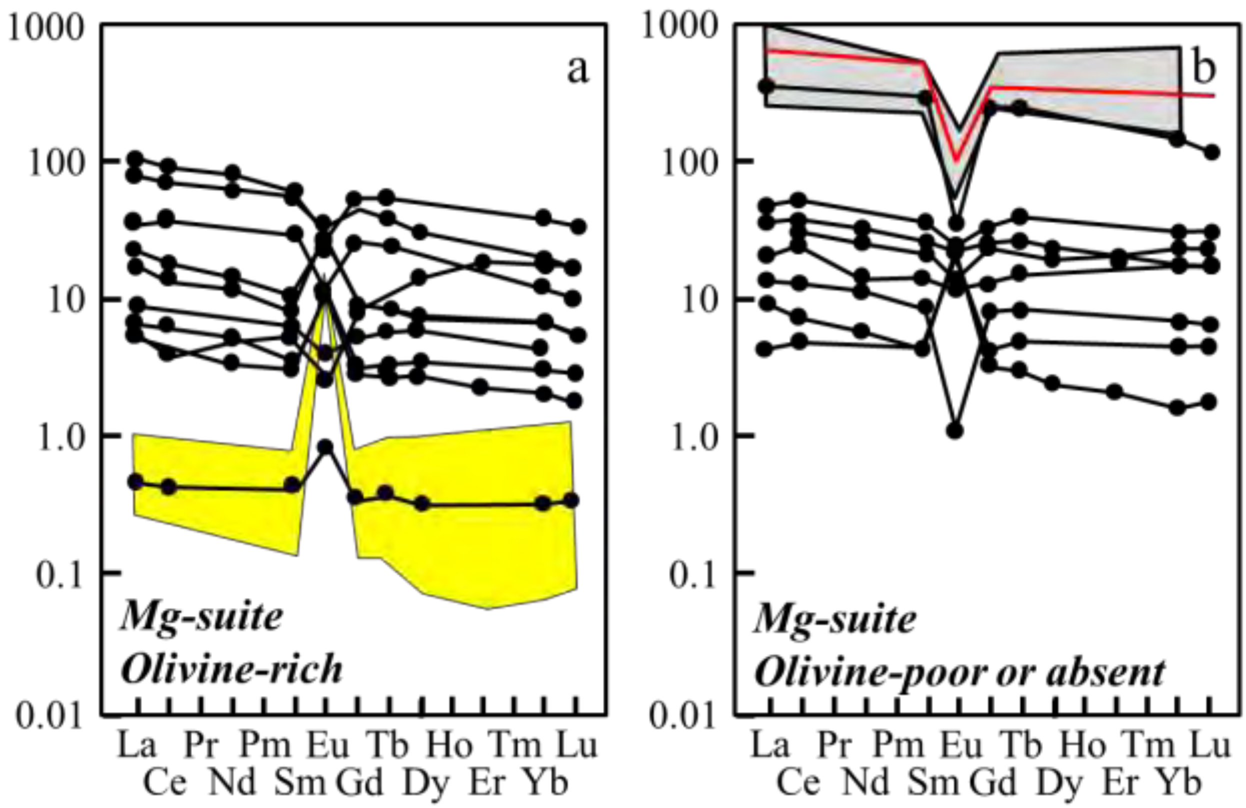
1000
100
10
1.0
0.1
0.01
a
Mg-suite
Olivine-rich
La Pr Pm Eu Tb Ho Tm Lu
Ce Nd Sm Gd Dy Er Yb
1000
100
10
1.0
0.1
0.01
b
Mg-suite
Olivine-poor or absent
La Pr Pm Eu Tb Ho Tm Lu
Ce Nd Sm Gd Dy Er Yb

Figure 10.

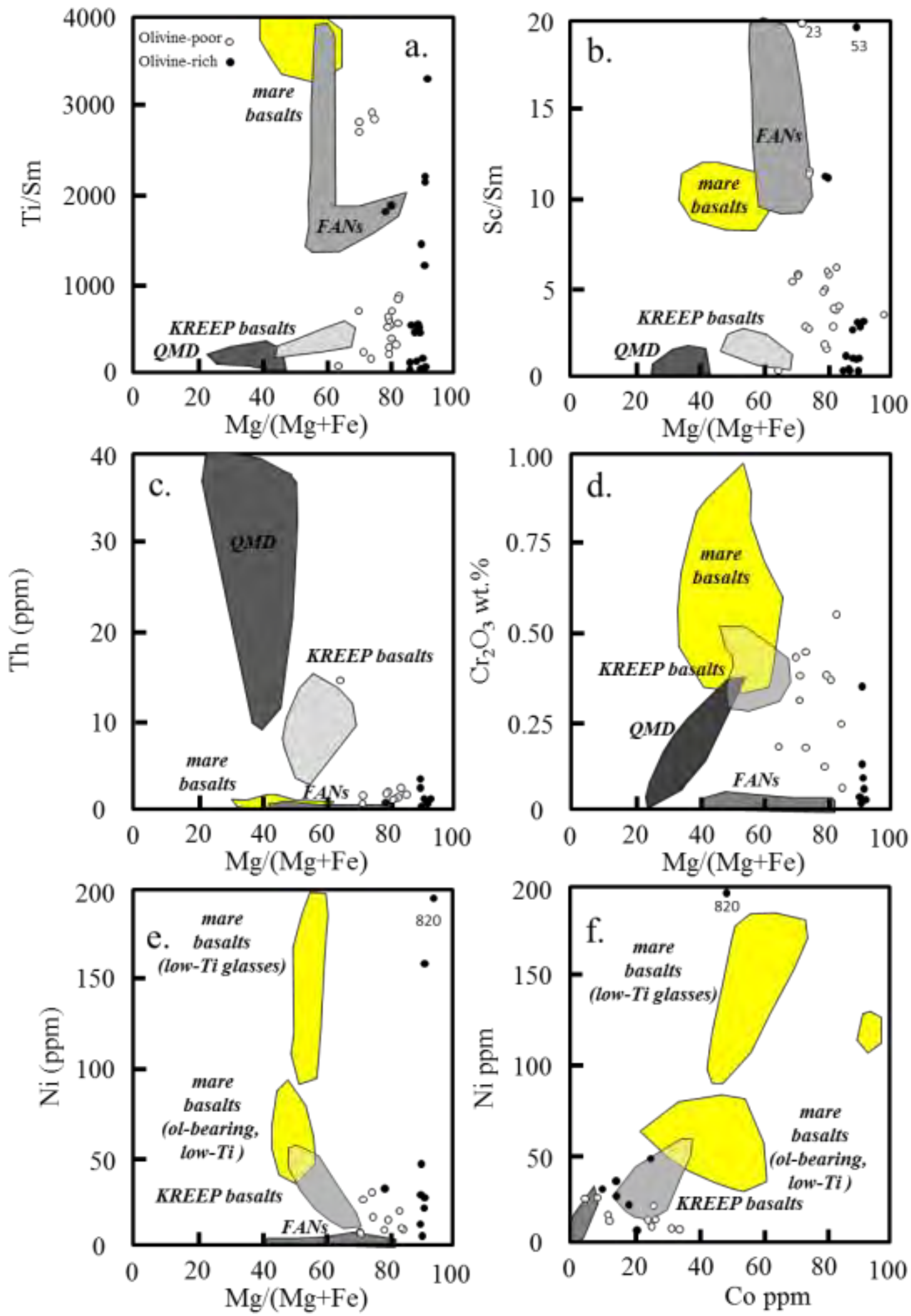
a.
Olivine-poor
Olivine-rich
mare basalts
FANs
KREEP basalts
QMD
Ti/Sm
Mg/(Mg+Fe)
b.
23
53
FANs
mare basalts
KREEP basalts
QMD
Sc/Sm
Mg/(Mg+Fe)
c.
QMD
KREEP basalts
mare basalts
FANs
Th (ppm)
Mg/(Mg+Fe)
d.
mare basalts
KREEP basalts
QMD
FANs
Cr_2O_3 wt.%
Mg/(Mg+Fe)
e.
820
mare basalts (low-Ti glasses)
mare basalts (ol-bearing, low-Ti)
KREEP basalts
FANs
Ni (ppm)
Mg/(Mg+Fe)
f.
820
mare basalts (low-Ti glasses)
mare basalts (ol-bearing, low-Ti)
KREEP basalts
Ni ppm
Co ppm

Figure 11.

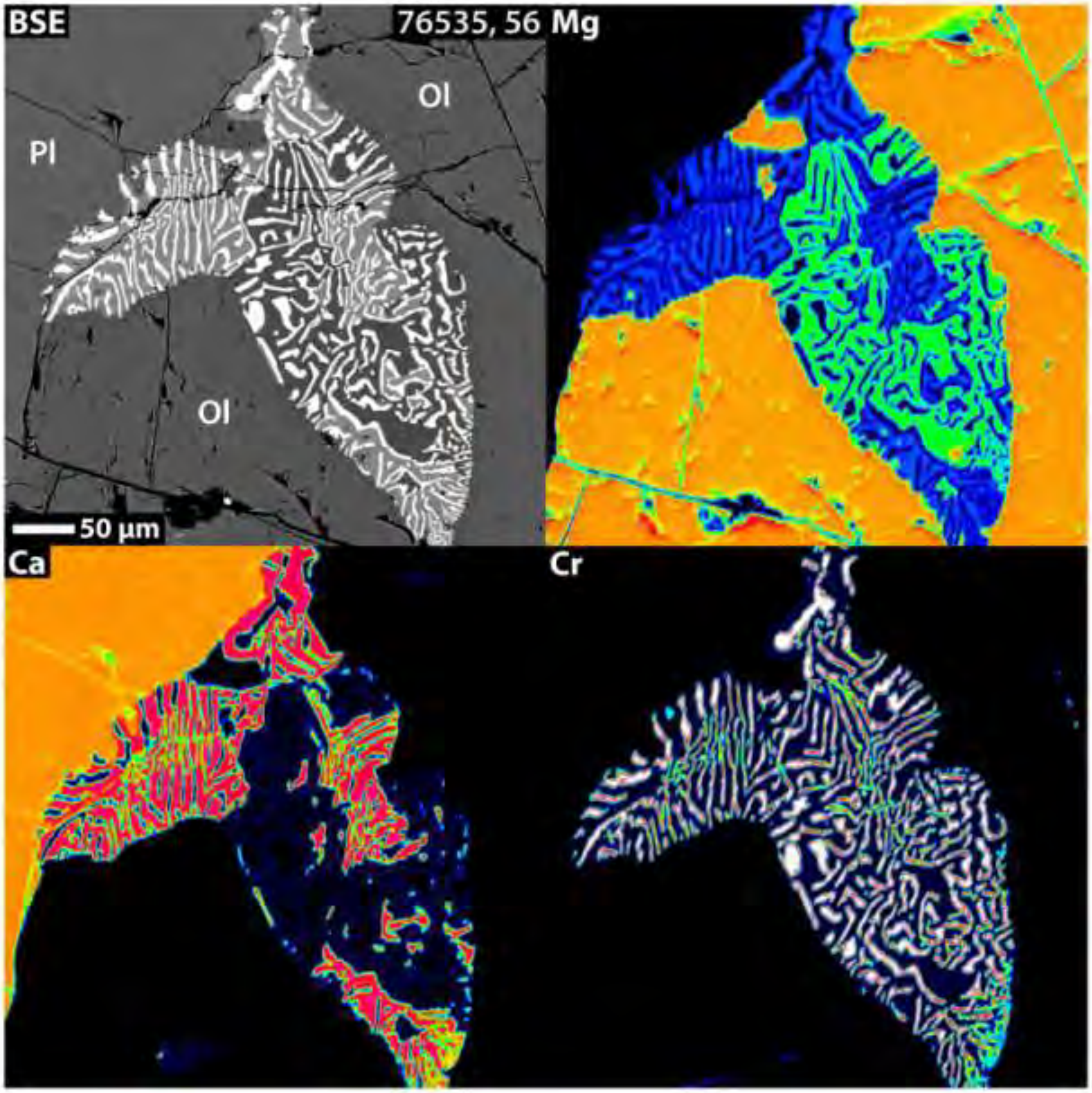

Figure 12.

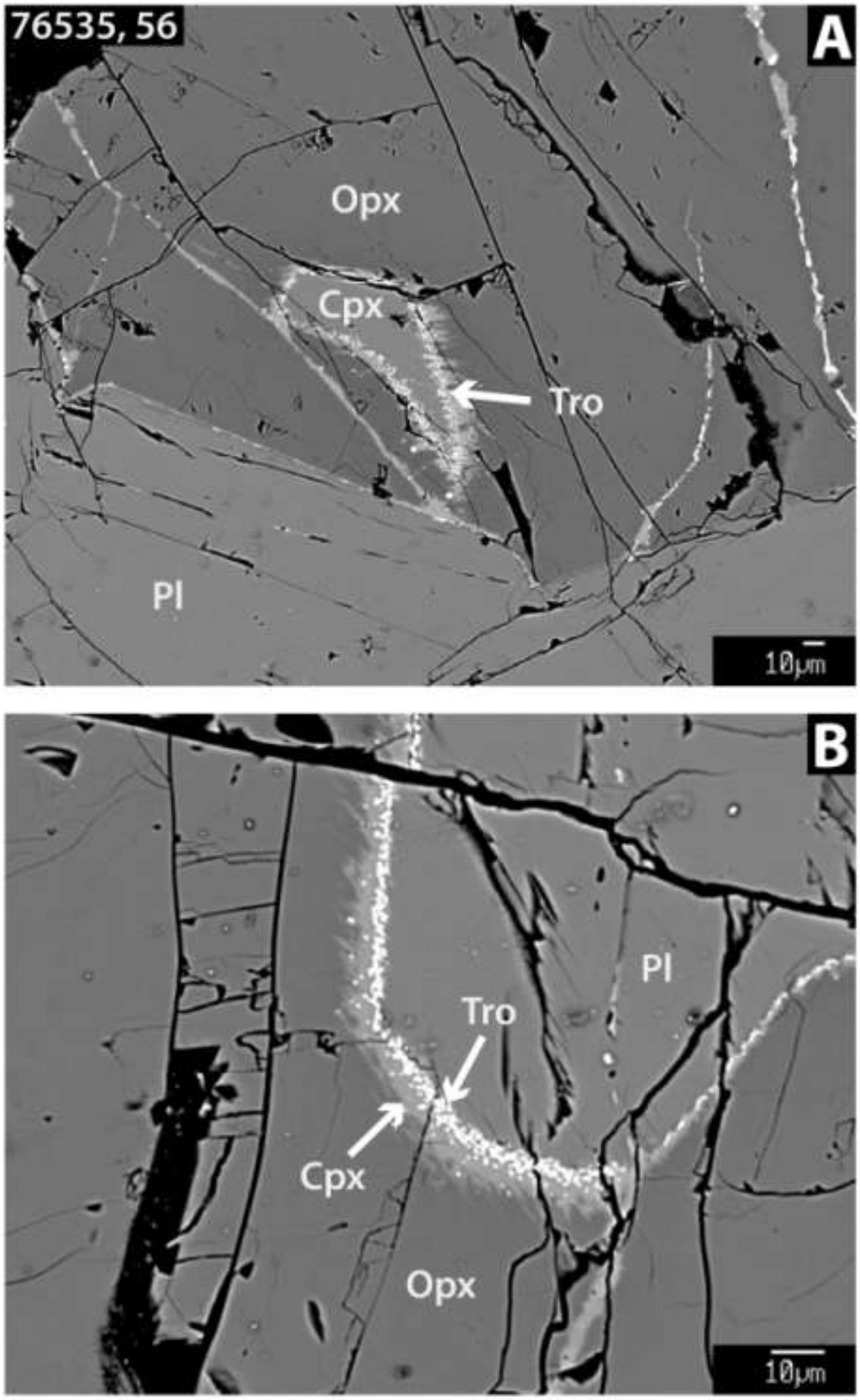

Figure 13.

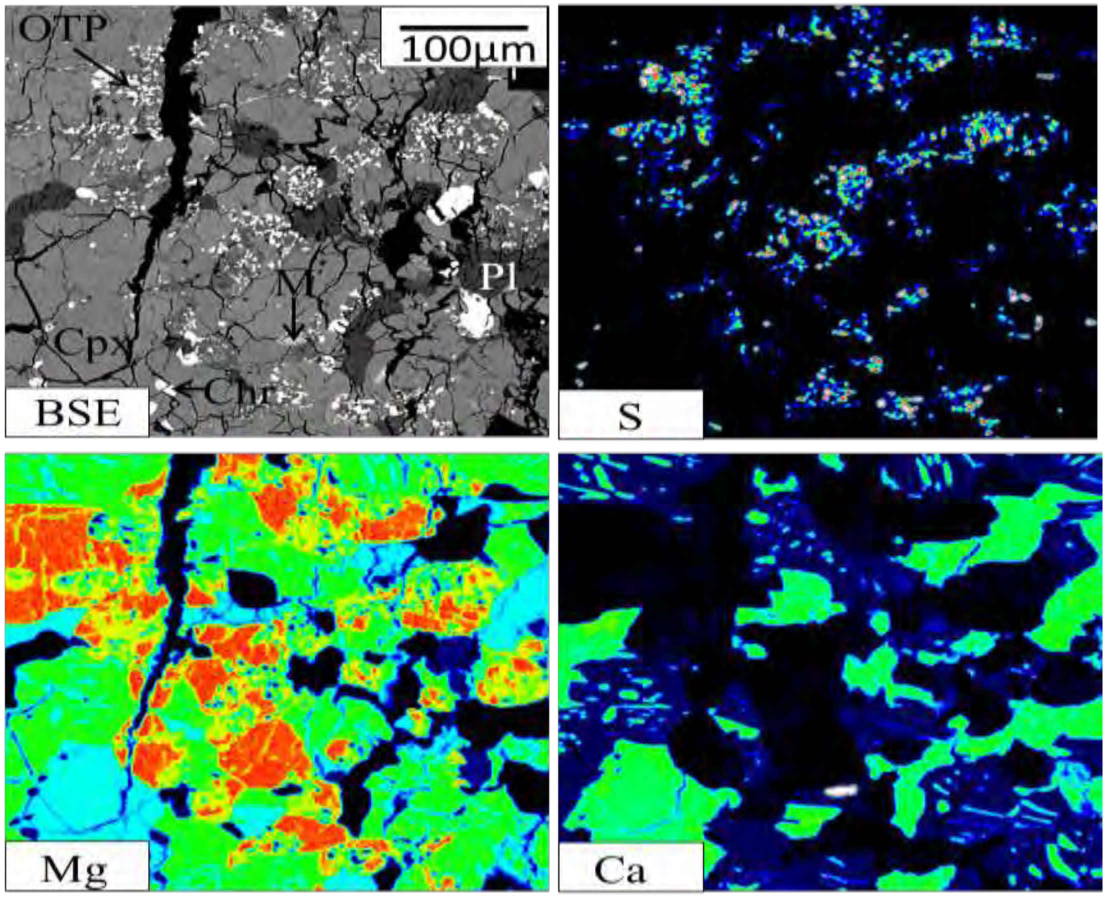

Figure 14.

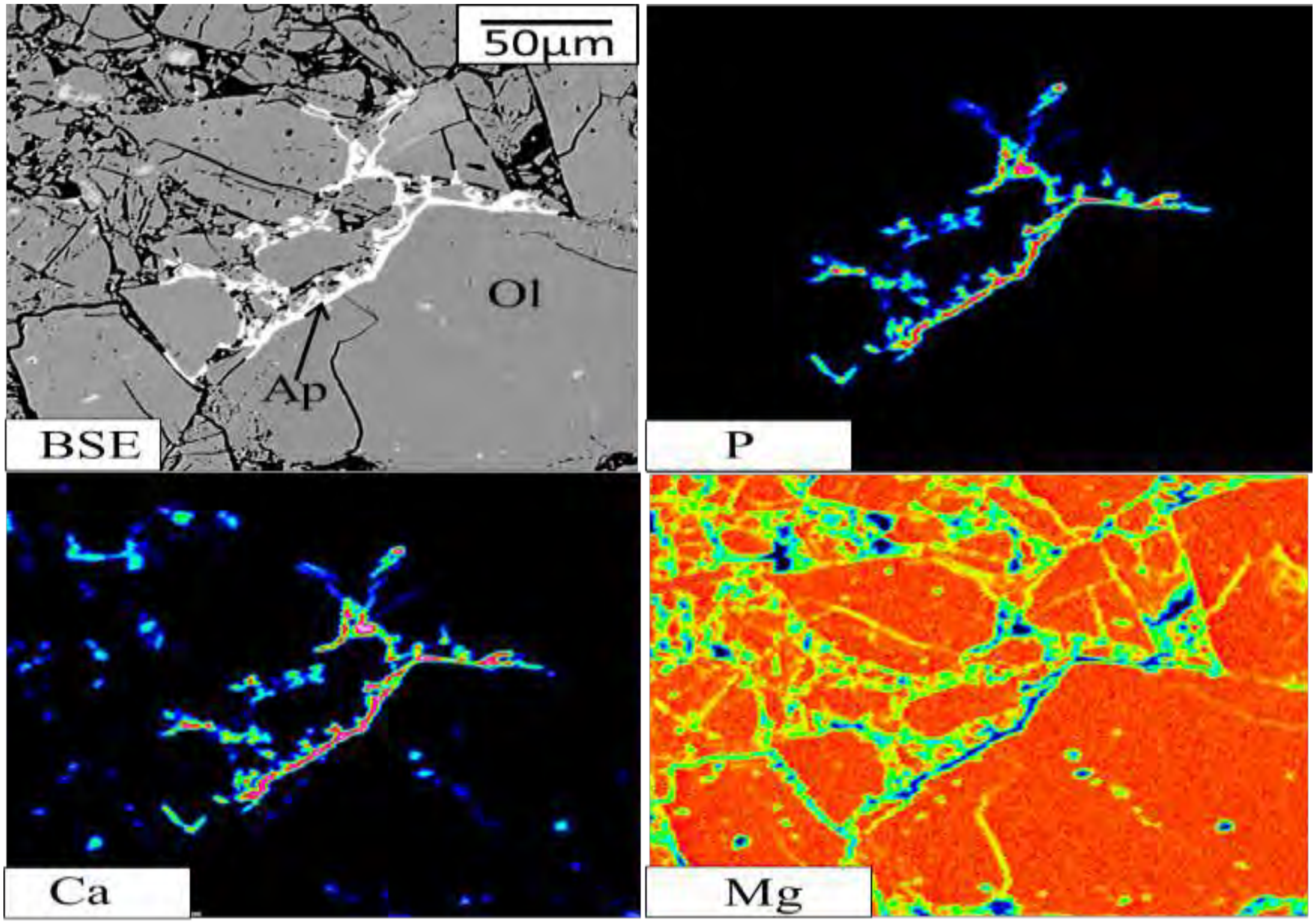

Figure 15.

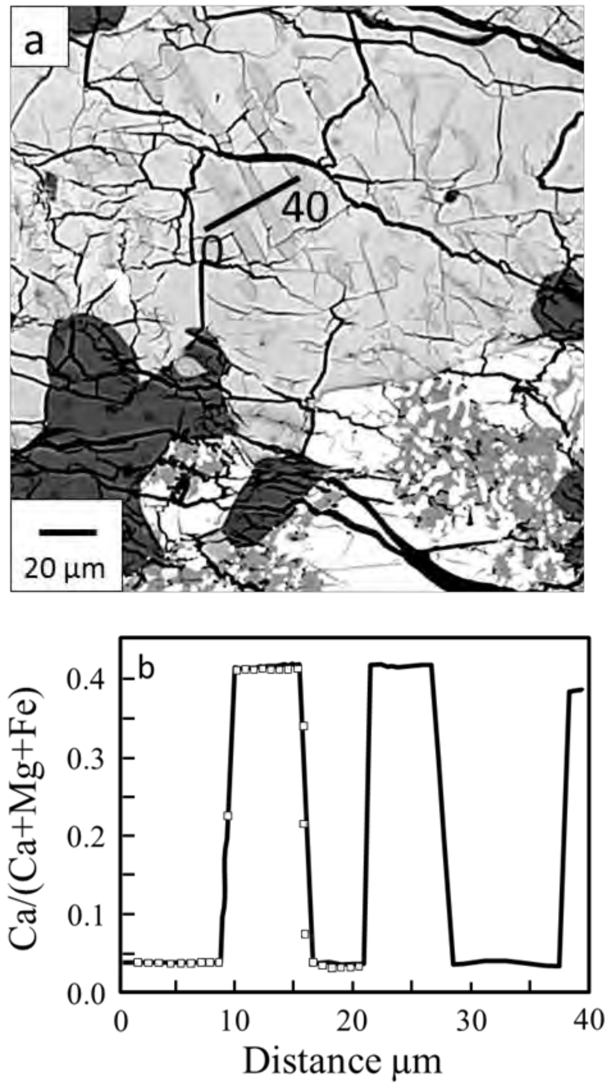

Figure 16.

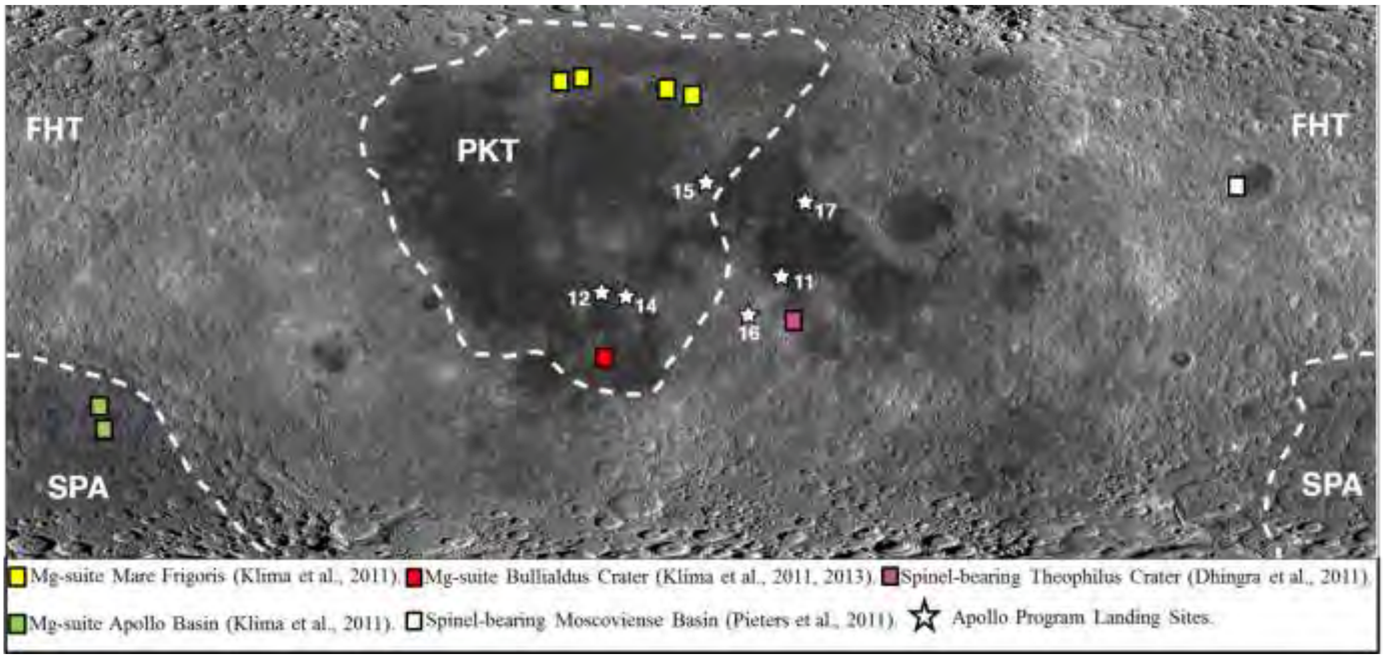
FHT
PKT
FHT
15
17
11
12
14
16
SPA
SPA
Mg-suite Mare Frigoris (Klima et al., 2011).
Mg-suite Bullialdus Crater (Klima et al., 2011, 2013).
Spinel-bearing Theophilus Crater (Dhingra et al., 2011).
Mg-suite Apollo Basin (Klima et al., 2011).
Spinel-bearing Moscoviense Basin (Pieters et al., 2011).
Apollo Program Landing Sites.

2440

2441

2442 Figure 17.

2443

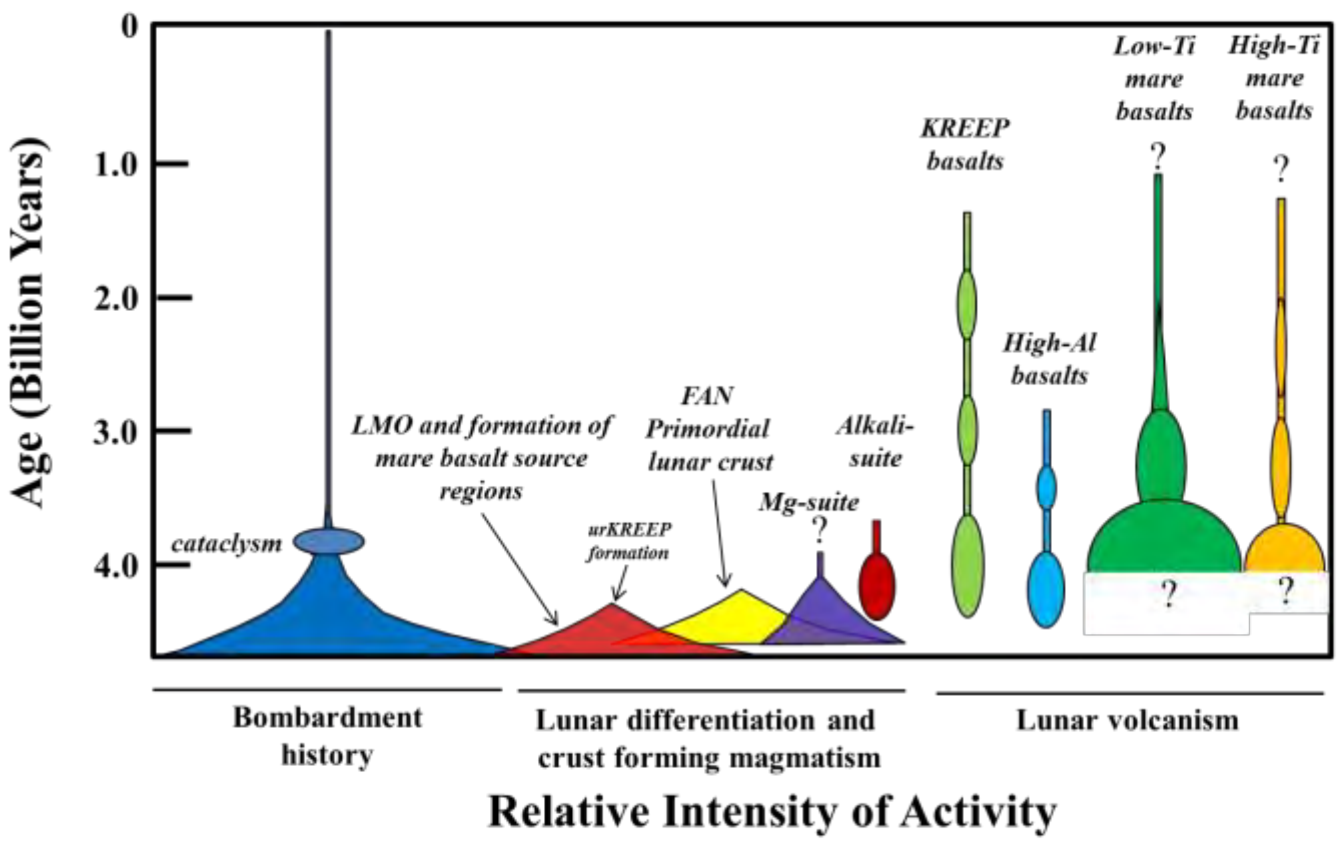

2444

2445

2446

Figure 18.

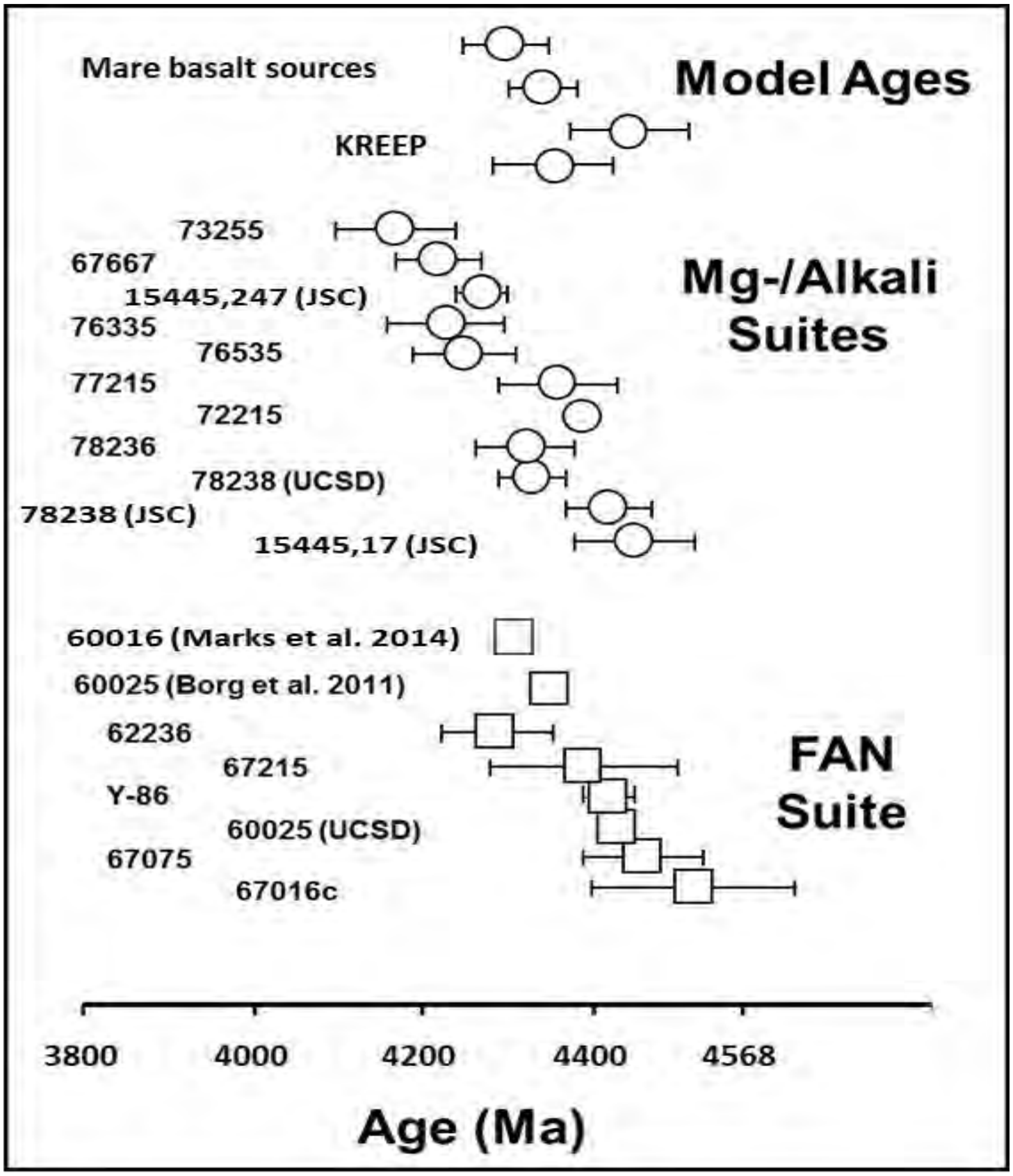
Mare basalt sources
Model Ages
KREEP
73255
67667
15445,247 (JSC)
76335
76535
77215
72215
78236
78238 (UCSD)
78238 (JSC)
15445,17 (JSC)
Mg-/Alkali Suites
60016 (Marks et al. 2014)
60025 (Borg et al. 2011)
62236
67215
Y-86
60025 (UCSD)
67075
67016c
FAN Suite
3800
4000
4200
4400
4568
Age (Ma)

Figure 19.

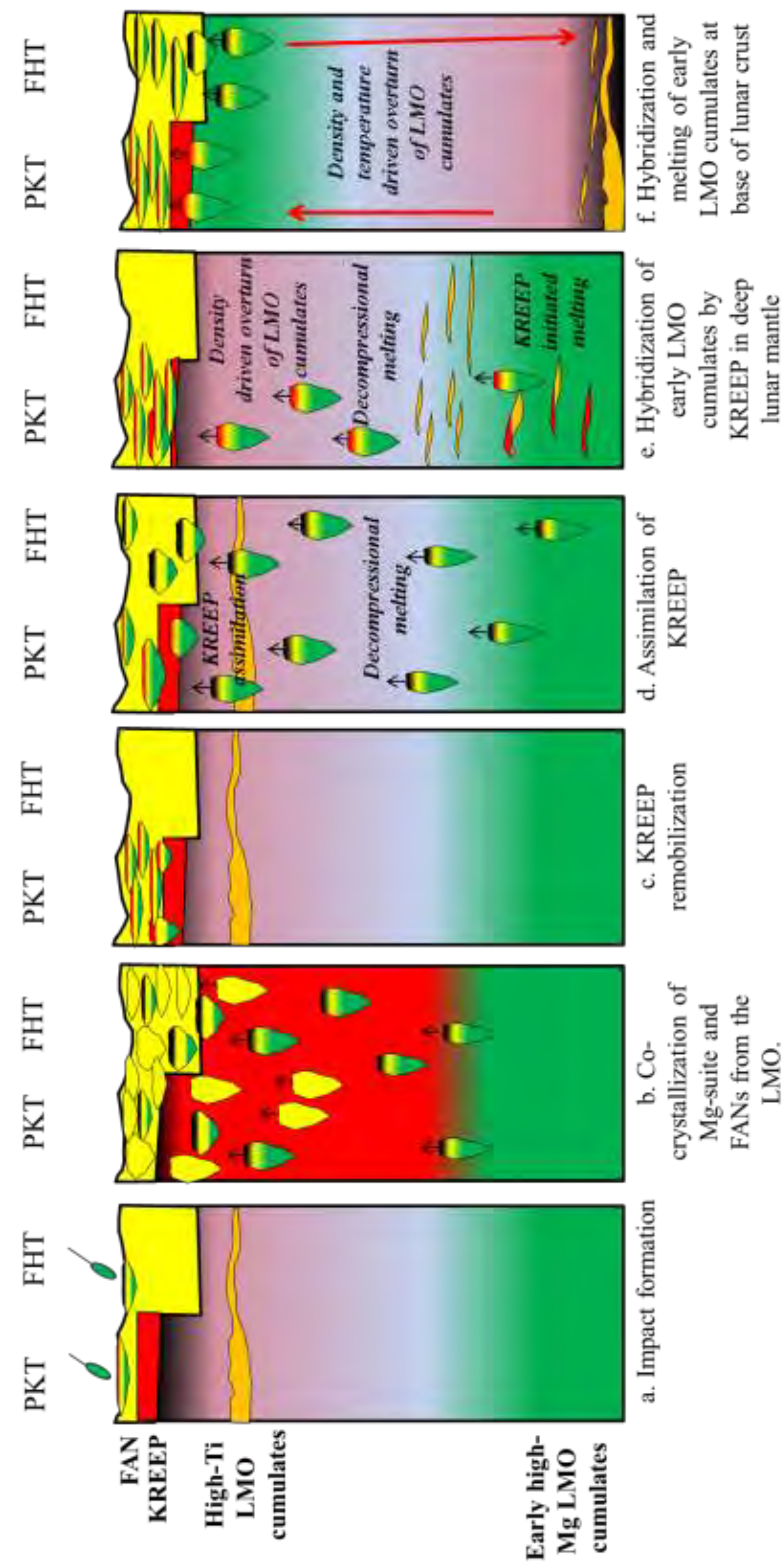
PKT
FHT
FAN
KREEP
High-Ti LMO cumulates
Early high-Mg LMO cumulates
a. Impact formation
b. Co-crystallization of Mg-suite and FANs from the LMO.
c. KREEP remobilization
KREEP assimilation
Decompressional melting
d. Assimilation of KREEP
Density driven overturn of LMO cumulates
Decompressional melting
KREEP initiated melting
e. Hybridization of early LMO cumulates by KREEP in deep lunar mantle
Density and temperature driven overturn of LMO cumulates
f. Hybridization and melting of early LMO cumulates at base of lunar crust